TECH LIBRARY KAFB, NM
0060473

NASA CONTRACTOR REPORT

NASA CR-1412

TECHNICAL LIBRARY BRANCH
AFWL (WLIL-2)
KIRTLAND AFB, N MEX

METHOD OF DERIVING ORBITAL PERTURBING PARAMETERS FROM ONBOARD OPTICAL MEASUREMENTS OF AN EJECTED PROBE OR A NATURAL SATELLITE

by C. B. Grosch and H. R. Paetznick

Prepared by
CONTROL DATA CORPORATION
Minneapolis, Minn.
for Langley Research Center

NATIONAL AERONAUTICS AND SPACE ADMINISTRATION • WASHINGTON, D. C. • AUGUST 1969

TECH LIBRARY KAFB, NM
0060473
NASA CR-1412

METHOD OF DERIVING ORBITAL PERTURBING PARAMETERS FROM ONBOARD OPTICAL MEASUREMENTS OF AN EJECTED PROBE OR A NATURAL SATELLITE

By C. B. Grosch and H. R. Paetznick

Distribution of this report is provided in the interest of information exchange. Responsibility for the contents resides in the author or organization that prepared it.

Issued by Originator as Control Data Project No. 9580

Prepared under Contract No. NAS 1-7540 by
CONTROL DATA CORPORATION
Minneapolis, Minn.

for Langley Research Center

NATIONAL AERONAUTICS AND SPACE ADMINISTRATION

For sale by the Clearinghouse for Federal Scientific and Technical Information
Springfield, Virginia 22151 – CFSTI price $3.00

ACKNOWLEDGMENT

The authors would like to acknowledge the assistance of Harold A. Hamer and Albert A. Schy, technical officers in charge of this study. They directed the study and pointed out many errors in the first draft. Also, Robert H. Tolson kindly furnished Control Data Corporation with the Lungfish program and written instructions to its use.

TABLE OF CONTENTS

METHOD OF DERIVING ORBITAL PERTURBING PARAMETERS FROM ONBOARD OPTICAL MEASUREMENTS OF AN EJECTED PROBE OR A NATURAL SATELLITE

INTRODUCTION

The principal objective of this analytical investigation is to evaluate the usefulness of a number of sightings taken from an orbiting spacecraft to another (secondary) satellite. The sightings determine the direction of the secondary satellite relative to the fixed stars by angle measurements only. The sightings are assumed to be made intermittently over periods ranging from a fraction of one orbit to many days. The secondary satellite may be a probe which is ejected from the spacecraft itself or a natural satellite.

This program has been exploratory in nature and, in general, is concerned with the possibility of deriving a knowledge of forces which perturb the orbit. From a theoretical viewpoint the feasibility of navigational systems of this type is already established. What is not known, however, is the effect of measurement errors on the accuracy of various perturbing parameters. Further, the determination of the perturbing parameters and the solution of the navigation problem constitutes a single problem for which solutions must be obtained simultaneously.

The study is conducted primarily with respect to spacecraft orbits about Mars, Venus, the Moon, and Earth. Some results are shown for Saturn. The study of Mars utilizes various combinations of one or both of its natural satellites and an ejected probe as secondaries. However, for orbits about Venus, the Moon, and Earth, the secondary is a single ejected probe. The speed of ejection is very small as compared with orbital speeds.

PROGRAM OBJECTIVES

Figure 1 indicates the geometry of the sightings and the parameters studied for the case of orbits about Mars and Venus. These parameters arise from gravitational forces. In a following study concerning the moon and the earth, a more complicated potential will be assumed for the moon, and non-gravitational forces will be considered for the earth.

As a starting point, effort has been concentrated on the problem of determining the higher order terms in the gravitational potential of Mars. Since

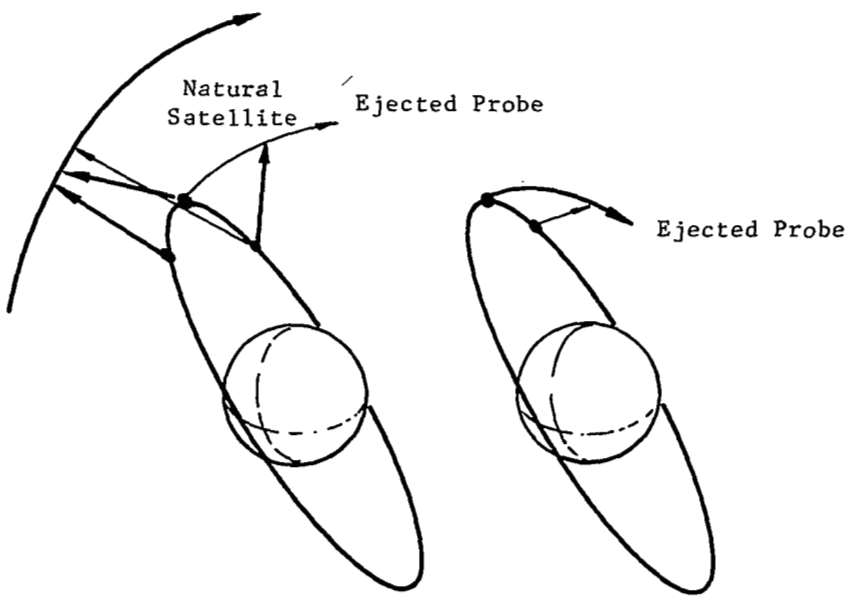

SOLAR SYSTEM BODY	Mars	Venus
REFERENCE TARGET	Natural Satellites and Probe	Ejected Test Probe
PERTURBING PARAMETERS OF PRIMARY INTEREST	(J_2, J_3, J_4), mass, and direction of axis of dynamic symmetry	Direction of axis of dynamic symmetry, (C_{21}, S_{21}, J_2)

Figure 1: Perturbing Parameter Study for Mars and Venus

Mars has two readily viewable natural satellites (Phobos and Deimos), it was first decided to base the investigation on angular observations of these bodies rather than to assume that an artificial probe was ejected. This, in turn, necessitated a prior navigational study involving 12 and 18 unknowns to determine the basic characteristics of such systems from the point of view of error propagation. As a result, it was found that systems in which our own satellite orbit was unknown as well as the orbits of Phobos and/or Deimos were indeed promising from a navigational point of view. Although the 18 unknown problem had satisfactory properties, it was decided that observations of a single orbiting body would be operationally simpler and thus the 12 unknown problem (our own satellite and Phobos) would form the starting point for Mars perturbing parameter studies.

After completing the Mars perturbing parameter study based on the use of Phobos as a secondary, consideration was given to including sightings on an ejected probe. This was done and proved to yield more accurate results, as will be shown.

The next phase of the investigation involved the determination of the gravitational potential of Venus. Since Venus has no known natural satellites, an ejected test probe of assumed ejection speed but unknown direction was used. The effect of an error in the assumed speed is also studied. The degree of interest in the various perturbing parameters is different for Venus than for Mars. Because Venus is rotating very slowly (rotational period of 247 days retrograde), it is probably the most nearly spherical of the planets. It turns out that considerable difficulty is encountered if the direction of the axis of dynamic asymmetry is treated as an unknown in the total problem.

In the moon study three separate orbits were chosen, each of which had an eccentricity of 0.1; the secondary being a probe ejected at 4 km/hr. In this case, problem emphasis is quite different from that of orbits about Mars or Venus for the following reasons:

(1) The moon has a complicated potential in that tesseral harmonics must be considered.

(2) Earth-based radar measurements are more effective in the case of the moon or the earth than Mars or Venus. Hence, our method must be compared with stronger competition.

As many as 10 unknown harmonics coefficients were chosen. In general, our error analysis yielded accuracies comparable to those obtained from Lunar Orbiter data.

Finally, low and high altitude Earth orbits were investigated. For this case the potential was assumed known, and unknown drag and radiation pressure terms were allowed. It was found that if a small error in the speed of probe ejection were made, a significant error in these parameters would be incurred. In order to overcome such errors, a geometry was studied in which the probe was simply released; drag and radiation pressure were then allowed to separate the probe and the spacecraft.

It is one of the principal objects of the investigation to determine the number of orbits over which measurements must be made in order to determine the values of the parameters for various degrees of accuracy. The criterion which is used in determining what constitutes an acceptable degree of accuracy is the accuracy with which the parameter in question is known at present. Thus, in the case of the earth, accuracies must be very great, whereas in the case of Mars and Venus, where large uncertainties exist, acceptable accuracies need not be as great.

Measurement Techniques

In performing the present study emphasis has been placed on the analytical problem and questions of measurement are subsidiary. However, it is desirable that mention be made of possible methods of measuring the position of the target relative to the celestial coordinate system as well as the problem of detecting the target under various viewing conditions.

It is assumed that the angular coordinates of the target are measured to an accuracy of ten seconds of arc for each sighting. For most of the problems simulated it was assumed that about 13 sightings were made per orbit. If the view of the target was blocked by the central body, then that sighting was omitted. Otherwise, the sightings were uniformly spaced.

In all cases the basic coordinate frame is that which is supplied by the catalogued position of the stars. Several types of detection instruments could be used to measure the direction of the target in this frame, e.g. a star tracker or an optical scanner. A review article describing optical scanners and their applications is given by reference [1].

Planetary Constants

The specific technique used in the study of the perturbing parameters depends on the physical constants of the planetary body in question. Tables I, II, and III contain relevant data. The quantities in parentheses behind each number indicate the source.

Table I gives some physical constants for Mars, Venus, Moon, and the Earth. As can be seen from this table, two of the bodies, the Earth and Mars, rotate sufficiently fast to have a measurable flattening which, in turn, permits the computation of the right ascension and declination of their spin axes as well as several terms in the gravitational potential. (As is shown in Table II, this is true even to a greater degree for Jupiter and Saturn.) The other two bodies, the Moon and Venus, are sufficiently close to spherical in shape that a more general representation of their irregular shape is necessary, and further, the gravitational perturbations only weakly define the orientation of the spin axis.

In studying Mars, we utilize the natural satellites, Phobos and/or Deimos. Some of the characteristics of their orbits are shown in Table III.

Table I: Physical Constants for Mars, Venus, Moon, and Earth

Constant	Mars	Venus	Moon	Earth
Ratio of body mass to Earth mass	0.10730 (7)	$.81500362 \pm .123 \times 10^{-5}$ (2)	$1/(81.3004) \pm .0007$ (2)	1.0
Radii (km)	$R_e = 3388 \pm 26$ $18 \leq R_e - R_p \leq 36$ (7)	$R_e = R_p = 6100 \pm 50$ (6)	$R_1 = 1738.549 \pm .061$ $R_2 = 1738.189 \pm .061$ $R_3 = 1737.470 \pm .061$ (9)	$R_e = 6378.15 \pm .05$ $R_p = 6356.63 \pm .05$
Reciprocal Flattening	150 ± 50 (7)	Large (nearly spherical)		$298.30 \pm .05$ (3)
Potential J_2	2.011×10^{-3} (11)		2.07×10^{-4}	$(1082.28 \pm .3) \times 10^{-6}$
J_3			-0.4461×10^{-4}	$(-2.3 \pm .2) \times 10^{-6}$
J_4			-0.2089×10^{-4} (4)	$(-2.12 \pm .5) \times 10^{-6}$
J_5				$(-.2 \pm .1) \times 10^{-6}$
J_6				$(1 \pm .8) \times 10^{-6}$ (3) *or* (9)
Rotational Period	$24^h\ 37^m\ 22.6689^s$ (7)	274 ± 4 days retrograde (6)	27.32166 days (9)	$23^h\ 56^m\ 4^s$
Spin Axis Direction r.a.	$316.55^\circ + .00675^\circ$ (t - 1905)	$272.75^\circ \pm 4^\circ$	$\sim -91^\circ$	undefined
dec.	$52.85^\circ + .00346^\circ$ (t - 1905) (7)	$71.50^\circ \pm 4^\circ$ (6)	$\sim 88.5^\circ$ *	90°

* On page 51 of the American Ephemeris and Nautical Almanac i and Ω' are tabulated. Declination = 90° - i, right ascension = $90^\circ - \Omega'$.

Table II: Physical Constants for Jupiter and Saturn, From [3]

Constant		Jupiter	Saturn
Ratio of Sun's mass to body mass		$1047.355 \pm .065$	$3,500 \pm 3$
Reciprocal Flattening		$15.2 \pm .1$	10.2
Major Radii (km)	R_1	$71,375 \pm 50$	$60,500 \pm 50$
	R_2	$66,680 \pm 50$	$54,550 \pm 50$
Potential	J_2	$.0148 \pm .0001$	$.0161 \pm .00001$
	J_4	$-.00035 \pm .00005$	$-.000865 \pm .000026$

Table III: Constants of Martian Satellites

Constant	Phobos		Deimos	
Mass	--		--	
Diameter (miles)	10	(7)	5	(7)
Characteristics of Orbit				
Orbital Period (days)	0.318910	(5)	1.262441	(5)
Semi-axis (sec at 1 AU)	12.895	(7)	32.389	(7)
Ellipticity	0.0210	(7)	0.0028	(7)
Orbital plane	see ref.	(7)	see ref.	(7)
Regression of ascending node (deg./yr.)	158.5	(7)	6.5	(7)
Mean distance from planet (km)	9.4×10^3	(5)	23.5×10^3	(5)

LIST OF MAJOR SYMBOLS

The following is a list of major symbols used in the sections ANALYTICAL STATEMENT OF THE PROBLEM and METHOD OF SOLUTION.

S_1 = celestial coordinate system

S_3 = inertial coordinate system with $\hat{k}_3$ parallel to planet's axis of symmetry

$R_{1i}(t)$ = coordinate system which is associated with the i^{th} Kepler arc which approximates the spacecraft's orbit for $(i - 1)\,\tau \leq t < i\tau$

$R_{2i}(t)$ = coordinate system which is associated with the i^{th} Kepler arc which approximates the secondary's orbit for $(i - 1)\,\tau \leq t < i\tau$

t = time

τ = fixed time length

ξ_1, ξ_2 = angles which define orientation of S_3 with respect to S_1

$\bar{R}_1(t)$ = position vector of spacecraft

$\bar{R}_2(t)$ = position vector of secondary

$\bar{k}$ = vector of unknown parameters (constants)

$$\bar{X}_j(t) = \begin{pmatrix} \bar{R}_j(t) \\ \dot{\bar{R}}_j(t) \end{pmatrix}, \quad j = 1, 2$$

e = declination of secondary's position as viewed from spacecraft

a = right ascension

$\bar{R}_{1iK}(t)$ = approximate position vector of spacecraft along i^{th} Kepler arc

$\bar{R}_{2iK}(t)$ = approximate position vector of secondary along i^{th} Kepler arc

$\delta\bar{X}_j(t) = \bar{X}_j(t) - \bar{X}_{jiK}(t)$, $(i - 1)\,\tau \leq t < i\tau$

$\tilde{e}$, $\tilde{a}$ = angles which define direction of probe ejection with respect to S_3

r_j, s_j, z_j = components of $\delta\bar{R}_j(t)$ expressed in $R_{ji}(t)$

Δv = ejection speed

In general,

U' = transpose of U

$\dot{} = \frac{d}{dt}$

$\hat{u}$ = implies $\hat{u} \cdot \hat{u} = 1$

δu = error in u

$\sigma(u)$ = standard deviation of a random variable u

ANALYTICAL STATEMENT OF THE PROBLEM

In general, if a second satellite is sighted from a primary satellite, the time-path observed is a function of:

(i) the position and velocity of the primary at $t = 0$,
(ii) the position and velocity of the secondary at $t = 0$.
(iii) the force field in which the two satellites are traveling.

Since the observed time-path is dependent upon these three factors, it may be possible to indirectly measure these factors by making measurements at known discrete times of the secondary's position with respect to the primary's.

Equations of Motion

Since the motions of the primary and secondary satellites are governed by a sixth order system of differential equations, it is possible to write

$$\ddot{\bar{R}}_1(t) = \bar{G}(\bar{R}_1(t), \dot{\bar{R}}_1(t), t, \bar{k}) \qquad (1)$$

$$\ddot{\bar{R}}_2(t) = \bar{G}(\bar{R}_2(t), \dot{\bar{R}}_2(t), t, \bar{k}) \qquad (2)$$

where $\bar{R}_1(t)$ = position of the primary as a function of time,
$\bar{R}_2(t)$ = position of the probe as a function of time, and
$\bar{k}$ = a vector of unknown parameters (constants).

Instead of writing the system of equations as three second-order equations, it is more convenient to consider six first-order equations. To this end, let

$$\bar{X}_i(t) = \begin{pmatrix} \bar{R}_i(t) \\ \dot{\bar{R}}_i(t) \end{pmatrix}, \text{ a } 6 \times 1 \text{ vector, } i = 1, 2.$$

Thus, Equations (1) and (2) may be written

$$\dot{\bar{X}}_i = \bar{F}(\bar{X}_i, t, \bar{k}), \quad i = 1, 2.$$

We will assume that $\bar{F}$ may be written as

$$\bar{F}(\bar{X}, t, \bar{k}) = \bar{F}_K(\bar{X}) + \sum_{j=1}^{n} k_j \bar{P}_j(\bar{X}, t)$$

where $\bar{F}_K$ is the vector which arises from the inverse square force field, and each $\bar{P}_j$ is a known function of its argument. Hence, (1) and (2) take the form

$$\ddot{\bar{X}}_i = \bar{F}_K(\bar{X}_i) + \sum_{j=1}^{n} k_j \bar{P}_j(\bar{X}_i, t), \quad i = 1, 2. \tag{3}$$

Constraint Equation

If measurements of the position of the secondary with respect to the primary are taken, these measurements imply a constraint on the motion of the two satellites. In this report, we will assume the measured quantities are the right ascension and declination of the vector from the primary to the secondary at known discrete times. That is,

$$\bar{R}_2(t_p) - \bar{R}_1(t_p) = \mu(\cos e \cos a\, \hat{i}_1 + \cos e \sin a\, \hat{j}_1 + \sin e\, \hat{k}_1) \tag{4}$$

where $\mu = |\bar{R}_2(t_p) - \bar{R}_1(t_p)|$

e = declination of $\bar{R}_2 - \bar{R}_1$ (measured)

a = right ascension of $\bar{R}_2 - \bar{R}_1$ (measured)

$\hat{i}_1, \hat{j}_1, \hat{k}_1$ = unit vectors associated with the celestial coordinate system. $\hat{i}_1$ in the celestial equatorial plane and in the direction of the first point of Aries. $\hat{k}_1$ in the direction of the North Pole, $\hat{j}_1$ completes the right-handed coordinate system.

Equation (4) requires that $\bar{R}_2 - \bar{R}_1$ be written with components in the celestial coordinate system (we will denote this system as S_1). However, this coordinate system may not be convenient when considering the equations of motion (3). In order to minimize n in (3), a new coordinate system is chosen with one axis parallel to the planet's principal axis of largest moment of inertia. Two angles, ξ_1 and ξ_2, are required to define the orientation of this new system, S_3, with respect to the celestial system S_1. Hence,

$\hat{i}_1 \rightarrow \hat{i}_2$ rotation $\xi_1 + 90^\circ$ about $\hat{k}_1 = \hat{k}_2$

$\hat{k}_2 \rightarrow \hat{k}_3$ rotation ξ_2 about $\hat{i}_2 = \hat{i}_3$.

Now, ξ_1 = the right ascension of the planet's principal axis of largest moment of inertia,

ξ_2 = the co-declination of this axis.

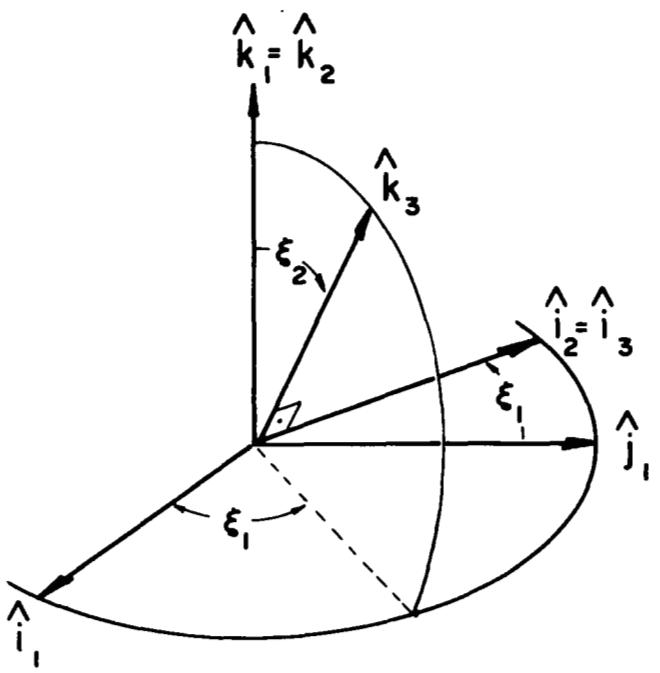

Figure 2: The angles ξ_1 and ξ_2

Generally, we will choose to write the equation of motion with components in S_3. Now,

$$\begin{pmatrix} \hat{i}_1 \\ \hat{j}_1 \\ \hat{k}_1 \end{pmatrix} = A \begin{pmatrix} \hat{i}_3 \\ \hat{j}_3 \\ \hat{k}_3 \end{pmatrix}$$

where

$$A = \begin{pmatrix} -\sin\xi_1 & -\cos\xi_1\cos\xi_2 & \cos\xi_1\sin\xi_2 \\ \cos\xi_1 & -\sin\xi_1\cos\xi_2 & \sin\xi_1\sin\xi_2 \\ 0 & \sin\xi_2 & \cos\xi_2 \end{pmatrix}$$

Hence, (4) becomes

$$\hat{d}(t_p) = \frac{1}{\mu} A \bar{x}(t_p) \tag{5}$$

where

$$\hat{d}(t_p) = \begin{pmatrix} \cos e \cos a \\ \cos e \sin a \\ \sin e \end{pmatrix}_{t_p}$$

$$\bar{x} = \bar{R}_2(t_p) - \bar{R}_1(t_p)$$
$$= x_1 \hat{i}_3 + x_2 \hat{j}_3 + x_3 \hat{k}_3$$

$$\mu = \sqrt{x_1^2 + x_2^2 + x_3^2} \quad .$$

Equation (5) then is the basic constraint equation implied by the measurements. This equation yields two independent relations which constrain $\bar{x}(t_p)$.

The Problem

The problem may now be stated as follows: Find initial conditions $\bar{X}_1(0)$, $\bar{X}_2(0)$, and force field parameters k_j, $j = 1, 2, \ldots, n$, which imply $\bar{X}_1(t)$ and $\bar{X}_2(t)$ as solutions to (3) such that $\bar{X}_1(t)$ and $\bar{X}_2(t)$ satisfy (5) at the discrete times t_p.

In some cases, the angles ξ_1 and ξ_2 must also be treated as unknowns. This is particularly true for the case of orbits about Venus. Also, if the secondary satellite is an ejected probe, then $\bar{R}_1 = \bar{R}_2$ at the time of ejection.

A complication to the analytical problem is that the number of measurements is expected to be much greater than the number of unknowns. Hence, because of various errors, no $\bar{X}_1(0)$, $\bar{X}_2(0)$, and $\bar{k}$ will exist such that all constraint equations (5) can be satisfied. Thus, some "best" value of the unknowns must be found.

METHOD OF SOLUTION

There are many methods of attacking the formulated problem, but we will discuss only one particular approach. The basic technique makes use of a linearization of the equations of motion and the constraint equation. The linear equations are then solved to yield improved values of the unknowns. An iterative computational procedure and an initial guess are required. Linearization of the constraint equation is as follows:

The total differential of (5) yields

$$\delta\hat{d} = \frac{1}{\mu} A[\delta\bar{x} - \frac{\bar{x}}{\mu}\delta\mu] + \frac{1}{\mu}\delta A\,\bar{x} \;;$$

but, $\mu\delta\mu = \bar{x} \cdot \delta\bar{x}$, since $\mu^2 = \bar{x} \cdot \bar{x}$.

So, $$\mu\delta\hat{d} = A[\delta\bar{x} - \frac{\bar{x} \cdot \delta\bar{x}}{\mu^2}\bar{x}] + \delta A\,\bar{x}$$

where

$$\delta\hat{d} = \begin{pmatrix} -\cos e \sin a\,\delta a & -\sin e \cos a\,\delta e \\ \cos e \cos a\,\delta a & -\sin e \sin a\,\delta e \\ & \cos e\,\delta e \end{pmatrix} .$$

So, $$\mu\delta a \cos e = (-\sin a\,A_1 + \cos a\,A_2)[\delta\bar{x} - \frac{\bar{x} \cdot \delta\bar{x}}{\mu^2}\bar{x}] + (-\sin a\,\delta A_1 + \cos a \cdot \delta A_2)\,\bar{x}$$

where $A_k = k^{th}$ row of A,
$\delta A_k = k^{th}$ row of δA.

Also,

$$\mu\delta e \cos e = A_3[\delta\bar{x} - \frac{\bar{x} \cdot \delta\bar{x}}{\mu^2}\bar{x}] + \delta A_3\,\bar{x}.$$

But,

$$\delta\bar{x} - \frac{\bar{x} \cdot \delta\bar{x}}{\mu^2}\bar{x} = \frac{1}{\mu^2}\begin{pmatrix} \mu^2 - x_1^2 & -x_1x_2 & -x_1x_3 \\ -x_1x_2 & \mu^2 - x_2^2 & -x_2x_3 \\ -x_1x_3 & -x_2x_3 & \mu^2 - x_3^2 \end{pmatrix}\delta\bar{x}$$

$$\delta A = \begin{pmatrix} -A_2 \\ A_1 \\ 0 \end{pmatrix}\delta\xi_1 + (0, A^3, -A^2)\,\delta\xi_2$$

where $A^k = k^{th}$ column of A.

Hence,

$$\begin{pmatrix} \delta a \cos e \\ \delta e \end{pmatrix} = E\,\delta\bar{x}(t_p) + F\begin{pmatrix} \delta\xi_1 \\ \delta\xi_2 \end{pmatrix} \qquad (6)$$

where

$$\mu^3 E = \begin{pmatrix} \cos(\xi_1 - a) & -\sin(\xi_1 - a)\cos\xi_2 & \sin(\xi_1 - a)\sin\xi_2 \\ 0 & \sin\xi_2 \sec e & \cos\xi_2 \sec e \end{pmatrix} \times \begin{pmatrix} \mu^2 - x_1^2 & -x_1x_2 & -x_1x_3 \\ -x_1x_2 & \mu^2 - x_2^2 & -x_2x_3 \\ -x_1x_3 & -x_2x_3 & \mu^2 - x_3^2 \end{pmatrix}$$

$$\mu F = \begin{pmatrix} \mu_1 & \mu_2 \\ 0 & \mu_4 \end{pmatrix}.$$

Here,

$$\mu_1 = -\sin(\xi_1 - a)\,x_1 - \cos(\xi_1 - a)\cos\xi_2\,x_2 + \cos(\xi_1 - a)\sin\xi_2\,x_3,$$

$$\mu_2 = \sin(\xi_1 - a)(\sin\xi_2\,x_2 + \cos\xi_2\,x_3),$$

$$\mu_4 = \sec e(\cos\xi_2\,x_2 - \sin\xi_2\,x_3).$$

Equation (6) is two independent relations in δa, δe, $\delta\xi_1$, $\delta\xi_2$, and $\delta\bar{x}(t_p) = \delta\bar{R}_2(t_p) - \delta\bar{R}_1(t_p)$.

Linearization of the Equations of Motion

For the present, let us drop the subscript i from Equation (3). Now let

$$\bar{X}(t) = \bar{X}_K(t) + \delta\bar{X}(t) \tag{7}$$
$$\bar{k} = \bar{k}_o + \delta\bar{k}$$

where $\bar{X}_K(t)$ is a reference trajectory (known) of possibly unconnected Kepler arcs. Thus,

$$\dot{\bar{X}}_K = \bar{F}_K(\bar{X}_K)$$

except for a finite set of points. Substituting (7) into (3) we obtain

$$\dot{\delta\bar{X}} = \nabla\bar{F}_K(\bar{X}_K)\ \delta\bar{X} + \ldots + \sum_{j=1}^{n} k_j(\bar{P}_j(\bar{X}_K, t) + \nabla\bar{P}_j(\bar{X}_K, t)\ \delta\bar{X} + \ldots)$$
$$\doteq \nabla\bar{F}_K(\bar{X}_K)\ \delta X + \sum_{j=1}^{n} (k_{o_j} + \delta k_j)\ \bar{P}_j(\bar{X}_K, t). \tag{8}$$

Thus, to a first approximation, $\delta\bar{X}$ satisfies a linear non-homogeneous differential equation. We may now write the solution to (8) as (Coddington and Levinson [8])

$$\delta\bar{X}(t) = \Phi(t, t_o)\left[\delta\bar{X}(t_o) + \int_{t_o}^{t} \Phi^{-1}(s, t) \sum_{j=1}^{n} k_j\ \bar{P}_j(\bar{X}_K(s), s)ds\right] \tag{9}$$

where

$$\dot{\Phi} = \nabla\bar{F}_K(\bar{X}_K)\ \Phi \text{ and } \Phi(t_o, t_o) = I.$$

The matrix Φ in (9) is commonly called the transition matrix in the terminology of orbital theory. It is the fundamental solution matrix of (8) in the terminology of differential equation theory.

An explicit solution of Φ is given by Kochi [10]. To utilize his solution the components of $\delta\bar{X}(t_o)$ and $\delta\bar{X}(t)$ must be expressed in preferred coordinate

systems. This point will be considered next. In any event, (9) gives a simple method of calculating an approximation to the deviation from a single Kepler orbit given $\delta\bar{X}(t_o)$ and $\bar{k}$.

In deriving an explicit expression for Φ, Kochi introduced a coordinate we will call R(t) which moves with the Kepler reference position $\bar{R}_K(t)$. Let R(t) have associated unit vectors $\hat{r}$, $\hat{s}$, $\hat{z}$ such that $\hat{r} = \bar{R}_K(t) / |\bar{R}_K(t)|$, $\hat{s}$ is in the plane of the Kepler orbit so that $\dot{\bar{R}}_K(t) \cdot \hat{s} \geq 0$, and $\hat{z}$ completes the right-handed system as shown in Figure 3.

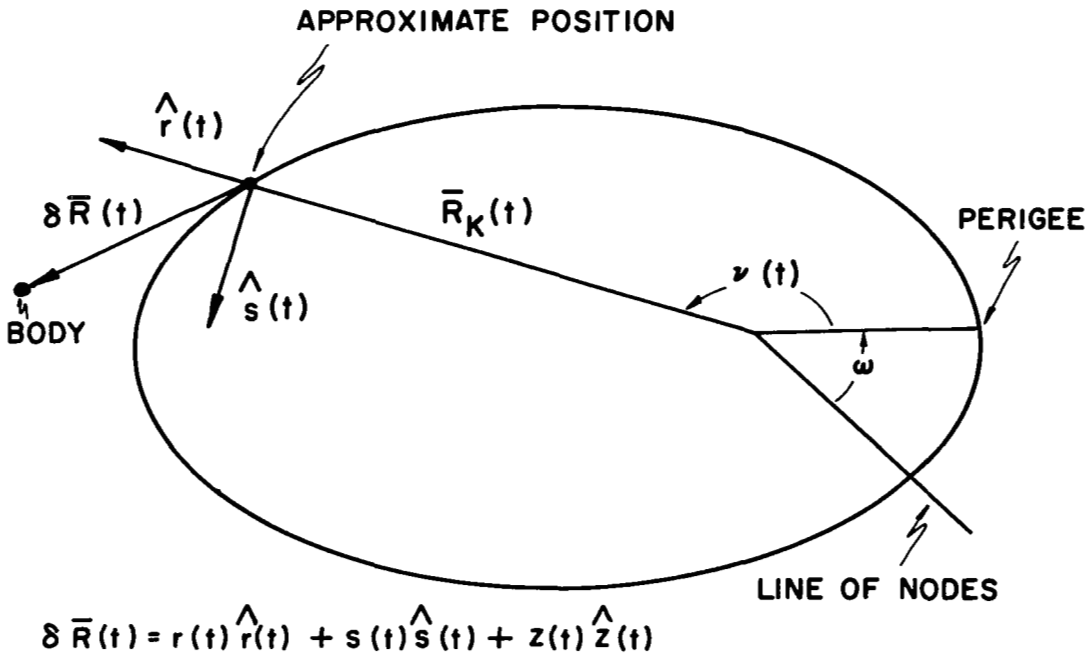

Figure 3: The Moving Coordinate System R(t)

With this definition, we may write

$$\begin{pmatrix} \hat{i}_3 \\ \hat{j}_3 \\ \hat{k}_3 \end{pmatrix} = B(t) \begin{pmatrix} \hat{r} \\ \hat{s} \\ \hat{z} \end{pmatrix}$$

where

$$B(t) = \begin{pmatrix} c\Omega\ c\omega' - s\Omega\ ci\ s\omega' & -c\Omega\ s\omega' - s\Omega\ ci\ c\omega' & s\Omega\ si \\ s\Omega\ c\omega' + c\Omega\ ci\ s\omega' & -s\Omega\ s\omega' + c\Omega\ ci\ c\omega' & -c\Omega\ si \\ si\ s\omega' & si\ c\omega' & ci \end{pmatrix}$$

where $c\theta = \cos\theta$

$s\theta = \sin\theta$

i = inclination of Kepler orbit

Ω = longitude of line of nodes

ω = argument of perigee

$\omega' = \omega + \nu(t)$

where

$\nu(t)$ = true anomaly.

Since we will use Φ as developed by Kochi, in (9) $\delta\overline{X}(t_o)$ must have position and velocity components expressed in $R(t_o)$ while $\delta\overline{X}(t)$ must have these components expressed in $R(t)$.

Since the perturbing forces $k_j\overline{P}_j$ are to be computed along the reference orbit, no single Kepler orbit can be expected to yield accurate results. We shall choose discontinuous arcs of Kepler orbits as a reference orbit as shown in Figure 4. Each arc is of time duration, τ.

In general, we have for $(i - 1)\tau \leq t < i\tau$

$$\delta\overline{X}(t) = \Phi_i(t, (i - 1)\tau)\left[\delta\overline{X}((i - 1)\tau) + \sum_{j=1}^{n} (k_{o\,j} + \delta k_j)\,\overline{F}_{ij}(t)\right]$$

where $\overline{X}_{iK}(t)$ is the position and velocity along the i Kepler arc,

Φ_i is evaluated using this arc as a reference.

$$\overline{F}_{ij}(t) = \int_{(i-1)\tau}^{t} \Phi_i^{-1}(s, (i - 1)\tau)\,\overline{P}_j(\overline{X}_{iK}(s), s)\,ds$$

$\delta\overline{X}((i - 1)\tau)$ must have components in $R_i((i - 1)\tau)$

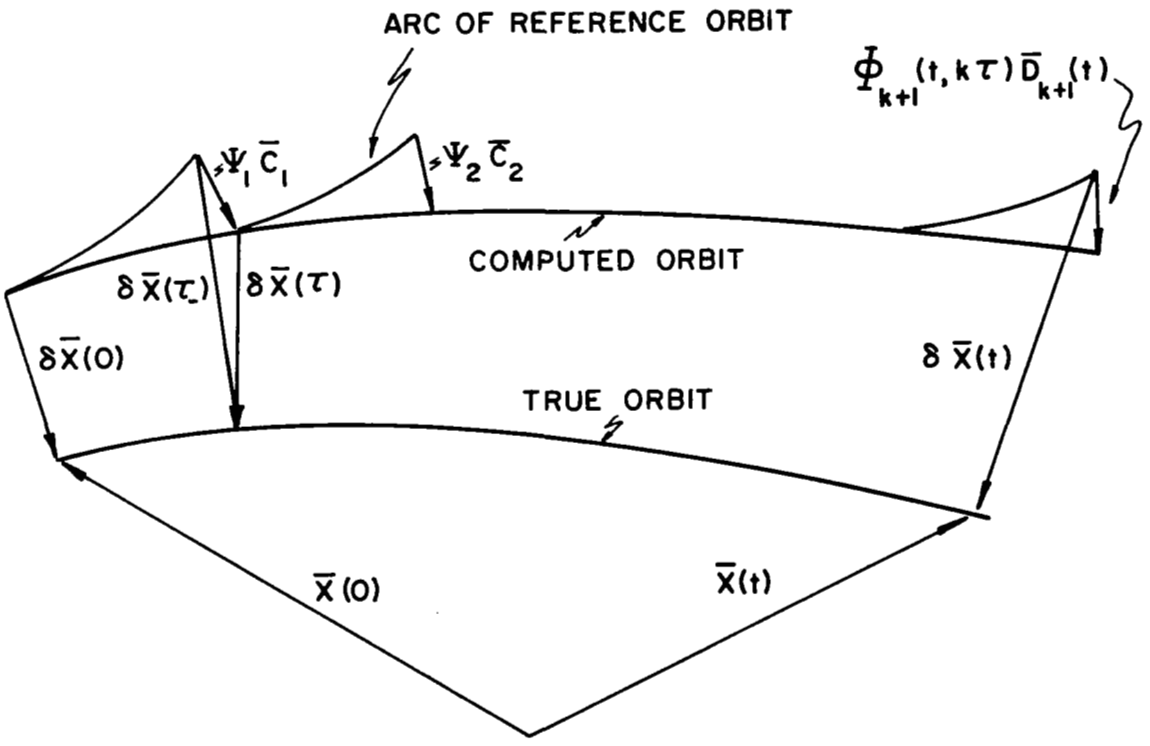

Figure 4: The True Orbit, Reference Orbit, and Computed Orbit

$\bar{P}_j(X_{iK}(s), s)$ must have components in $R_i(s)$

$\delta\bar{X}(t)$ must have components in $R_i(t)$.

But we will choose to define $\delta\bar{X}(i\tau)$ so that.

$$\delta\bar{X}(i\tau) = \psi_i\left[\delta\bar{X}((i-1)\tau) + \sum_{j=1}^{n} \delta k_j \bar{E}_{ij}\right]$$

where $\psi_i = \Phi_i(i\tau, (i-1)\tau)$

$\bar{E}_{ij} = \bar{F}_{ij}(i\tau)$.

Thus, to generate the i + 1 Kepler arc, we use the conditions

$$\bar{X}_{i+1,K}(i\tau) = \bar{X}_{iK}(i\tau) + \sum_{j=1}^{n} k_{oj} \begin{pmatrix} B_i(i\tau) & 0 \\ 0 & B_i(i\tau) \end{pmatrix} \psi_i \bar{E}_{ij} \qquad (10)$$

In (10) $\bar{X}_{iK}$ and $\bar{X}_{i+1,K}$ must be expressed with components in S_3. After computing $\bar{X}_{i+1,K}(i\tau)$, we may find the orbital elements of the $i+1^{th}$ Kepler arc, and hence $\Phi_{i+1}(t, i\tau)$. So, for $i\tau \le t < (i+1)\tau$,

$$\delta\bar{X}(t) = \Phi_{i+1}(t, i\tau)\left[\delta\bar{X}(i\tau) + \sum_{j=1}^{n} k_j \bar{F}_{i+1,j}(t)\right]$$

$$\delta\bar{X}(t) = \Phi_{i+1}(t, i\tau)\left[\begin{pmatrix} B'_{i+1}(i\tau)\, B_i(i\tau) & 0 \\ 0 & B'_{i+1}(i\tau)\, B_i(i\tau) \end{pmatrix} \psi_i \right.$$
$$\left. \times \left[\delta\bar{X}(i-1)\tau) + \sum_{j=1}^{n} \delta k_j \bar{E}_{ij}\right] + \sum_{j=1}^{n} k_j \bar{F}_{i+1,j}(t)\right]$$

the matrix $B'_{i+1}(i\tau)\, B_i(i\tau)$ differs from the 3 x 3 identity matrix, but its effect is second order. Hence, for $i\tau \le t < (i+1)\tau$

$$\delta\bar{X}(t) = \Phi_{i+1}(t, i\tau)\left[M_i \delta\bar{X}(0) + \sum_{j=1}^{n} \delta k_j (\bar{V}_{ij} + \bar{F}_{i+1,j}(t)) + \sum_{j=1}^{n} k_{oj} \bar{F}_{i+1,j}(t)\right]$$

$i\tau \le t < (i+1)\tau$

$$\delta\bar{X}((i+1)\tau) = M_{i+1}\, \delta\bar{X}(0) + \sum_{j=1}^{n} \delta k_j \bar{V}_{i+1,j} \qquad (11)$$

where

$$\bar{V}_{ij} = \psi_i \bar{E}_{ij} + \psi_i \psi_{i-1} \bar{E}_{i-1,j} + \cdots + \psi_i \psi_{i-1} \cdots \psi_1 \bar{E}_{1j}$$
$$M_i = \psi_i \psi_{i-1} \cdots \psi_1.$$

So that,

$$\bar{V}_{i+1,j} = \psi_{i+1}(\bar{E}_{i+1,j} + \bar{V}_{ij})$$

$$M_{i+1} = \psi_{i+1} M_i .$$

Equation (11) thus gives us the deviation in position and velocity of the reference position and velocity from the time quantities at t, $i\tau \leq t < (i+1)\tau$, in terms of these deviations at t = 0, $\bar{k}_o$, and $\delta\bar{k}$. In this equation $\delta\bar{X}(t)$ has components in $R_{i+1}(t)$.

Linear Equation in Unknowns

Equation (6) is two independent equations expressing a relationship between errors in the measured direction to the secondary satellite, errors in the two angles which define the planetary coordinate system with respect to the celestial coordinate system, and errors in the position of the secondary with respect to the primary. This equation is useless in itself, for if errors in the measured quantities are specified (δa and δe) the equations contain more unknowns than independent relations. The dynamics of the problem, however, do not allow the vectors $\delta\bar{R}_1$ to move at random. In fact, if $\delta\bar{R}_i(0)$, $\delta\dot{\bar{R}}_i(0)$, and $\bar{k}$ are specified, then $\delta\bar{R}_i(t)$ and $\delta\dot{\bar{R}}_i(t)$ are determined for all time, t. This dependence is analytically stated by Equation (11). In this section, we will utilize Equations (6) and (11) to obtain a relationship between δa, δe, $\delta\xi_1$, $\delta\xi_2$, $\delta\bar{k}$, $\delta\bar{X}_1(0)$ and $\delta\bar{X}_2(0)$.

A trivial transformation yields

$$\delta\bar{R}_i(t) = K\,\delta\bar{X}_i(t)$$

where K = (I, 0), I being the 3 x 3 identity; 0 being the 3 x 3 zero. So, (6) becomes

$$\begin{pmatrix} \delta a \\ \cos e\,\delta e \end{pmatrix} = E\,K(\delta\bar{X}_2(t_p) - \delta\bar{X}_1(t_p)) + F\begin{pmatrix} \delta\xi_1 \\ \delta\xi_2 \end{pmatrix} .$$

In the above equation $\delta\bar{X}_2$ and $\delta\bar{X}_1$ must have components in S_3. In order to utilize this equation, it is necessary to rewrite it so that $\delta\bar{X}_2(t_p)$ has components in $R_{2i}(t_p)$ while $\delta\bar{X}_1(t_p)$ has components in $R_{1i}(t_p)$, where

$$(i - 1)\,\tau \leq t_p < i\tau.$$

Hence,

$$\begin{pmatrix} \delta a \\ \delta e \end{pmatrix}_{\cos e} = E(B_{2i}(t_p)\ K\ \delta\bar{X}_2(t_p) - B_{1i}(t_p)\ K\ \delta\bar{X}_1(t_p)) + F\begin{pmatrix} \delta\xi_1 \\ \delta\xi_2 \end{pmatrix}$$

So, Equation (11) yields

$$-D_2 + D_1 + \begin{pmatrix} \delta a \\ \delta e \end{pmatrix}_{\cos e} = (\mathcal{U}_2, -\mathcal{U}_1, \mathcal{V}_{21} - \mathcal{V}_{11}, \mathcal{V}_{22} - \mathcal{V}_{12}, \ldots \mathcal{V}_{2n} - \mathcal{V}_{1n}, F) \times \delta\bar{Y}(0) \qquad (12)$$

where $D_2 = E\ B_{2i}\ K\ \Phi_{2i}\ (t, i\tau) \sum_{j=1}^{n} k_{o_j}\ \bar{E}_{2,i,j}(t_p)$

$$D_1 = E\ B_{1i}\ K\ \Phi_{1i}\ (t, i\tau) \sum_{j=1}^{n} k_{o_j}\ \bar{E}_{1,i,j}(t_p)$$

$$\mathcal{U}_2 = E\ B_{2i}(t_p)\ K\ \Phi_{2i}(t_p, (i - 1)\tau)\ M_{2,\,i-1}$$

$$\mathcal{U}_1 = E\ B_{1i}(t_p)\ K\ \Phi_{1i}(t_p, (i - 1)\tau)\ M_{1,\,i-1}$$

$$\mathcal{V}_{2j} = E\ B_{2i}(t_p)\ K\ \Phi_{2i}\ (t_p, (i - 1)\ \tau)\ (\bar{V}_{2,\,i-1,\,j} + \bar{F}_{2,\,i,\,j}(t_p))$$

$$\mathcal{V}_{1j} = E\ B_{1i}\ (t_p) K\ \Phi_{1i}\ (t_p, (i - 1)\ \tau)\ (\bar{V}_{1,\,i-1,\,j} + \bar{F}_{1,\,i,\,j}(t_p))$$

$$\delta\bar{Y}(0) = \begin{pmatrix} \delta\bar{X}_2(0) \\ \delta\bar{X}_1(0) \\ \delta\bar{k} \\ \delta\xi_1 \\ \delta\xi_2 \end{pmatrix}, \text{ a } (14 + n) \times 1 \text{ vector.}$$

Thus, (12) is two equations in $\delta\bar{Y}(0)$. If a sufficiently large number of measurements are specified we may solve for $\delta\bar{Y}(0)$. After finding this vector $\delta\bar{X}_2(t)$ and $\delta\bar{X}_1(t)$ may be found from (11). Since (12) is only an approximate equation, an iterative computational process is necessary.

Let us now suppose the secondary satellite is a probe which was ejected from the primary with a known speed but poorly known direction at $t = 0$. Then,

$$\bar{R}_2(0) = \bar{R}_1(0) \ ,$$

and

$$\dot{\bar{R}}_2(0) = \dot{\bar{R}}_1(0) + \Delta v \ \hat{u}$$

where Δv = speed of ejection (assumed known) and $\hat{u}$ defines the ejection direction. We may choose the reference trajectories so that

$$\bar{R}_{21K}(0) = \bar{R}_{11K}(0)$$

$$\dot{\bar{R}}_{21K}(0) = \dot{\bar{R}}_{11K}(0) + \Delta v \ \hat{u}_o \text{, where } \hat{u}_o \text{ is an estimate of } \hat{u}.$$

So, $\delta\bar{X}_2(0) = \delta\bar{X}_1(0) + \Delta v \begin{pmatrix} 0 \\ \delta\hat{u} \end{pmatrix}$.

Now let $\hat{u} = \cos\tilde{e}\cos\tilde{a}\,\hat{i}_3 + \cos\tilde{e}\sin\tilde{a}\,\hat{j}_3 + \sin\tilde{e}\,\hat{k}_3$. Thus,

$$\delta\bar{X}_2(0) = \delta\bar{X}_1(0) + \begin{pmatrix} 0 \\ 0 \\ 0 \\ Q \begin{pmatrix} \cos\tilde{e}\,\delta\tilde{a} \\ \delta\tilde{e} \end{pmatrix} \end{pmatrix}. \qquad (13)$$

where

$$Q = \Delta v \begin{pmatrix} -\sin\tilde{a} & -\sin\tilde{e}\cos\tilde{a} \\ \cos\tilde{a} & -\sin\tilde{e}\sin\tilde{a} \\ 0 & \cos\tilde{e} \end{pmatrix}$$

and the components of $\delta\bar{X}_2(0)$ and $\delta\bar{X}_1(0)$ are in S_3.

In (12), $\delta\bar{X}_2(0)$ has components in $R_{21}(0)$ while $\delta\bar{X}_1(0)$ has components in $\bar{R}_{11}(0)$; (13) cannot be substituted into (12) without rewriting (12) such that $\delta\bar{X}_2(0)$ and $\delta\bar{X}_1(0)$ have components in the same coordinate system. To this end, let us rewrite (12) so that $\delta\bar{X}_2(0)$ and $\delta\bar{X}_1(0)$ have components in S_3. Hence,

$$-D_2 + D_1 + \begin{pmatrix} \delta a \cos e \\ \delta e \end{pmatrix} = (\mathcal{W}_2, -\mathcal{W}_1, \mathcal{V}_{21} - \mathcal{V}_{11}, \ldots, \mathcal{V}_{2n} - \mathcal{V}_{1n}, F)\ \delta\bar{Y}(0) \quad (14)$$

where

$$\mathcal{W}_2 = \mathcal{U}_2 \begin{pmatrix} B'_{21}(0) & 0 \\ 0 & B'_{21}(0) \end{pmatrix} \qquad (2 \times 6) \text{ matrix}$$

$$\mathcal{W}_1 = \mathcal{U}_1 \begin{pmatrix} B'_{11}(0) & 0 \\ 0 & B'_{11}(0) \end{pmatrix} \qquad (2 \times 6) \text{ matrix}$$

and $\delta\bar{X}_2(0)$ and $\delta\bar{X}_1(0)$ have components in S_3. Hence, (13) allows us to rewrite (14) as

$$-D_2 + D_1 + \begin{pmatrix} \delta a \cos e \\ \delta e \end{pmatrix}$$

$$= (\mathcal{W}_2 - \mathcal{W}_1, \mathcal{V}_{21} - \mathcal{V}_{11}, \ldots, \mathcal{V}_{2n} - \mathcal{V}_{1n}, F, \beta_2 Q) \begin{pmatrix} \delta\bar{X}_1(0) \\ \delta\bar{k} \\ \delta\xi_1 \\ \delta\xi_2 \end{pmatrix}$$

where β_2 is a 2 x 3 matrix defined by the last three columns of $\mathcal{W}_2$.

Other cases may be considered. For example, $\Delta\bar{v}$ unknown; Δv unknown; the time of ejection unknown; etc.

Summary of Equations

We now list the equations as developed in the previous sections.

1. We are given
   (a) $\bar{X}_1(0)$ and $\bar{X}_2(0)$ in S_3
   (b) $k_{01}, k_{02}, \ldots, k_{0n}$
   (c) $\bar{P}_1, \bar{P}_2, \ldots, \bar{P}_n$ as a function of spherical coordinates and with components in R(t) (for both trajectories)
   (d) times of observation t_k, k = 1, 2, ..., f
   (e) ξ_1, ξ_2
   (f) τ
   (g)
$$A = \begin{pmatrix} -\sin\xi_1 & -\cos\xi_1\cos\xi_2 & \cos\xi_1\sin\xi_2 \\ \cos\xi_1 & -\sin\xi_1\cos\xi_2 & \sin\xi_1\sin\xi_2 \\ 0 & \sin\xi_2 & \cos\xi_2 \end{pmatrix}$$

2. $M_{10} = M_{20} = I$ (6 x 6), $\bar{V}_{10j} = \bar{V}_{20j} = 0$ (6 x 1)

3. $\bar{X}((i-1)\tau) = \bar{X}_{iK}((i-1)\tau)$ (for both trajectories in S_3)

4. Find orbital elements

5. If $t_k \geq i\tau$
   (a) $\psi_i = \Phi_i(i\tau, (i-1)\tau)$
   (b) $M_i = \psi_i M_{i-1}$
   (c) $\bar{E}_{ij} = \bar{F}_{ij}(i\tau) = \int_{(i-1)\tau}^{i\tau} \Phi_i^{-1}(s, (i-1)\tau)\, \bar{P}_{ij}(s)\, ds$
   (d) $\bar{V}_{ij} = \psi_i(\bar{E}_{ij} + \bar{V}_{i-1,j})$
   (e) $\bar{C}_i = \sum_{j=1}^{n} k_{0j}\, \psi_i\, \bar{E}_{ij}$
   (f)
$$\bar{X}_{i+1,K}(i\tau) = \begin{pmatrix} B_i(i\tau) & 0 \\ 0 & B_i(i\tau) \end{pmatrix} (\bar{X}_{iK}(i(\tau)) + \bar{C}_i) \quad \text{in } S_3$$
   (g) $i \rightarrow i + 1$

6. If $t_k < i\tau$, we obtain two linear equations in the unknowns.
Use i Kepler arc to compute

(a) mean anomaly at t_k

(b) true anomaly

(c) $$r_j = \frac{a_j(1 - e_j^2)}{1 + e_j \cos \nu_j} = \frac{p_j}{1 + e_j \cos \nu_j}$$

(d) In S_3

$$\bar{R}_{jiK}(t_k) = B_{ji}(t_k) \begin{pmatrix} r_j \\ 0 \\ 0 \end{pmatrix} \quad j = 1, 2$$

(e) $$\bar{x}(t_k) = x_1(t_k)\, \hat{i}_3 + x_2(t_k)\, \hat{j}_3 + x_3(t_k)\, \hat{k}_3$$
$$= \bar{R}_{2iK}(t_k) - \bar{R}_{1iK}(t_k)$$

(f) $$\mu = |\bar{x}|$$

(g) $$\begin{pmatrix} \cos e \cos a \\ \cos e \sin a \\ \sin a \end{pmatrix} = \frac{1}{\mu} A\, \bar{x}, \text{ determines } \sin e, \cos e, \sin a, \cos a$$

(h) $$E = \begin{pmatrix} \cos(\xi_1 - a) & -\sin(\xi_1 - a)\cos \xi_2, & \sin(\xi_1 - a)\sin \xi_2 \\ 0 & \frac{\sin \xi_2}{\cos e} & \frac{\cos \xi_2}{\cos e} \end{pmatrix}$$

$$x \frac{1}{\mu^3} \begin{pmatrix} \mu^2 - x_1^2 & -x_1x_2 & -x_1x_3 \\ -x_1x_2 & \mu^2 - x_2^2 & -x_2x_3 \\ -x_1x_3 & -x_2x_3 & \mu^2 - x_3^2 \end{pmatrix}$$

$$F = \frac{1}{\mu} \begin{pmatrix} \mu_1 & \mu_2 \\ 0 & \mu_4 \end{pmatrix}$$

$$\mu_1 = -\sin(\xi_1 - a)\, x_1 - \cos(\xi_1 - a) \cos \xi_2\, x_2 + \cos(\xi_1 - a) \sin \xi_2 x_3$$

$$\mu_2 = \sin(\xi_1 - a) \sin \xi_2 x_2 + \sin(\xi_1 - a) \cos \xi_2 x_3$$

$$\mu_4 = \frac{\cos \xi_2}{\cos e}\, x_2 - \frac{\sin \xi_2}{\cos e}\, x_3$$

(i) $$\bar{F}_{ij}(t_k) = \int_{(i-1)\tau}^{t_k} \Phi_i^{-1}(s, (i-1)\tau)\, \bar{P}_{ij}(s)\, ds$$

$$j = 1, 2, \ldots, n$$

$$\mathcal{U} = E\, B_i(t_k) K\, \Phi_i(t_k, (i-1)\tau)\, M_{i-1}$$

$$\mathcal{V}_j = E\, B_i(t_k) K\, \Phi_i(t_k, (i-1)\tau)(\bar{V}_{i-1,j} + \bar{F}_{i,j}(t_k))$$

(j) $$A_k = (\mathcal{U}_2, -\mathcal{U}_1, \mathcal{V}_{21} - \mathcal{V}_{11}, \mathcal{V}_{22} - \mathcal{V}_{12}, \ldots, \mathcal{V}_{2n} - \mathcal{V}_{1n}, F)$$

7. $$a = \begin{pmatrix} A_1 \\ A_2 \\ \cdot \\ \cdot \\ \cdot \\ A_k \end{pmatrix} \qquad 2k \times (14 + n)$$

8. After all measurements the covariance matrix of the output errors is given by

$$E(\delta Y^T(0)\ \delta Y(0)) = \sigma^2 (a^T a)^{-1}.$$

PERTURBING FORCES

In this study, the only perturbing forces acting on orbits about Mars, Venus, and the moon for which numerical results will be shown are those which arise from higher order terms in a gravitation potential. Let us now give a short discussion of the gravitation potential.

Let (X, Y, Z) be an arbitrary set of right-handed orthogonal axis, and let (r, ϕ, θ) be the spherical coordinates of a point, P, external to a body whose density is sectionally continuous (Figure 5).

The potential of a unit mass at P due to the body may be written as

$$V(r, \phi, \theta) = -G \iiint_B \frac{D(\bar{P}')\, dv}{|\bar{P}' - \bar{P}|} \qquad (15)$$

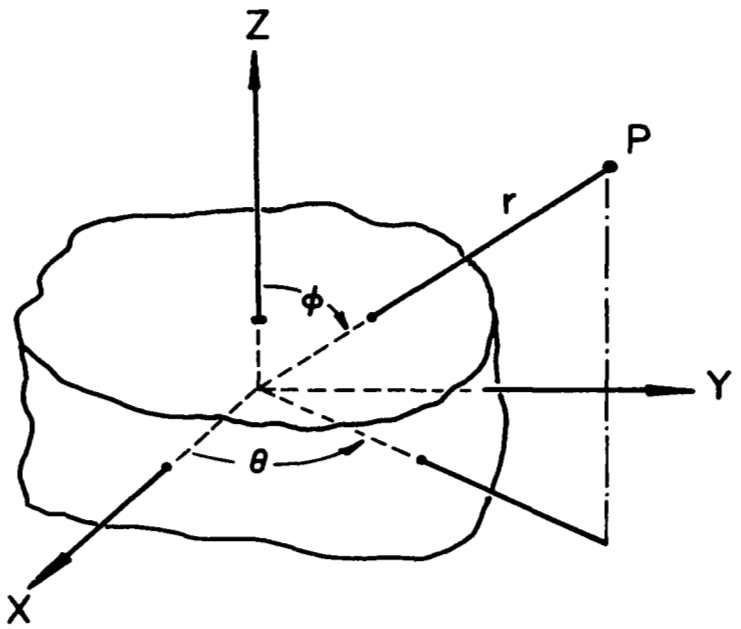

Figure 5: The Body and External Point, P

where B = region occupied by the body

$\bar{P}'$ = generic position within the body

$\bar{P}$ = position of external point, P

G = universal gravitational constant

$D(\bar{P}')$ = density of body at $\bar{P}'$

dv = element of volume of $\bar{P}'$.

Now, $-\nabla V$= the gravitational force on a unit mass at P due to the body.

It would be most convenient if the integrand of (15) could be written as $f(\bar{P}')\, g(\bar{P})$; for if this were the case, then,

$$V(r, \phi, \theta) = -G\, g(\bar{P}) \iiint_B f(\bar{P}')\, dv$$

$$= G_1\, g(\bar{P}),$$

where G_1 is a constant which depends only on the shape and mass distribution of the body. Hence, the force on a unit mass would be known except for a single

multiplicative constant. Unfortunately, the integrand of (15) cannot be written so simply, instead we must write it in the form

$$\sum_{i=1}^{\infty} f_i(\bar{P}')\, g_i(\bar{P}) \ .$$

So,

$$V(r, \phi, \theta) = \sum_{i=1}^{\infty} G_i\, g_i(\bar{P}) \tag{16}$$

where each G_i is independent of $\bar{P}$ and dependent only on the shape and mass distribution of the body. The exact form of (16) may be found in [9], and can be written as

$$V(r, \phi, \theta) = -\frac{Gm}{r}\left[1 + \sum_{n=1}^{\infty}\sum_{m=0}^{n}\left(\frac{r_e}{r}\right)^n P_n^m(\cos\phi)(C_{nm}\cos m\theta + S_{nm}\sin m\theta)\right] \tag{17}$$

where C_{nm} and S_{nm} are constants which are dependent on the mass distribution of the body,

m = total mass of body

r_e = equatorial radius of body

G = universal gravitational constant

$P_k^j(x)$ = associated Legendre function of the first kind of degree k and order j.

A tremendous simplification of (17) occurs if the body is symmetric about the Z axis. If this is the case, then

$$C_{nm} = 0, \ m \neq 0$$
$$S_{nm} = 0$$

and (17) is customarily written in the form

$$V(r, \phi) = -\frac{Gm}{r}\left[1 - \sum_{k=1}^{\infty} J_k\left(\frac{r_e}{r}\right)^k P_k(\cos\phi)\right]$$

where J_k are constants ($J_k = -C_{ko}$)

$P_k(x)$ = Legendre polynomial of degree k = $P_k^o(x)$

In addition, if the origin of the axes (X, Y, Z) is the center of mass of the body, the $J_1 = 0$, thus (17)becomes

$$V(r, \phi) = -\frac{Gm}{r}\left[1 - \sum_{k=2}^{\infty} J_k \left(\frac{r_e}{r}\right)^k P_k (\cos \phi)\right] \qquad (18)$$

We will use this form in the study of Mars and Venus in this report. Recall that the validity of this form rests on two assumptions:

(1) the Z axis from which the angle ϕ is measured is an axis of symmetry of the body, and

(2) the distance r is measured from the center of mass of the body.

The assumption that Mars and Venus have an axis of symmetry appears to be a good approximation, for there are some reasons to believe that these planets are more homogeneous than Earth. However, the direction of the axis of symmetry with respect to the celestial coordinate is not well known beforehand. Hence, if we choose to use form (18) we are forced to introduce two angles which define the direction of the axis of symmetry with respect to the celestial system as unknowns.

The assumption that the coordinate system may be located at the center of mass of the body introduces no significant difficulties and will be used here.

Let us now investigate the change in the coefficients of (18) for the case in which the coordinate system chosen lies close to the preferred system.

As before, let S_1 be the celestial coordinate system. Also, let S_3 be a system with associated unit vectors, $\hat{i}_3$, $\hat{j}_3$, and $\hat{k}_3$ such that $\hat{k}_3$ is parallel to the axis of symmetry. Let ξ_1 and ξ_2 be the azimuth and coelevation of $\hat{k}_3$ with respect to S_1 (Figure 5). Then, the potential has the form (18).

Now suppose we do not utilize the preferred system, S_3, but instead write the potential in a system defined with respect to S_1 by angles $\xi_1 + \delta\xi_1$ and $\xi_2 + \delta\xi_2$. It may be shown that for small $\delta\xi_1$ and $\delta\xi_2$

$$V(r, \tilde{\phi}, \tilde{\theta}) = -\frac{Gm}{r}\left[1 - \sum_{k=2}^{\infty} \tilde{J}_k \left(\frac{r_e}{r}\right)^k P_k (\cos \tilde{\phi})\right] + \sum_{k=2}^{\infty} \left(\frac{r_e}{r}\right)^k P_k^1 (\cos \tilde{\phi})\left[C_{k1} \cos \tilde{\theta} + S_{k1} \sin \tilde{\theta}\right]$$

where $\tilde{J}_k = J_k$

$C_{k1} = -J_k \, \delta\xi_2/\sqrt{2}$

$S_{k1} = -J_k \sin \xi_2 \, \delta\xi_1/\sqrt{2}$

$\tilde{\phi}$ = coelevation of P in new system

$\tilde{\theta}$ = azimuth of P in new system.

Thus, to a first approximation, Legendre functions of the first order must be included in the potential if a coordinate system slightly removed from a preferred system is utilized to describe the position and velocity of a satellite.

NUMERICAL RESULTS

We now will give some results of an error analysis for a series of different cases for orbits about Mars and Venus, Moon, and Earth. However, let us first briefly describe the method of the error analysis.

It has been shown that it is possible to write

$$\delta\bar{m} + \bar{D} = A \, \delta\bar{Y}(0) \tag{19}$$

where $\delta\bar{m}$ = a vector of angle deviations from the directions which would be computed if the primary and secondary were on the reference orbits,

$\bar{D}$ = a vector which arises because the reference orbits were chosen to be Kepler orbits,

A = a 2n x m matrix, n is the number of sightings of the secondary, and m is the number of unknowns in the problems,

$\delta\bar{Y}(0)$ = a 1 x m vector which represents deviations from their true values of the initial conditions and the multiplicative constants of the perturbing forces.

Equation (19) was derived by a linearization technique, and hence is only an approximation. However, we will assume errors in the measured angles to be 10 seconds of arc. For these small errors, we may regard (19) as exact.

Let us assume $E(\overline{\delta m} + \overline{D}) = 0$, i.e., the expected value of each of the measured angles is its true value. Also, the distributions of each measured angle are independent. And, finally, the standard deviation of each measurement is 10 seconds of arc. More precisely, for each i

$$\sigma = \sigma(\delta a_i \cos e_i) = \sigma(\delta e_i) = 10 \text{ seconds of arc.}$$

In general, $2n > m$; i.e., there are more equations in (19) than unknowns. Since this is the case, a "least squares" solution of (19) may be sought. If the columns of A are linearly independent vectors, then the "least squares" solution of (19) yields

$$E(\delta\overline{Y}(0)) = 0$$

and

$$E(\delta\overline{Y}(0)\ \delta\overline{Y}(0)') = \sigma^2(A'A)^{-1}.$$

Hence, the mean of the outputs will be their true values. However, even though the input errors are uncorrelated, the output error may be highly correlated. In any event, as a measure of the error in outputs due to the input errors, we will use the standard deviation of the output.

The unit of length is chosen as the kilometer, and the unit of time is the hour.

Mars

For orbits about Mars, the secondary will first be chosen as one or both of its known natural satellites, Phobos and Deimos. Later, the effect of using an ejected probe will be studied. We assume Mars has an axis of dynamic symmetry, and hence we are justified in assuming a potential of the form (18) if the direction of this axis is included in the unknowns.

Position and Velocity Only.- Let us first investigate the errors in position and velocity for the case in which the only force field is an inverse square central field; i.e., that is, no perturbing force exists.

The orbital elements chosen for the spacecraft, Phobos, and Deimos are given in Table IV.

Table IV

Orbital Elements of Spacecraft, Phobos, and Deimos

Body	a (km)	e	i	ω	Ω	T_p (hrs)
Spacecraft	4056.4	0	45^o	0	0	0
Phobos	9400.	0.017	0.95^o	270^o	319^o	0
Deimos	23500.	0.0028	1.3^o	0	305^o	0

In Figure 6 is a plot of the distance between the spacecraft and Deimos, the spacecraft and Phobos, and the intervals of time over which these secondaries will be obscured by Mars.

Table V gives the resulting errors in position and velocity at t = 0. For this case, 132 sightings were uniformly spaced over 10 orbital periods of the satellite. Each sighting yields two equations, since both azimuth and elevation of the secondary were utilized. No sightings were utilized during the time interval in which the secondary was obscured by Mars.

Table V gives the results for various cases. Given are the standard deviations of the position and velocity errors at t = 0. The components of these error vectors are resolved in the system $R_{j1}(0)$; i.e., they are given in the radial, tangential, and cross-track directions (j = 1, 2). The 12 unknown case is that in which both the orbit of the spacecraft and Phobos are unknown. Two 6 unknown cases are presented; one in which the orbit of Phobos is known, and sightings on it are used to compute only the orbit of the spacecraft. The second 6 unknown case utilizes Deimos instead of Phobos. Finally, an 18 unknown case is given in which sightings of both Phobos and Deimos are utilized to compute all the orbits of all three bodies.

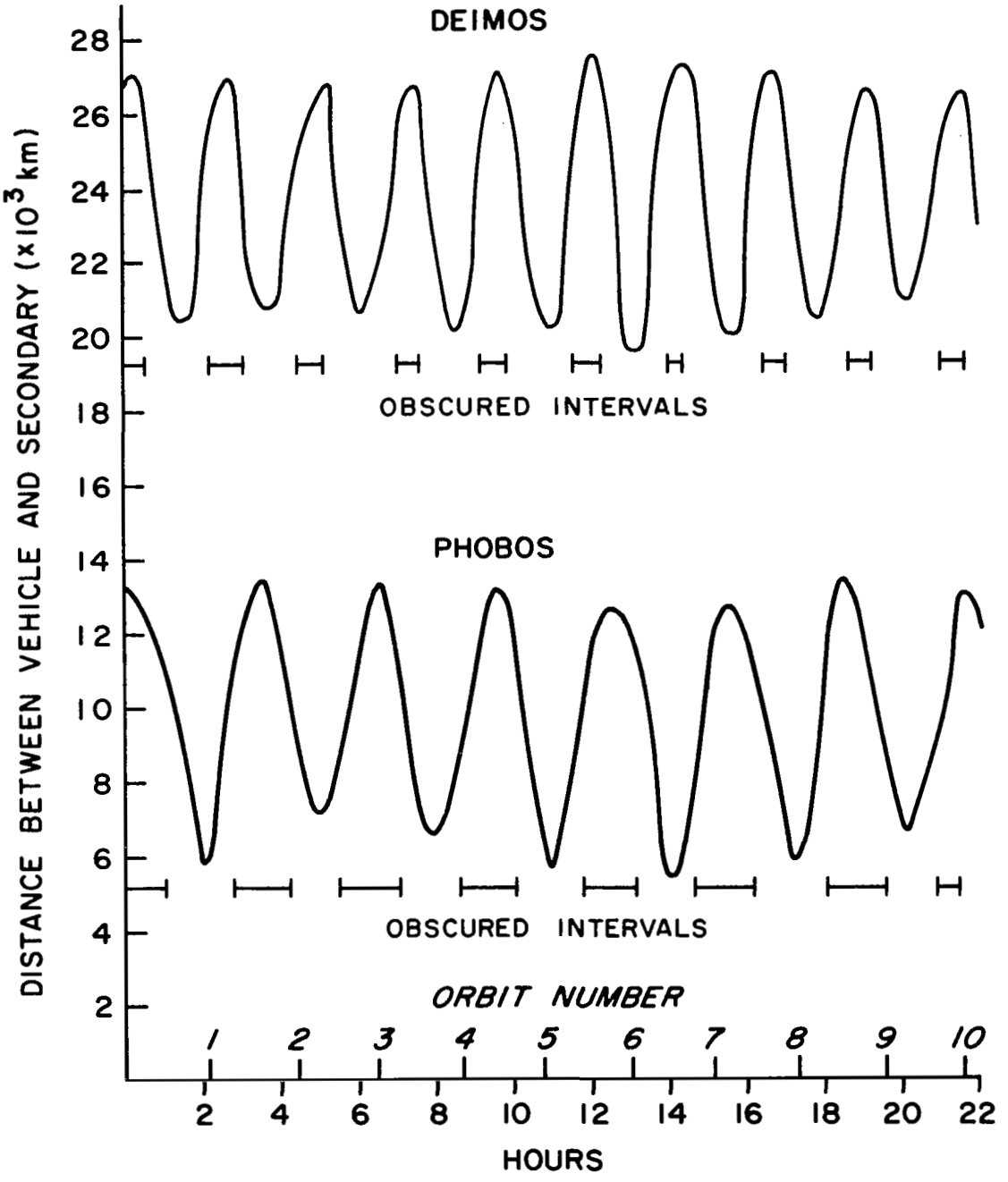

Figure 6: Distance Between Spacecraft and Secondaries as a Function of Time

In all cases, the results indicate that the positions and velocities may be computed within a reasonable error. As might be expected, the case which yields the smallest errors is that in which an accurately known orbit of Phobos is utilized. Note that if the orbit of Phobos is treated as unknown, then the accuracy to which the spacecraft's position is determined is only slightly poorer.

From this table, the overall conclusion is that the navigational problem is well conditioned. Moreover, the proper choice of problems is a 12 unknown problem in which the orbits of Phobos and the spacecraft are determined. Little is gained by utilizing sightings of Deimos.

Table V was obtained by using a spacecraft orbital inclination of $i = 45^{\circ}$. Several different inclinations were also utilized. The results were that the largest error was obtained for $i = 0^{\circ}$, and the smallest for $i = 90^{\circ}$. The spread, however, was not great.

Table V

Position and Velocity Errors at t = 0

132 Sightings, 10 Orbital Periods

	Position Errors (km)				Velocity Errors (km/hr)			No. of
Body	$\sigma(r)$	$\sigma(s)$	$\sigma(z)$	Σ	$\sigma(\dot{r})$	$\sigma(\dot{s})$	$\sigma(\dot{z})$	Unknowns
S/C	.044	.141	.081	.168	.380	.126	.246	6 Phobos known
S/C	.113	.401	.214	.468	1.06	.330	.583	6 Deimos known
Phobos	.071	.190	.079	.217	.116	.059	.060	
Deimos	.375	.432	.167	.596	.112	.058	.037	18
S/C	.117	.147	.102	.214	.391	.338	.237	
Phobos	.075	.197	.082	.226	.119	.062	.062	
S/C	.125	.159	.112	.231	.420	.362	.262	12

$$\Sigma = \sqrt{\sigma^2(r) + \sigma^2(s) + \sigma^2(z)}$$

r = error in radial direction

s = error in tangent direction

z = cross-track error

Finally, in Figure 7 we plot what is defined as the total navigational error for the cases examined in Table V. We define total navigational error as,

$$\frac{1}{T}\int_{(q-1)T}^{qT}\sqrt{\sigma^2(r(t)) + \sigma^2(s(t)) + \sigma^2(z(t))}\,dt$$

$$q = 1, 2, \ldots$$

where T = orbital period of the spacecraft and all measurements are utilized such that $0 \leq t \leq qT$.

Unknown Potential Parameters and Coordinate Direction but Mass Known.-Let us now assume the mass of Mars is accurately known (in the next section, we allow for an unknown mass) and the potential is given by

$$V(r, \phi) = \frac{Gm}{r}\left[-1 + \sum_{k=2}^{4} J_k\left(\frac{r_e}{r}\right)^k P_k(\cos\phi)\right].$$

We assume J_2, J_3, J_4, ξ_1, and ξ_2 are poorly known. The angles ξ_1 and ξ_2 define the direction of the spin axis of Mars.

In the previous section, we showed little was gained by sighting of Deimos (at least for the navigation problem and a low altitude spacecraft orbit). Thus, for the rest of our study of Mars, we will only utilize Phobos as the secondary body. The orbit of Phobos will be treated as unknown. The number of unknowns in the total problem is then 17 or 15 (in two cases we give results in which ξ_1 and ξ_2 are known).

Four different orbits of the spacecraft were investigated. These four orbits are defined in Table VI. For all orbits, $\omega = \Omega = T_p = 0$.

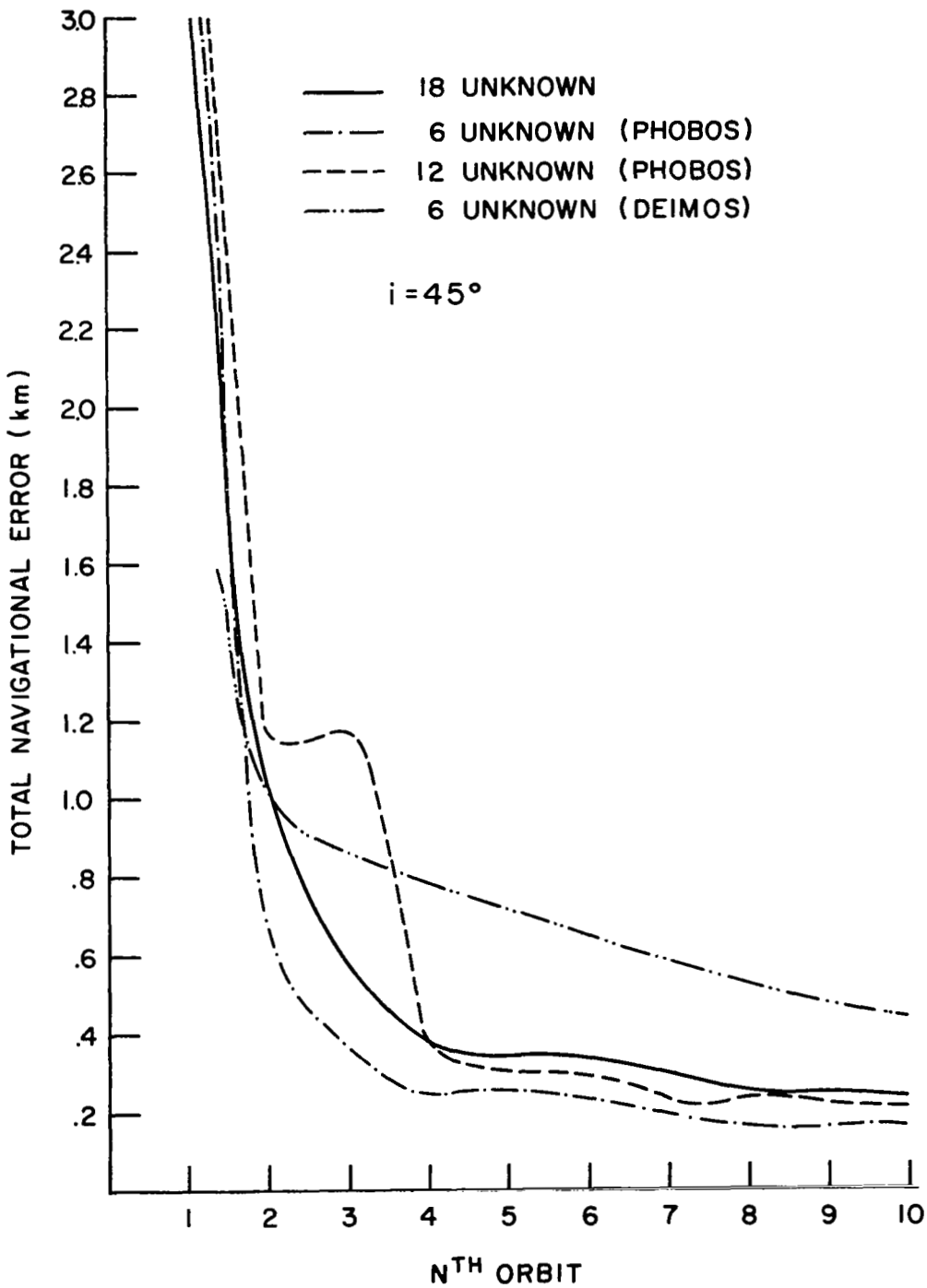

Figure 7: Total Navigational Error of the Spacecraft as a Function of the Orbit Number and Various Cases

Table VI

Spacecraft Orbit

Orbit No.	a (km)	e	i	Periapsis ht. (km)	Apoapsis ht. (km)
1	4056.40	0	45^{o}	672.06	672.06
2	4056.40	0	0^{o}	672.06	672.06
3	3930.34	0.114494	60^{o}	100	1000.
4	8880.34	0.506737	60^{o}	1000	10000.

Values of the parameters were chosen as follows:

$\xi_1 = 317.9^{o}$

$\xi_2 = 35.3^{o}$ from [7]

$J_2 = 2.011 \times 10^{-3}$ from [11]

$J_3 = J_4 = 0$ when orbits 1 and 2 were used

$J_3 = -5 \times 10^{-6}$, $J_4 = -4 \times 10^{-6}$ when orbits 3 and 4 were used

No estimates of J_3 or J_4 are given in the literature.

As expected, the position and velocity errors are now greater than those obtained for the case in which no perturbating forces exist (compare Table V with Table VII). Also, for any particular case of the 17 unknown problem, $\sigma(\dot{z})>\sigma(\dot{r})>\sigma(\dot{s})$. Deletion of the direction of the axis of symmetry as an unknown reduces $\sigma(z)$ and $\sigma(\dot{z})$ more than the other position and velocity error components, respectively. However, this deletion has little effect in reducing the potential parameter errors.

At present, astronomic measurements yield $\sigma(\delta J_2) \doteq 10^{-3}$, $\sigma(\delta \xi_1) \doteq \sigma(\delta \xi_2) = 1^{o}$. Hence, the sighting can be expected to yield considerable improvement in our knowledge of the Martian potential.

Unknown Mass, Potential Parameters, and Coordinate Direction.-Let us now consider exactly the same case as that presented by Orbit No. 3 in Table VII except we now assume that the mass of Mars is unknown. Hence, the problem now has 18 unknowns. Results of this case are shown in Table VIII.

From this table, we see the method is very poor if the mass of Mars and the orbit of Phobos are unknown. Note the large values of $\sigma(r)$, $\sigma(\dot{s})$, and $\sigma(\delta m)$. The

132 Sightings

Orbit No.	No. of Orbits	Body	Position Errors at t = 0 (km)			Velocity Errors at t = 0 (km/hr)			Potential Parameter Errors x 10^5			Axis Direction (secs. of arc)		No. of Unknowns
			$\sigma(r)$	$\sigma(s)$	$\sigma(z)$	$\sigma(\dot{r})$	$\sigma(\dot{s})$	$\sigma(\dot{z})$	$\sigma(\delta J_2)$	$\sigma(\delta J_3)$	$\sigma(\delta J_4)$	$\sigma(\delta\xi_1)$	$\sigma(\delta\xi_2)$	
1	10	Phobos	.08	4.41	19.54	3.74	.06	17.1	1.57	.26	7.15	125	622	17
		S/C	.14	.37	.24	1.03	.43	35.4						
1	20	Phobos	.07	.81	2.49	.68	.05	2.28	1.49	.12	6.79	25	81	17
		S/C	.14	.13	.51	.34	.42	4.65						
1	10	Phobos	.07	.21	.09	.13	.06	.06	1.57	.23	7.13	---	---	15
		S/C	.14	.16	.22	.40	.42	.32						
1	20	Phobos	.06	.21	.08	.12	.05	.07	1.46	.12	6.65	---	---	15
		S/C	.14	.12	.19	.30	.42	.30						
2	10	Phobos	.22	.36	5.61	.23	.18	4.1	3.66	1.44	35.7	6	165	17
		S/C	.17	.33	.17	.55	.46	9.4						
2	20	Phobos	.11	.27	2.74	.16	.10	2.0	1.40	1.41	8.81	5	81	17
		S/C	.15	.29	.16	.45	.41	4.6						
3	10	Phobos	.10	5.95	29.4	5.06	.07	21.6	.57	1.21	1.05	168	863	17
		S/C	.16	.37	2.90	1.35	.54	55.9						
3	20	Phobos	.07	.91	4.49	.76	.06	3.37	.29	.52	.40	28	133	17
		S/C	.15	.28	.53	.91	.51	8.58						
4	10	Phobos	.09	.43	5.59	.32	.08	4.0	.65	.36	1.15	16	162	17
		S/C	.10	.62	.40	1.31	.20	10.6						
4	20	Phobos	.08	.23	3.03	.14	.06	2.17	.24	.14	.55	3	88	17
		S/C	.09	.44	.10	.89	.18	5.61						

Table VII: Position, Velocity, and Parameter Errors (Mass of Mars Known)

		Position Errors at t = 0 (km)			Velocity Errors at t = 0(km/hr)			Potential Parameter Errors				Axis Direction (sec.of arc)	
No. of Orbits	Body	$\sigma(r)$	$\sigma(s)$	$\sigma(z)$	$\sigma(\dot{r})$	$\sigma(\dot{s})$	$\sigma(\dot{z})$	$\sigma(\delta J_2)$	$\sigma(\delta J_3)$	$\sigma(\delta J_4)$	$\frac{\sigma(\delta m)}{m}$	$\sigma(\delta \xi_1)$	$\sigma(\delta \xi_2)$
10	Phobos	547	5.66	27.0	4.8	464	20	1.97×10^{-5}	1.26×10^{-5}	3.33×10^{-5}	.18	160	792
	S/C	206	.37	2.8	1.3	791	51						
20	Phobos	358	.85	4.1	.71	304	3.1	1.23×10^{-5}	5.61×10^{-5}	2.06×10^{-5}	.11	25.8	121
	S/C	135	.28	.50	.93	518	7.8						

Table VIII: Position, Velocity, and Parameter Errors (Mass of Mars Unknown)

analytic reason for these poor results is obvious, for the equations of motion are of the form

$$\ddot{\bar{r}} = \frac{G\,m\,\bar{r}}{|\bar{r}|^3} + \bar{g}\,(\bar{r})$$

where $\bar{g}\,(\bar{r})$ is small if J_2, J_3, and J_4 are small.

Now let $\lambda\bar{R} = \bar{r}$

$\lambda^3 M = m$, where λ is a constant.

Since no lengths are measured, the factor λ does not appear in the constraint equations if these equations are expressed in the new variables. However, in terms of the new variables, the equations of motion become

$$\ddot{\bar{R}} = \frac{G\,M\,\bar{R}}{|\bar{R}|^3} + \bar{g}\,(\lambda\bar{R}).$$

Thus, we note, if $\bar{g} \equiv 0$, then the equations of motion are independent of λ. Since $\bar{g}$ is small, it can be expected that $\bar{r}$ and m are nearly dependent, and thus cannot be well determined by the measurements. A penalty thus must be paid for not measuring lengths.

In summary, sighting of Phobos from a spacecraft yields accurate determination of the spacecraft's orbit, the orbit of Phobos, and the potential parameters. However, the mass of Mars cannot be treated as unknown in the total problem.

Ejected Probe.-Thus far, we have utilized only Phobos as the secondary satellite in determining the potential of Mars. We have observed that if the orbit of Phobos and the mass of Mars are treated as unknown, then intolerably large errors are produced. This result occurs because no lengths are measured.

Let us now investigate the total problem again utilizing Orbit No. 3 of Table VII for the case in which an ejected probe of known ejection speed is utilized. Note that the ejected speed introduces a known length.

Let the probe be ejected so that

Δv = 4 km/hr (ejection speed)

$\alpha_o = 0^o$

$\epsilon_o = 45^o$.

The angles α_o and ϵ_o determine the direction of ejection as shown in Figure 8. We will assume these angles to be unknown, but Δv known.

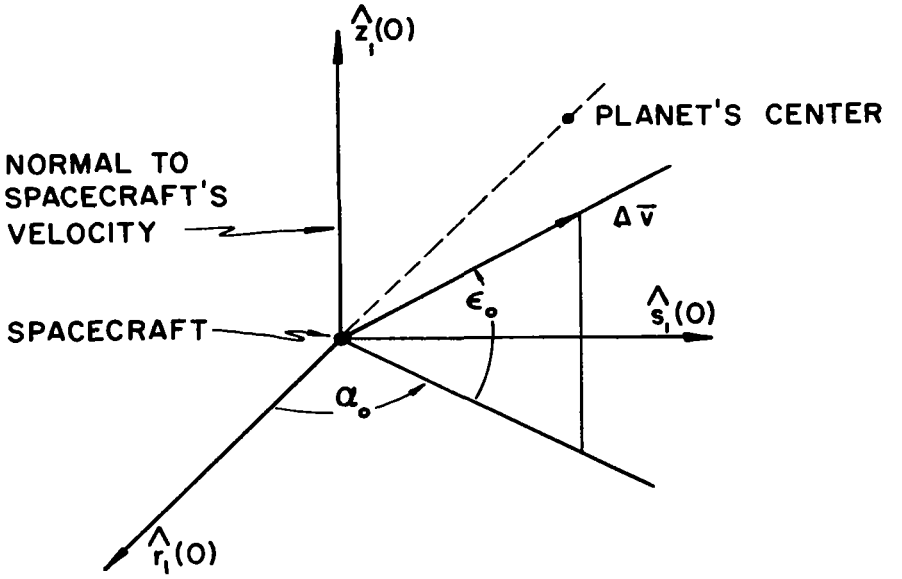

Figure 8: Direction of Ejection with Respect to System which Moves with Spacecraft

In Figures 9, 10, and 11 results of two cases are presented. One case utilizes 10 sightings per spacecraft orbital period on the ejected probe and 10 sightings per period on Phobos; the other utilizes only the sightings on the probe. The first case in which Phobos is used contains six more unknowns than the second case. The two cases have 20 and 14 unknowns, respectively.

Figure 9 gives the error in mass of Mars, navigational error of the spacecraft, and error in J_3 for both cases as a function of the number of orbital periods over which the data is gathered. Here, navigational error is defined as

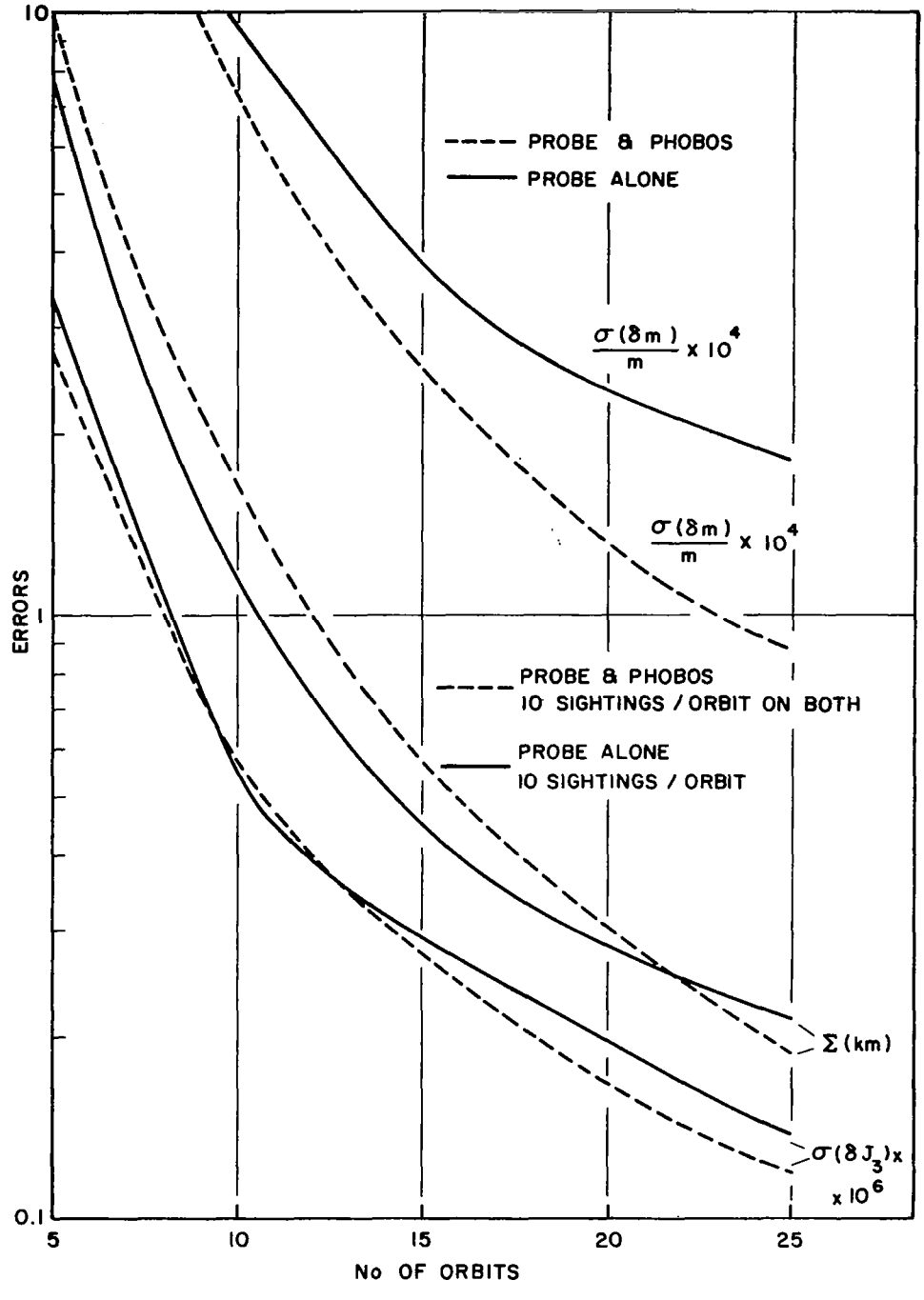

Figure 9: Total Navigation Error, Mass Error, and J_3 Error. Sighting of Probe Alone, and Probe and Phobos

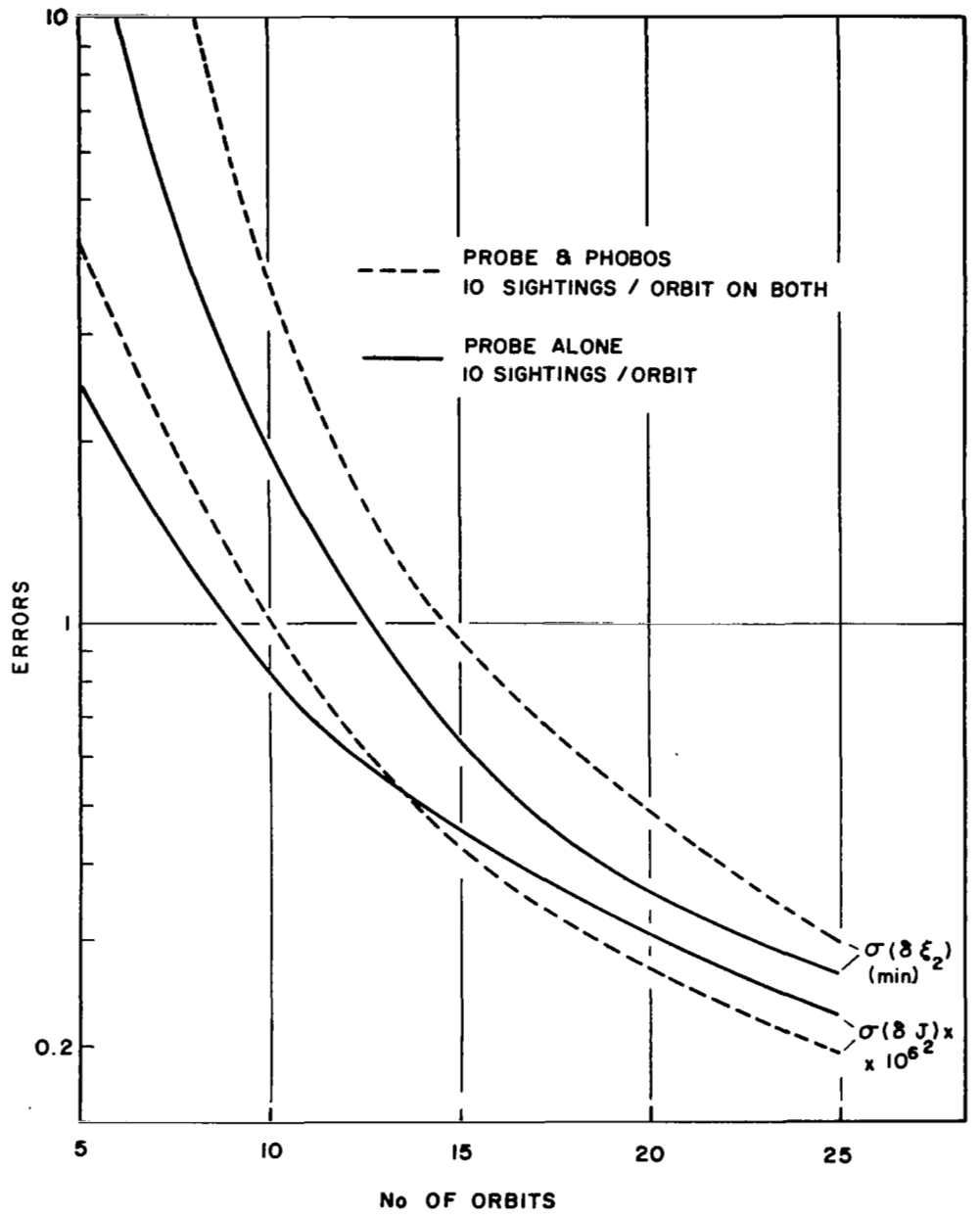

Figure 10: Error in J_2 and ξ_2 by Sighting of Probe Alone, and Probe and Phobos

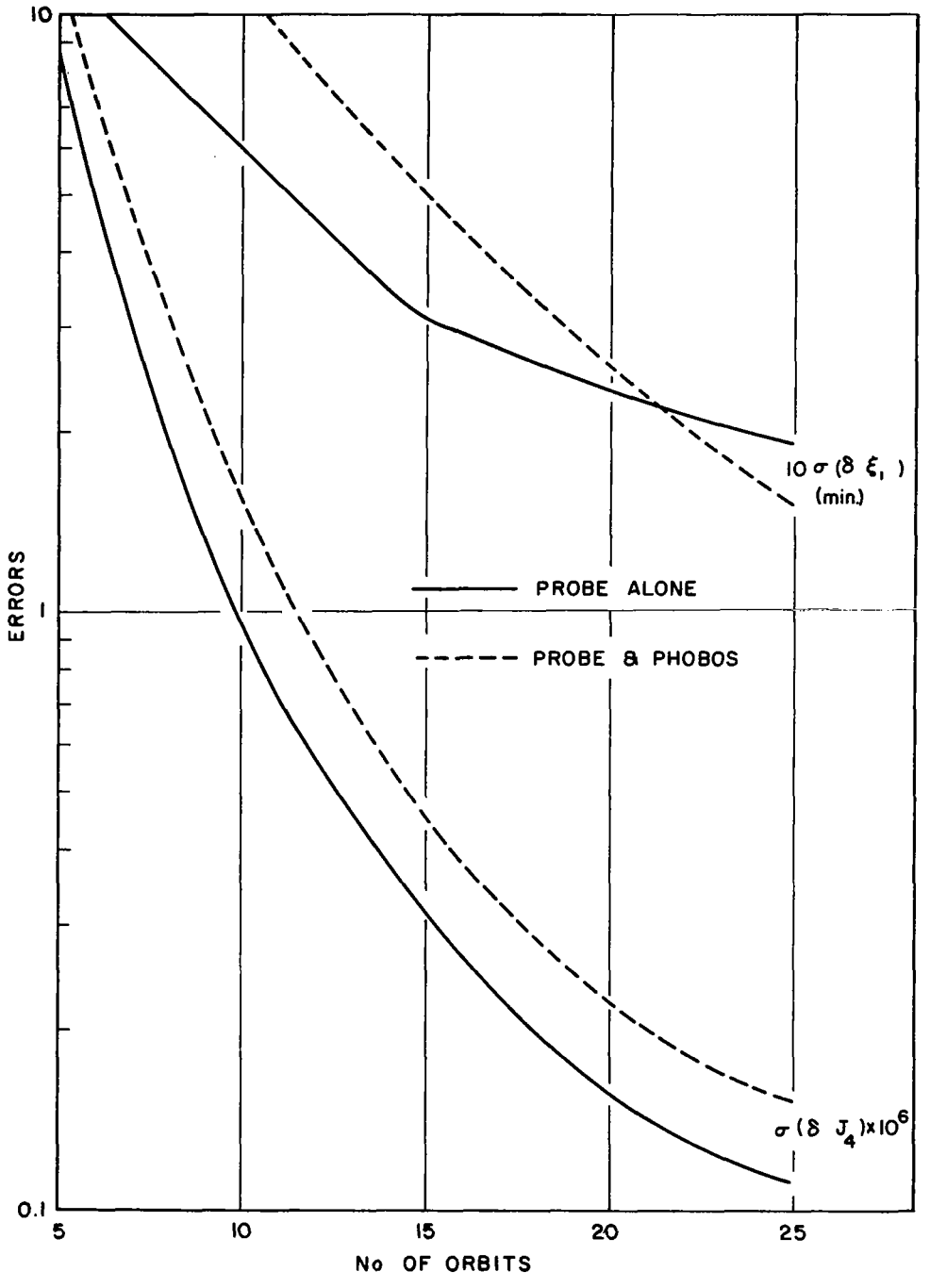

Figure 11: Errors in J_4 and ξ_1 Sighting of Probe Alone, and Probe and Phobos

$$\Sigma = \sqrt{\sigma^2(r) + \sigma^2(s) + \sigma^2(z)} \qquad \text{at } t = 0,$$

and r, s, and z are defined in Figure 3. Note that the mass determination is always better if Phobos is used in conjunction with the probe.

In Figure 10 we plot the error in ξ_2 and J_2 for the two cases. ξ_2 is the codeclination of the axis of symmetry of Mars. Finally, in Figure 11 we plot the error in ξ_1 (right ascension) and J_4.

In general, there is no greatly significant difference between results obtained with and without sightings of Phobos along with the probe; except that in the first case, an accurate orbit of Phobos is determined.

It is somewhat difficult to evaluate the improvement in accuracy afforded by sighting of the probe over that obtained by sighting Phobos alone from the data we have presented. Recall that Table VII (sighting of Phobos alone) was constructed by utilizing the assumption that the mass of Mars was known; however, in Figures 9, 10, and 11 we assumed the mass to be unknown. Even though this is the case, the improvement obtained by the probe is about a factor of three for position, 15 for J_2, 30 for J_3, 23 for J_4, and five for the direction of the axis of symmetry.

If sightings of the probe and Phobos are utilized, the improvement in the orbit determination of Phobos (versus Phobos alone) is given in Table IX.

Table IX

Comparison of Accuracy of Position and Velocity at t = 0 of Phobos With and Without Probe Sightings, Orbit No. 3. Martian Mass Unknown With Probe, Known Without Probe.

No. of Orbits	No. of Measurements		Σ (km)		$\dot{\Sigma}$ (km/hr)	
	With Probe	Without Probe	With Probe	Without Probe	With Probe	Without Probe
10	150	264	8.82	30.0	5.94	22.2
20	300	264	1.46	4.58	0.84	3.46

Venus

J_2 and Direction of Axis of Symmetry Unknown - Known Ejection Speed.-Of all the planets, Venus is the most nearly spherical. Its equatorial and polar radii are both estimated to be 6100 $\pm$ 50 kilometers. Thus, it is difficult to determine the coefficients of the higher order terms in the potential. No estimates are given in the literature. Here we assume all coefficients are zero except J_2.

The orbit chosen for the spacecraft is defined by

a = 6587 kilometers

e = .0151814

$i = 60^{\circ}$

$\Omega = \omega = T_p = 0.$

These elements imply a periapsis and apoapsis altitude of 387 and 587 kilometers, respectively.

We assume the spin axis to be coincident with the axis of dynamic symmetry of Venus. This assumption and data from [6] thus implies

$\xi_1 = 272.75^{\circ}$ (right ascension of spin axis)

$\xi_2 = 18.5^{\circ}$ (co-declination).

Venus has no known natural satellites, hence the secondary must be an ejected probe. We assume that the probe is ejected with known speed, but poorly known direction. It turns out that the total problem is unstable if the ejection speed is treated as unknown. We will discuss this point later. Also, we will show the effect of an error in the ejection speed.

We define the direction of ejection with respect to the coordinate $R_{11}(0)$ by two angles, α_o and ϵ_o, as pictured in Figure 8.

Let us set

Δv = 4 km/hr

$\alpha_o = 36^{\circ}$

$\epsilon_o = 49^{\circ}.$

These parameters imply that the maximum distance between the spacecraft and probe in 10 orbital periods is 86.39 km, 86.50 km, and 86.51 km for $J_2 = 10^{-3}$, 10^{-4}, and 10^{-5}, respectively. Assume no errors in the mass of Venus and the ejection speed. There are 11 unknowns in the problem. These unknowns are given in Table X, along with results for various values of J_2.

From Table X we note that as J_2 becomes smaller, the errors become larger. In fact, for $J_2 \leq 10^{-6}$ the problem becomes so ill-conditioned that no solution could be found. The physical reason for this fact is that for small J_2, the direction of the planet's axis of symmetry is poorly defined. It is undefined for $J_2 = 0$.

For rapidly rotating planets (e.g. Jupiter and Saturn), J_2 can probably be estimated closely by assuming the planet to be in hydrostatic equilibrium. However, for such a slowly rotating planet (sidereal period = 243.2 days retrograde), the effect of centrifugal force is second order. It is difficult for us to estimate J_2 for Venus, but it is highly likely that it is smaller than that of the Earth or moon.

In Table XI we show the effect of adding the mass of Venus as an unknown. Recall that for the case of Mars, adding mass as an unknown greatly increased the errors. A significant, but not intolerable, increase in position and velocity errors are shown for the present case. This is because the ejection speed supplies a length measurement which was missing when only the direction of Phobos was measured. The accuracy of the mass determination, however, is not impressive. Our present knowledge (Table I) gives $\delta m/m = 1.5 \times 10^{-6}$.

Note that (Table XI) deleting the direction of the axis of symmetry from the unknowns greatly decreases the errors in all remaining unknowns except (disappointingly) the mass.

In Figure 12 we plot the errors as a function of the number of orbital periods over which data was gathered. Here $J_2 = 10^{-3}$, and 13 sightings/10 orbital periods were utilized.

Table X: Errors in $\overline{X}_1$ (0), J_2, Direction of Axis of Symmetry, and Direction of Ejection: Speed of Ejection and Mass of Venus Known

Chosen J_2	Position Errors (km) $\sigma(\delta x)$	$\sigma(\delta y)$	$\sigma(\delta z)$	Velocity Errors (km/hr) $\sigma(\delta \dot{x})$	$\sigma(\delta \dot{y})$	$\sigma(\delta \dot{z})$	$\sigma(\delta J_2)$ x 10^6	Axis Dir. (min) $\sigma(\delta \xi_1)$	$\sigma(\delta \xi_2)$	Ejection Dir. (min) cos $\tilde{e}$ $\sigma(\delta \tilde{a})$	$\sigma(\delta \tilde{e})$
10^{-3}	.042	.451	1.65	4.63	170	98.1	3.1	.85	27	15	17
10^{-4}	.041	2.12	6.60	18.2	1790	1030	3.3	3.6	280	157	183
10^{-5}	.041	21.0	62.9	172	19600	11300	3.6	35	3058	1710	2000
10^{-6}	--	--	--	--	--	--	--	--	--	--	--
10^{-7}	--	--	--	--	--	--	--	--	--	--	--

10 orbital periods of data - 130 sightings

Table XI: Effect of Adding Mass as an Unknown. Also Effect of Deleting Direction of Axis of Symmetry

Chosen J_2	No. of Unknowns	Position Error Σ(km)	Speed Error $\dot{\Sigma}$(km/hr)	$\sigma(\delta J_2)$ x 10^6	Axis Direction (min) $\sigma(\delta \xi_1)$	$\sigma(\delta \xi_2)$	Ejection Direction (min) cos $\tilde{e}$ $\sigma(\delta \tilde{a})$	$\sigma(\delta \tilde{e})$	$\frac{\sigma(\delta m)}{m}$
10^{-3}	12	30.9	238.9	3.2	.90	28	17	18	.014
10^{-4}	12	317	2694	3.4	3	294	165	192	.185
10^{-3}	10	29.4	115	.77	---	---	1	1	.013
10^{-4}	10	37.8	148	.82	---	---	1	1	.174

10 orbital periods of data - 130 sightings

$$\Sigma = \sqrt{\sigma^2(\delta x) + \sigma^2(\delta y) + \sigma^2(\delta z)}$$

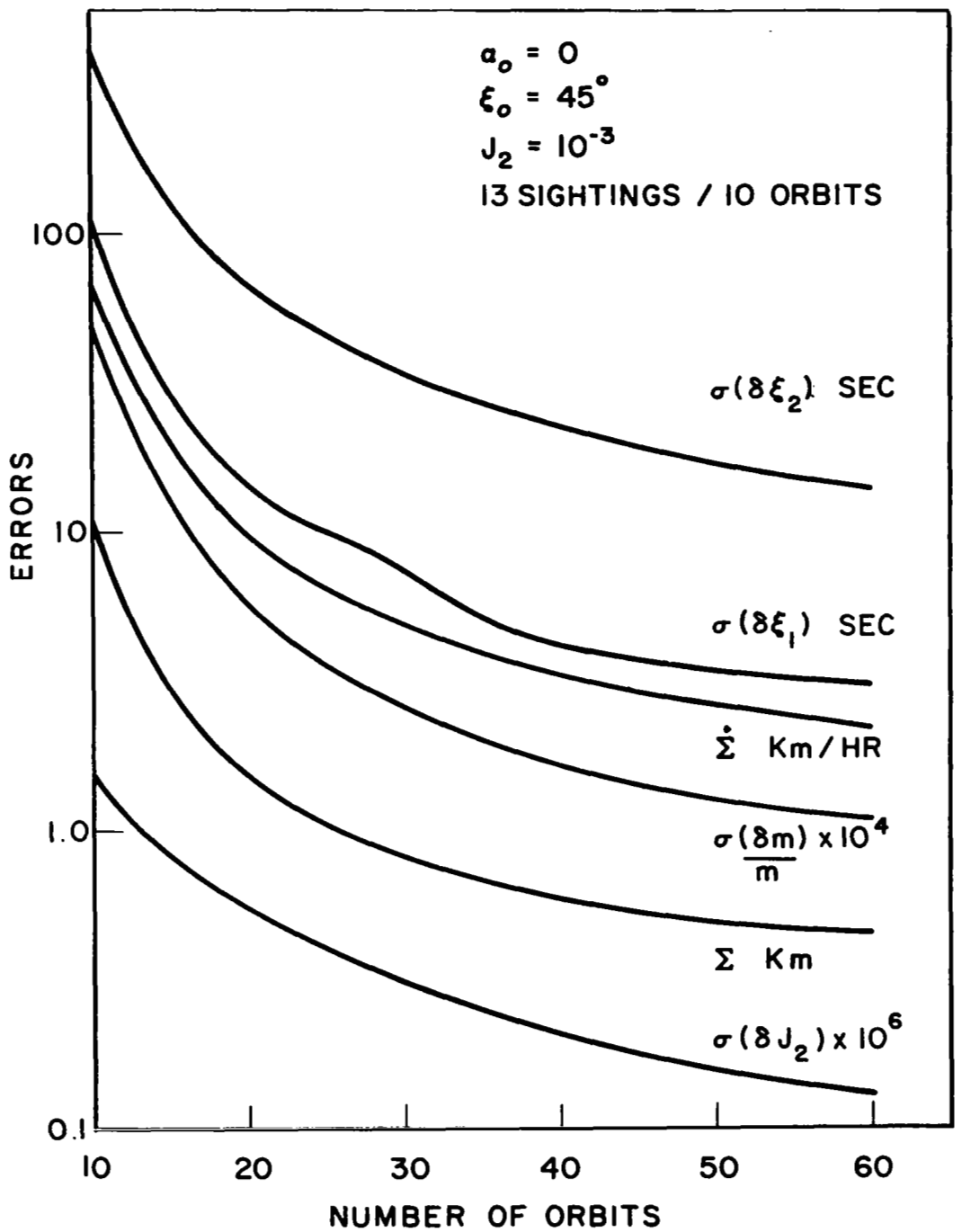

Figure 12: Effect of Additional Measurements and Orbits on Errors

In order to assure that the probe is not too far from the spacecraft, the angles of ejection for the case shown in Figure 12 were changed so that

$\alpha_o = 0$
$\epsilon_o = 45^o$, where these angles are defined in Figure 8.

This ejection direction will be used in the rest of the analysis. Setting $\alpha_o = 0$ insures (at least to a first order) that no secular dependence is present in the distance between the probe and the spacecraft. During a period of 100 orbits the maximum distance between the probe and spacecraft is 3.91 kilometers.

Note that even though more sightings were used for the case presented in Table XI than that presented in Figure 12, after 10 orbits the errors are smaller in the latter case. This results because a more judicious choice of the ejection direction yields a smaller distance between the spacecraft and probe.

Several other cases were tried in which the planet's mass was unknown, but errors in the mass determination were always quite large. At this point, we conclude that our method is somewhat poorly conditioned if the planet's mass is unknown In the rest of the analysis we assume the planet's mass is given.

Let us look at one more case before leaving this section:

(1) Mass known
(2) $\alpha_o = 0$
    $\epsilon_o = 45^o$
(3) $\Delta v = 4$ km/hr
(4) five sightings/orbit
(5) $J_2 = 10^{-5}$ and 10^{-6}.

Conditions (1), (2), (3), and (4) will be used in the rest of our study of Venus. Results of this case are shown in Figures 13 and 14. Note that all errors are significantly larger for the smaller value of J_2 except $\sigma(\delta J_2)$ itself.

J_2, C_{21}, and S_{21} Unknown.-In order to overcome the singularity inherent in the above formulation for $J_2=0$, a different and more conventional formulation will now be made.

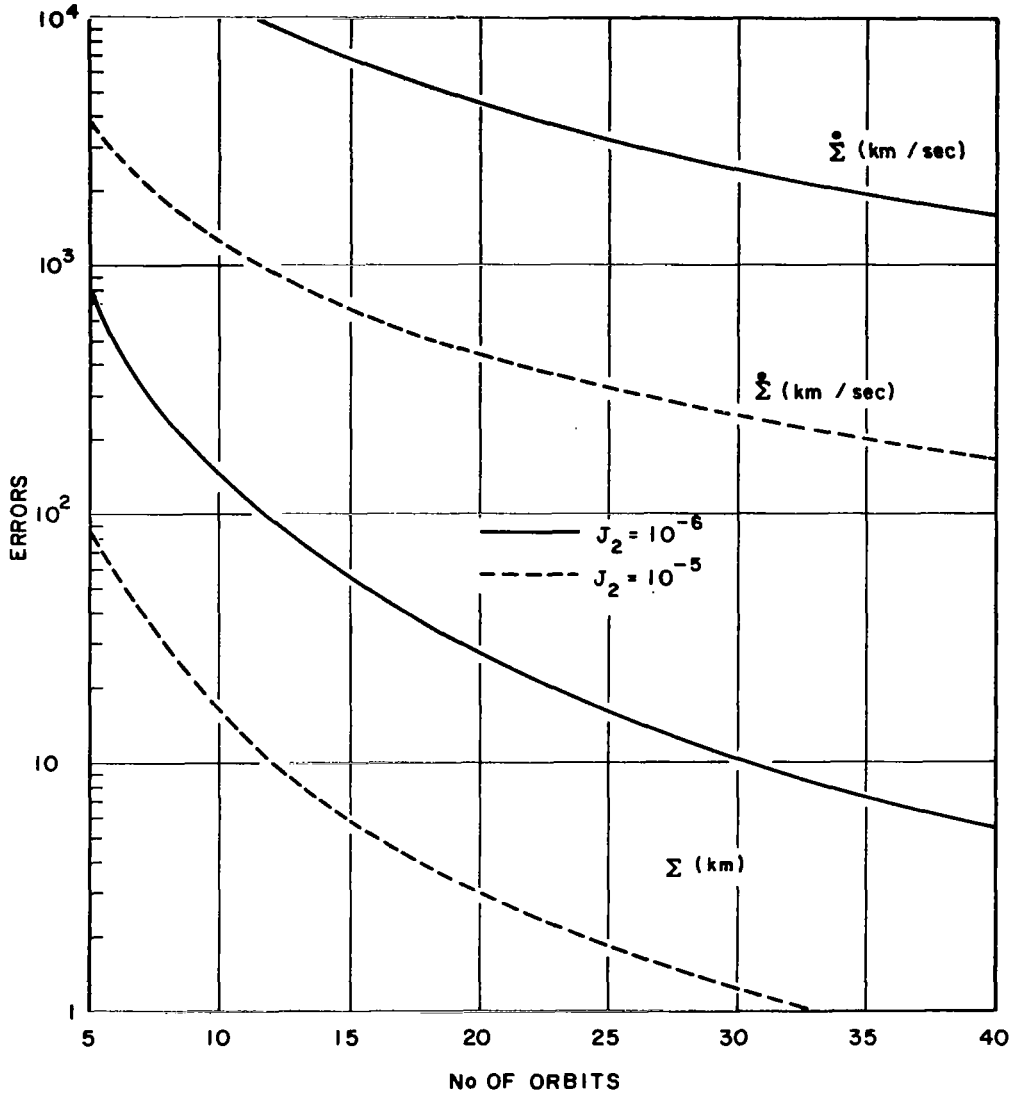

Figure 13: Error in Initial Position and Velocity. $J_2 = 10^{-5}$ 10^{-6}. $\alpha_o = 0$, $\epsilon_o = 45^o$, Five Sightings per Orbit. Mass Known

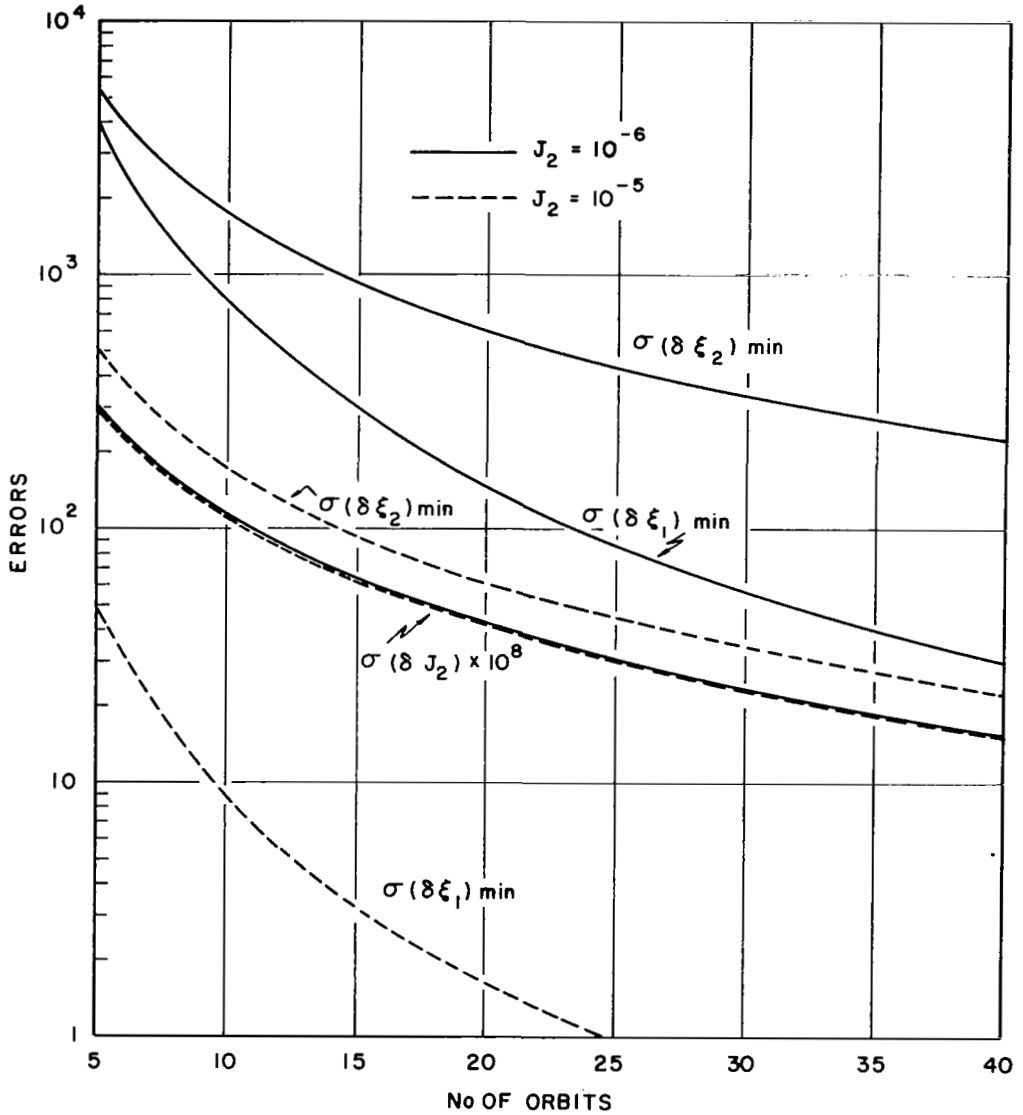

Figure 14: Error in Direction of Symmetric Axis, and J_2. $J_2 = 10^{-5}$ and 10^{-6}. $\alpha_o = 0$, $\epsilon_o = 45^o$. Five Sightings Per Orbit. Mass Known

Assume a body has an axis of symmetry and a potential which includes terms with Legendre polynomials up to degree k when the preferred coordinate system is utilized. Then as was observed in our discussion of the potential, a system slightly removed from the preferred system introduces first order Legendre functions if the removed system is utilized to express its potential.

We now assume the potential of Venus to be

$$V(r, \phi, \theta) = -\frac{Gm}{r}\left[1 - J_2\left(\frac{r_e}{r}\right)^2 P_2(\cos\phi) + (C_{21}\cos\theta + S_{21}\sin\theta)\left(\frac{r_e}{r}\right)^2 P_2^1(\cos\phi)\right]$$

So, C_{21} and S_{21} are now used as unknowns instead of ξ_1 and ξ_2. Note that even if $J_2 = 0$, C_{21} and S_{21} have physical significance, but ξ_1 and ξ_2 do not.

For the present study we set the direction of ejection so that $\alpha_o = 0$, $\epsilon_o = 45^o$. All orbital parameters are the same as before. However, five sightings are spread uniformly over an orbital period. Moreover, it is assumed the ejection speed is known as is 4 km/hr. The present problem has 11 unknowns.

Results for the case $J_2 = 10^{-5}$, $C_{21} = 10^{-7}$, and $S_{21} = 0$, are shown in Table XII. However, two other cases viz. $J_2 = 10^{-7}$, $C_{21} = S_{21} = 0$; and $J_2 = C_{21} = S_{21} = 0$ yields almost identical results. This result is in sharp contrast with those obtained for the formulation in which the direction of the axis of symmetry was unknown instead of S_{21} and C_{21}. Also, the error in initial velocity is much smaller in the present formulation.

Table XII: Errors in Initial Position and Velocity, J_2, C_{21}, and S_{21} as a Function of Number of Orbits, Mass known

No. of Orbits	Σ(km)	$\dot{\Sigma}$ (km/hr)	$\sigma(\delta J_2)\times10^6$	$\sigma(\delta C_{21})\times10^8$	$\sigma(\delta S_{21})\times10^9$
5	1.15	1.37	2.80	28.7	65.0
10	.82	.95	.98	5.84	11.3
15	.67	.85	.54	2.19	4.10
20	.58	.67	.35	1.10	2.03
25	.52	.60	.25	.63	1.14
30	.48	.55	.19	.40	.72
35	.44	.51	.15	.27	.49
40	.41	.48	.13	.20	.35

Effect of Ejection Speed Errors

Extremely large errors in all parameters are obtained if the ejection speed is taken as an additional unknown in the total problem. The reason for this fact is that

$$\bar{R}_2(t) - \bar{R}_1(t) \doteq \Delta v \, \phi_2(t) \, \hat{u}_o, \quad \phi_2(0) = 0,$$

where $\bar{R}_2 - \bar{R}_1$ = position of probe with respect to spacecraft,
Δv = ejection speed,
ϕ_2 = 3 x 3 matrix, and
$\hat{u}_o$ = ejection direction.

Thus, the direction to the probe as a function of time is nearly independent of the ejection speed. Since only this direction is measured, the measurements weakly determine the ejection speed.

The situation with respect to the direction of ejection is just the opposite. That is, the generic direction is strongly dependent on the ejection direction and thus the ejection direction is always accurately determined by the measurements.

In all our previous analyses, we assumed the ejection speed was known exactly. More precisely, we assumed no systematic errors. The random errors in the measurement of the probe's direction then gives rise to random errors in the output parameters with mean zero and the reported standard deviation.

Let us now investigate the effect of a systematic error in the ejection speed. In general, any systematic error will force upon us errors in the output parameters with non-zero means, but the standard deviation will be unaffected. Thus, our previous results may still be interpreted as the standard deviation of the parameter .

Let us now give the systematic error produced by an error in the ejection speed for the five principal cases studied previously. (See Table XIII.) For these cases, we assume the mass of Venus known.

Figure 15 is a plot of the systematic error in the spacecraft's initial position and velocity, while Figure 16 yields the systematic errors in J_2, C_{21}, and S_{21}. These plots are for Cases III, IV, and V (Table XIII) and $\delta\Delta v = .01\ \Delta v$ (the error in the ejection speed is 1/100 of the true ejection speed). We define the position and velocity errors plotted in Figure 15 as the square root of the sum of the squares of the component errors. For the case shown the true magnitudes of the initial position and velocity are 6,487 kilometers and 25,367 km/hr, respectively.

From these figures, three main generalizations may be made as follows:

(1) Smaller perturbations yield smaller systematic errors due to ejection speed errors.

(2) In general (Case V in which the perturbing forces are zero offers exceptions), the systematic errors in initial position, velocity, and C_{21} increase with increasing number of measurements and measurement time interval. This is in contrast with the effect of random input error which always imply a decrease in output errors as more measurements and a longer time interval are used.

(3) If the error in ejection speed is on the order of 1% or less, the resulting output errors are reasonably small.

Table XIII: Cases for Which Systematic Error has Been Studied

Case No.	Parameters	Random Error Results	Comments
I	$J_2 = 10^{-5}$ ξ_1, ξ_2	Figures 13 and 14	Systematic errors slightly larger in Case I than in II, but random errors were significantly larger in II than in I.
II	$J_2 = 10^{-6}$ ξ_1, ξ_2		
III	$J_2 = 10^{-5}$ $C_{21} = 10^{-7}$, $S_{21} = 0$	Table XII, Cases III, IV, and V yield almost identical results.	Systematic errors smaller for smaller perturbations but random error nearly independent of magnitude of perturbations.
IV	$J_2 = 10^{-7}$ $C_{21} = S_{21} = 0$		
V	$J_2 = C_{21}$ $= S_{21} = 0$		

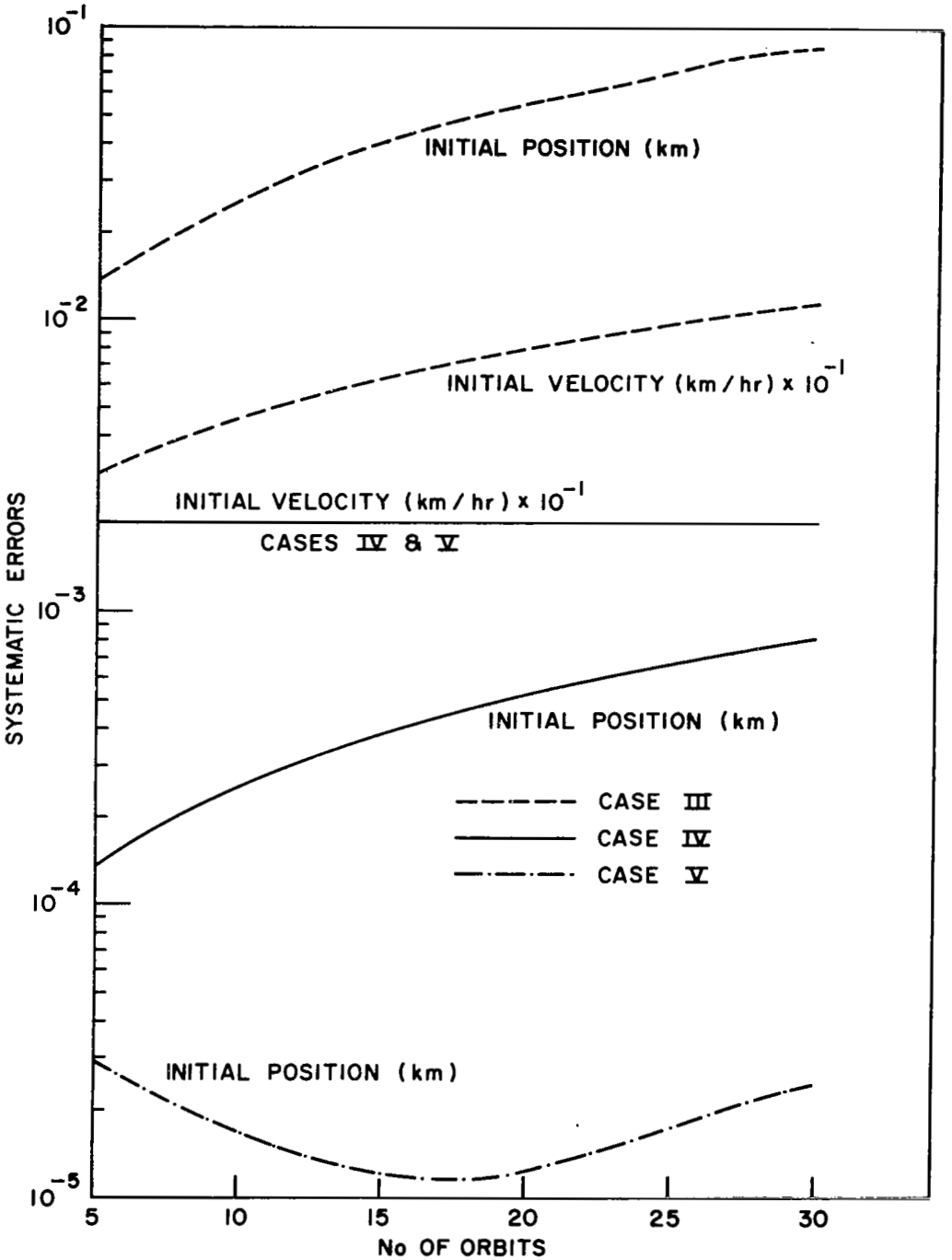

Figure 15: Mean Error in Initial Position and Velocity as a Function of Number of Orbits. $\delta\Delta v = .01\ \Delta\Delta$. Cases III, IV, and V

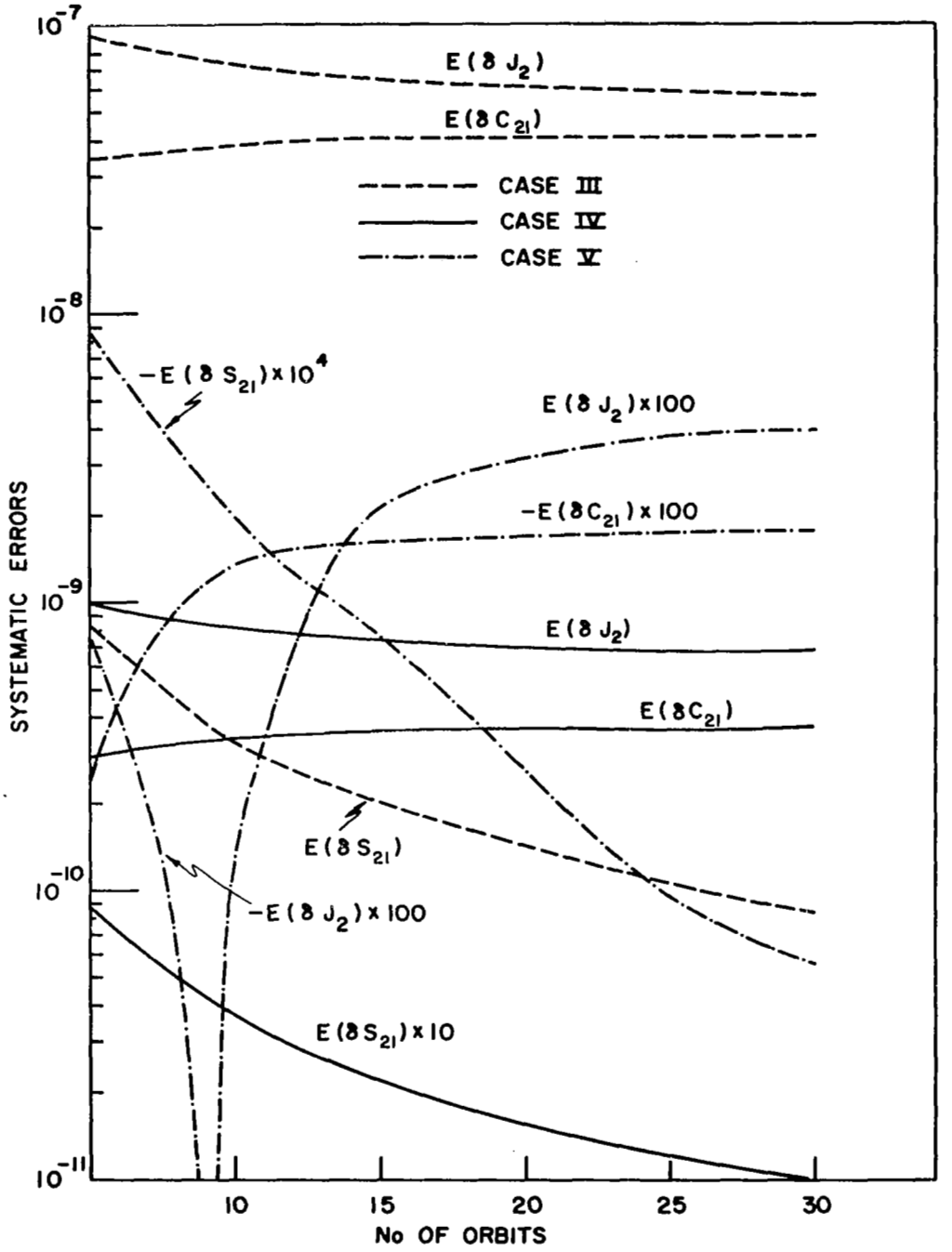

Figure 16: Mean Errors in J_2, C_{21}, and S_{21} as a Function of Number of Orbits. $\delta\Delta v = .01\ \Delta v$. Cases III, IV, and V

Finally, in Figures 17 and 18 we plot the value of $|\delta\Delta v|/\Delta v$ which will produce a systematic error in any one parameter equal to the random error in that parameter. For example, from Figure 18 we see that for Case III after 20 orbits of measurements, the magnitude of the systematic error in the spacecraft's initial velocity is equal to the random error if $|\delta\Delta v| = .086\,\Delta v$. If $|\delta\Delta v| < .086\,\Delta v$, then the magnitude of the systematic error will be less than the random error. For Case IV, only the parameter C_{21} requires $|\delta\Delta v| < |\Delta v|$, for all other parameters $|\delta\Delta v| > |\Delta v|$. That is, the error in the ejection speed is actually greater than this speed, to yield a systematic error in these other parameters equal to their respective random error. For Case V, no parameter requires $|\delta\Delta v| < |\Delta v|$.

Moon

We assume the moon has a potential of the form

$$V(r, \phi, \theta) = -\frac{Gm}{r}\left[1 + \sum_{j=2}^{4}\sum_{i=0}^{j}\left(\frac{r_e}{r}\right)^j P_j^i(\cos\phi)\right.$$

$$\left. \times \left(C_{ji}\cos i\theta + S_{ji}\sin i\theta\right)\right] \qquad (20)$$

where r, ϕ, θ = spherical coordinates of generic external point,

G = universal gravitation constant,

m = mass of the moon, and

r_e = equatorial radius $\doteq$ 1738.09 km.

Also, we assume all forces on the spacecraft and probe are given by $-\nabla V$.

Three orbits about the moon will be utilized. The initial position and velocity and initial orbital elements are given in Table XIV. The maximum distance between the probe and spacecraft is dependent on the choice

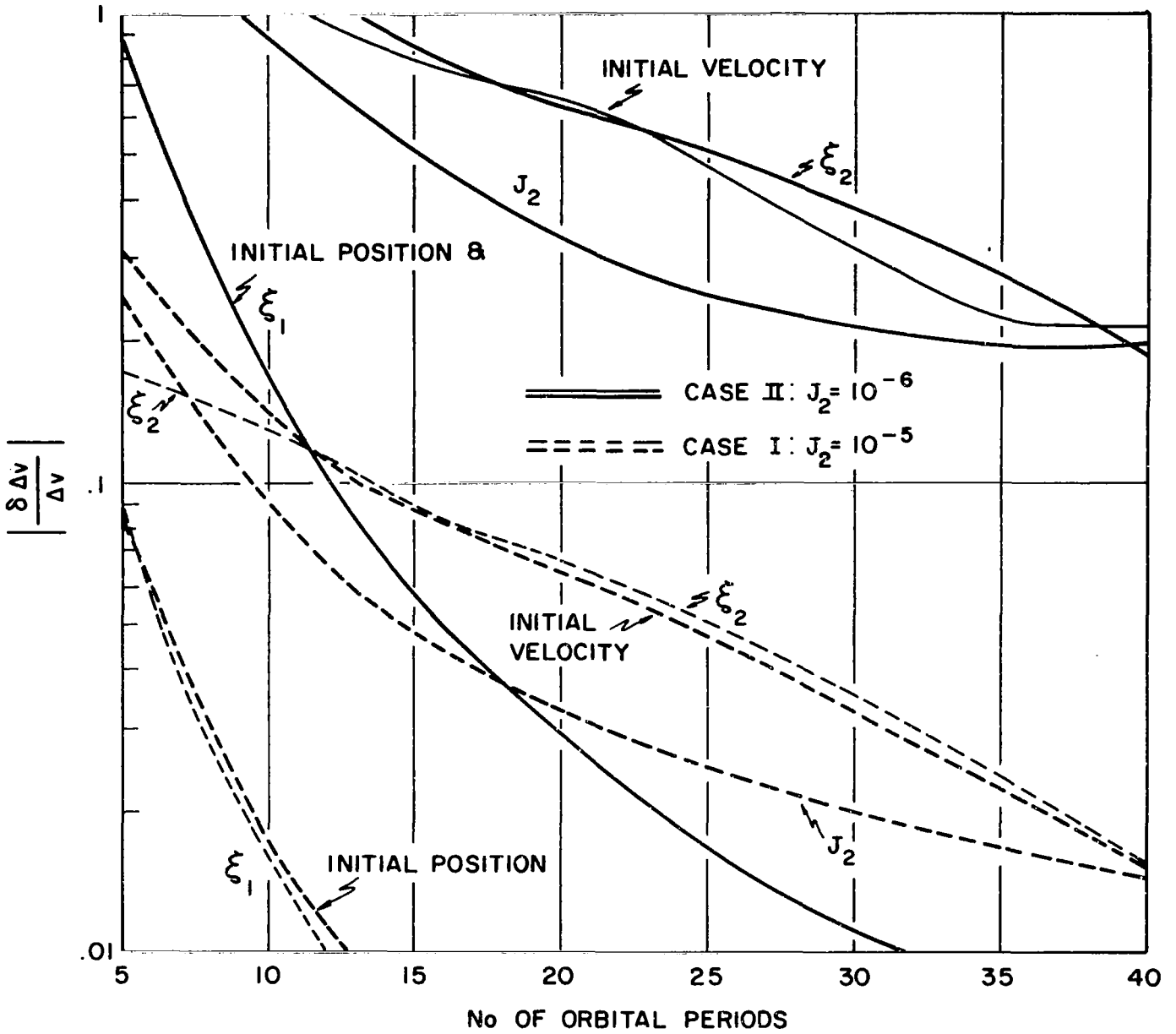

Figure 17: Fractional Error in Ejection Speed Which Implies a Systematic Error in Output Parameters Equal in Magnitude to its Random Error. Case I and II.

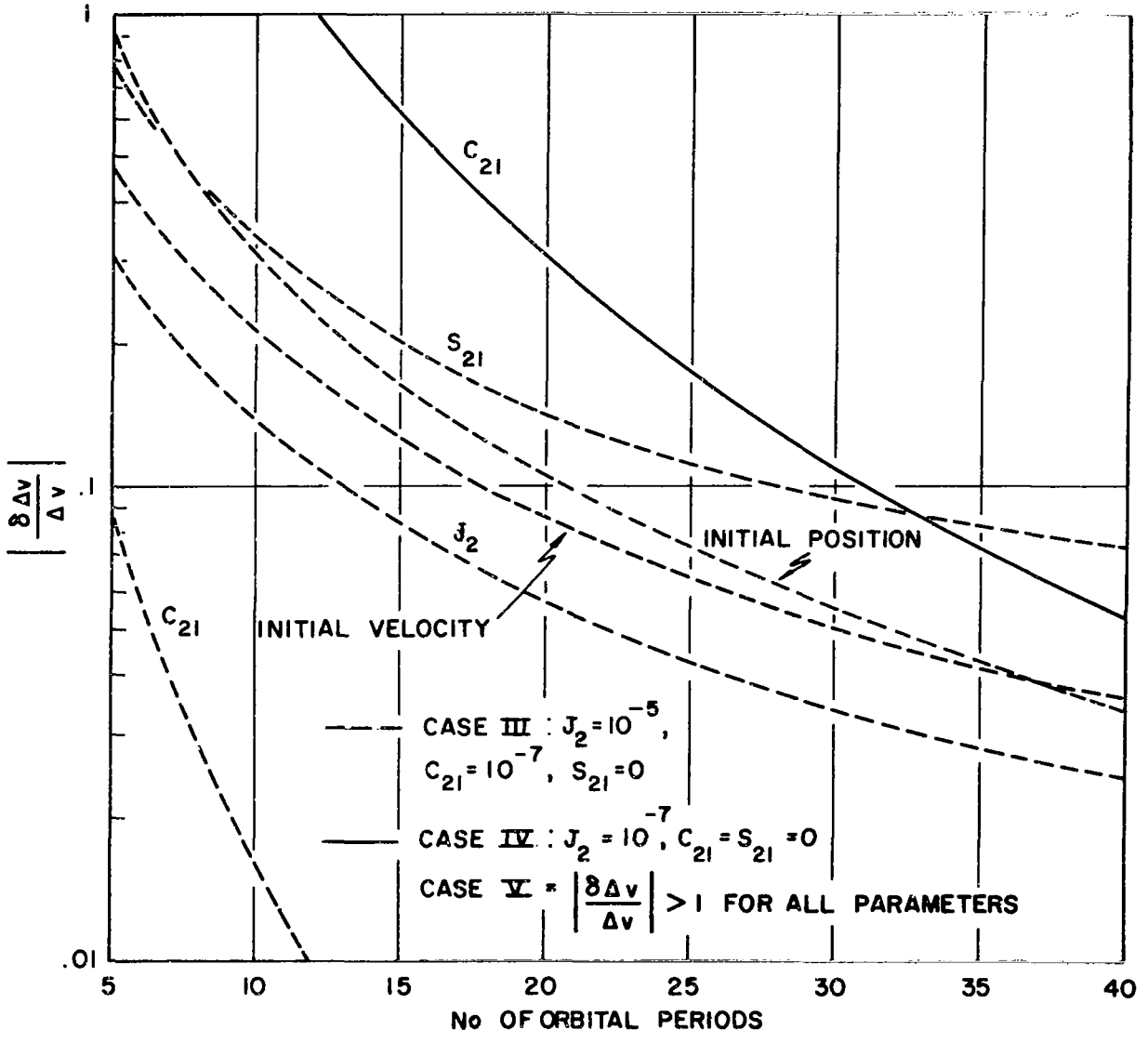

Figure 18: Fractional Error in Ejection Speed which Implies a Systematic Error in Output Parameters Equal in Magnitude to its Random Error. Case III, IV, and V

TABLE XIV: Initial Position, Velocity, and Orbital Elements of Orbits 1, 2, and 3

Parameter	Orbit 1		Orbit 2		Orbit 3	
	S/C	Probe	S/C	Probe	S/C	Probe
x (km)	2160	2160	1935	1935	1797.3	1797.3
y (km)	0	0	0	0	0	0
z (km)	0	0	0	0	0	0
$\dot{x}$ (km/hr)	0	2.828	0	2.828	0	2.828
$\dot{y}$ (km/hr)	2844.16	2841.71	3004.974	3002.524	3117.963	3115.513
$\dot{z}$ (km/hr)	4926.23	4927.65	5204.767	5206.182	5400.470	5401.884
a (km)	2400	2400.00145	2150	2150.00116	1997	1997.001
e	.1	.100002	.1	.100002	.1	.1
i	60^{o}	60.03^{o}	60^{o}	60.03^{o}	60^{o}	60.03^{o}
Ω	0	0	0	0	0	0
ω	0	$-.31^{o}$	0	$-.29^{o}$	0	$-.29^{o}$
T_p (hr)	0	-.002	0	-.002	0	-.001
Period (hr)	2.930	2.930	2.484	2.484	2.224	2.224
h_p (km)	421.91	421.91	196.91	196.91	59.21	59.21
h_a (km)	901.91	901.92	626.91	626.92	458.61	458.61

of C_{ji} and S_{ji}, but over a time duration of 25 orbital periods, it is roughly 1.32 kilometers for Orbit 1 and 1.12 kilometers for Orbit 2. These distances are small because of a judicious choice of the ejection direction. In general, no secular dependence will be present in the distance between the probe and spacecraft if a zero component of velocity in the direction which is tangent to the spacecraft's orbital path is given to the probe. Thus, if a zero tangential component is achieved, the distance between the probe and spacecraft will be oscillatory and bounded. However, a non-zero component causes this distance to increase roughly linearly with time. For Orbits 1, 2, and 3 the probe was ejected so that equal velocity components were given in the radial and normal directions of the orbit and the ejection speed was 4 km/hr.

In Table XV, we present the four cases for which we will give results. The values of C_{ji} and S_{ji} were taken from Reference [4]. In all cases we set $C_{21} = C_{41} = C_{42} = C_{33} = C_{43} = C_{44} = S_{32} = S_{33} = S_{44} = 0$. Case 2 utilizes the same orbit as Case 1. Cases 3 and 4 are the same as 2 except that 3 utilizes a lower altitude orbit, while 4 utilizes the lowest altitude orbit (Table XIV).

TABLE XV: Cases for Which Numerical Results will be Given (Multiply all values by 10^{-4})

Constant	Case 1	Case 2	Case 3	Case 4
C_{20}	-2.07	-2.07	Same as Case 2	Same as Case 2
C_{30}	.4461	.4461		
C_{40}	.2089	.2089		
C_{31}	.4346	.4346		
C_{22}	.2761	.2761		
C_{32}	0	-.0522		
S_{21}	-.4106	-.4106		
S_{31}	.1701	0		
S_{41}	-.1018	-.1018		
S_{42}	0	-.0834		
S_{43}	0	-.0259		
Orbit No.	1	1	2	3
Total No. of Unknowns	16	18	18	18

The unknowns of the problem are the position and velocity of the spacecraft at the time of ejection, the direction of ejection, and the potential parameters that are not identically zero in Table XV.

For all results presented on the moon problem we chose to utilize 10 sightings of the probe per orbital period of the spacecraft. Each sighting yields two equations.

Effect of Random Error in Direction

Let us now investigate the effect of random error in the measurement of the direction of the probe as seen from the spacecraft. These errors will imply an error in each of the outputs.

Let us restate our major assumptions as follows:

(1) No systematic error exists, and the only error source is random errors in each measured direction to the probe.

(2) The expected value of each measured angle is its true value.

(3) The error distributions of each measured angle are independent and identical with a standard deviation of 10 seconds of arc.

(4) The random input errors are so small that each output error is a linear combination of the input errors.

(5) Ten sightings per orbital period are made. Each sighting implies two equations.

In Figure 19 we plot the initial position and velocity errors of the spacecraft due to the random input errors as a function of the number of orbits of the spacecraft. From this figure we note the following trends:

(1) As the number of unknowns increases (Case 1 to Case 2), the position and velocity errors increase.

(2) As the orbital altitude is lowered (Case 2 to Case 3), the position errors decrease, but the velocity errors increase. In order not to crowd the graph, Case 4 (the lowest altitude orbit) is not shown, but its plot supports this conclusion.

(3) The improvement in accuracy is rather gradual after 15 spacecraft orbital periods.

In Figures 20, 21, and 22 we plot the normalized errors in the parameters for Cases 1, 2, and 3, respectively. Here we define normalized error as $\tilde{C}_{ji} = |\sigma(\delta C_{ji})/C_{ji}|$, with similar definitions for the S's. Results for Case 4 are not plotted, but a comparison of Cases 2, 3, and 4 is given in Table XVI. These three figures and the table yield the following generalization:

(1) The potential parameter errors increase as the number of unknowns increases (Case 1 to Case 2).

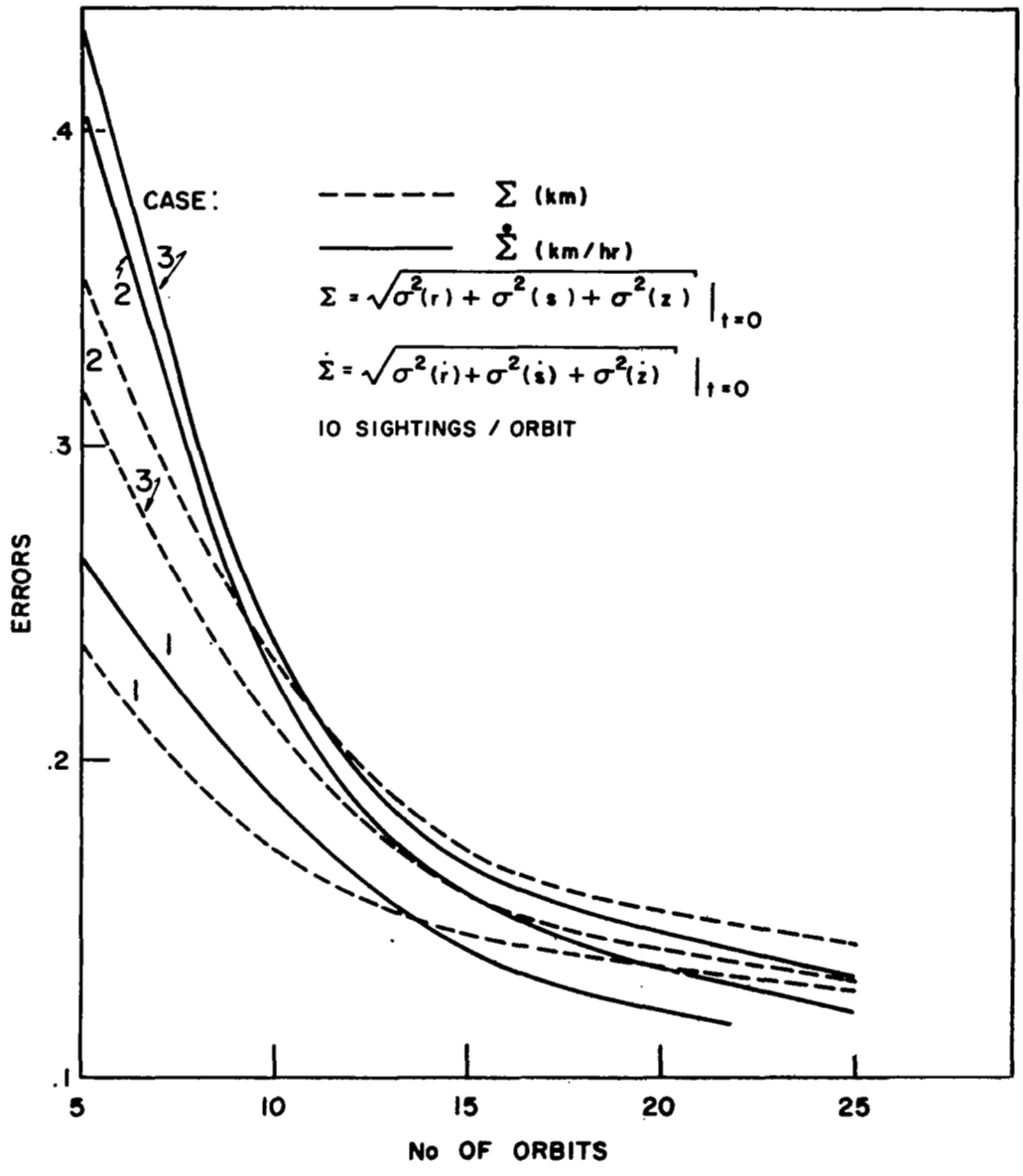

Figure 19: Σ and $\dot{\Sigma}$ as Function of Number of Orbits Over Which Data is Taken. Cases 1, 2 and 3

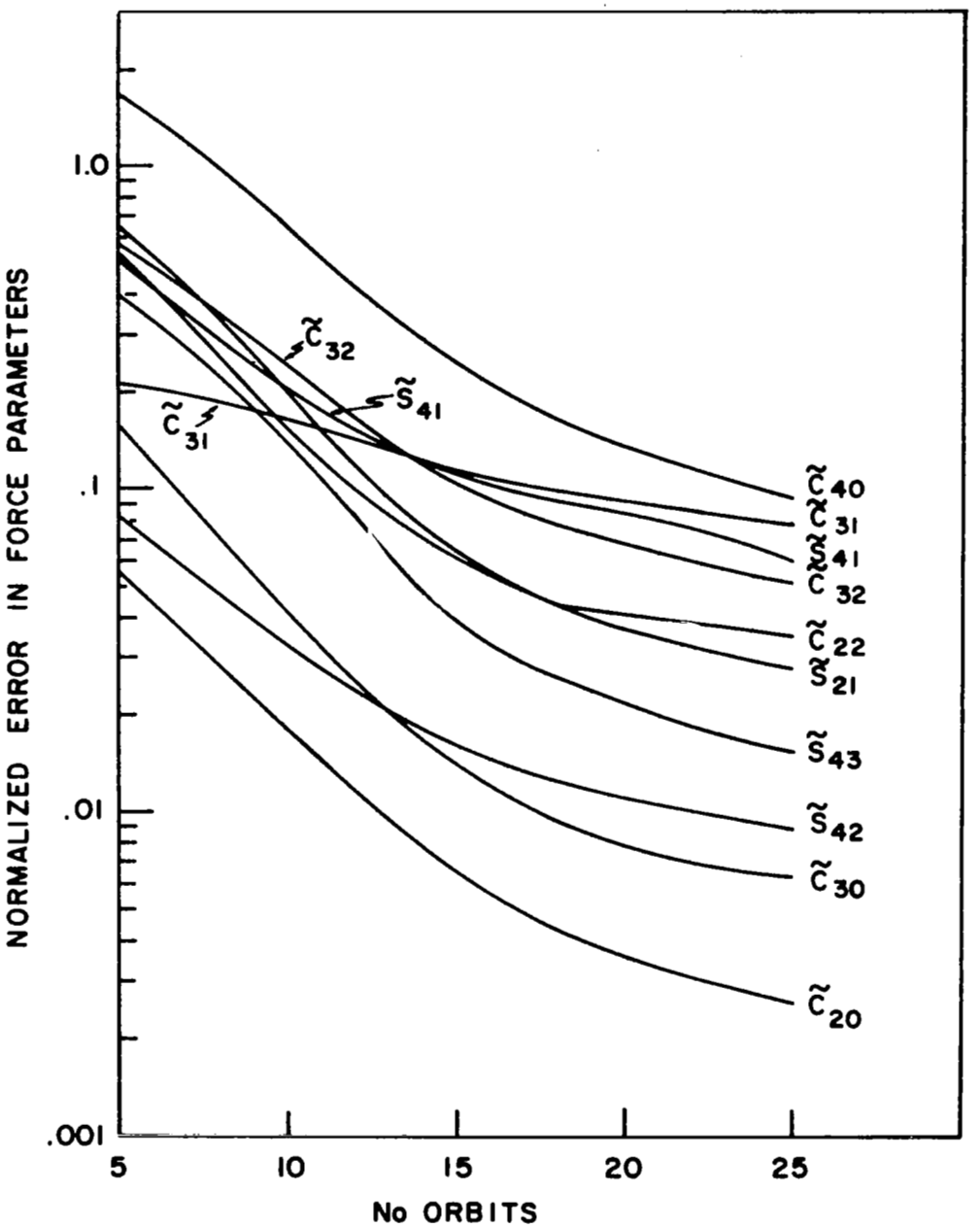

Figure 20: Normalized Error in Parameters as a Function of Data Interval. Case 1

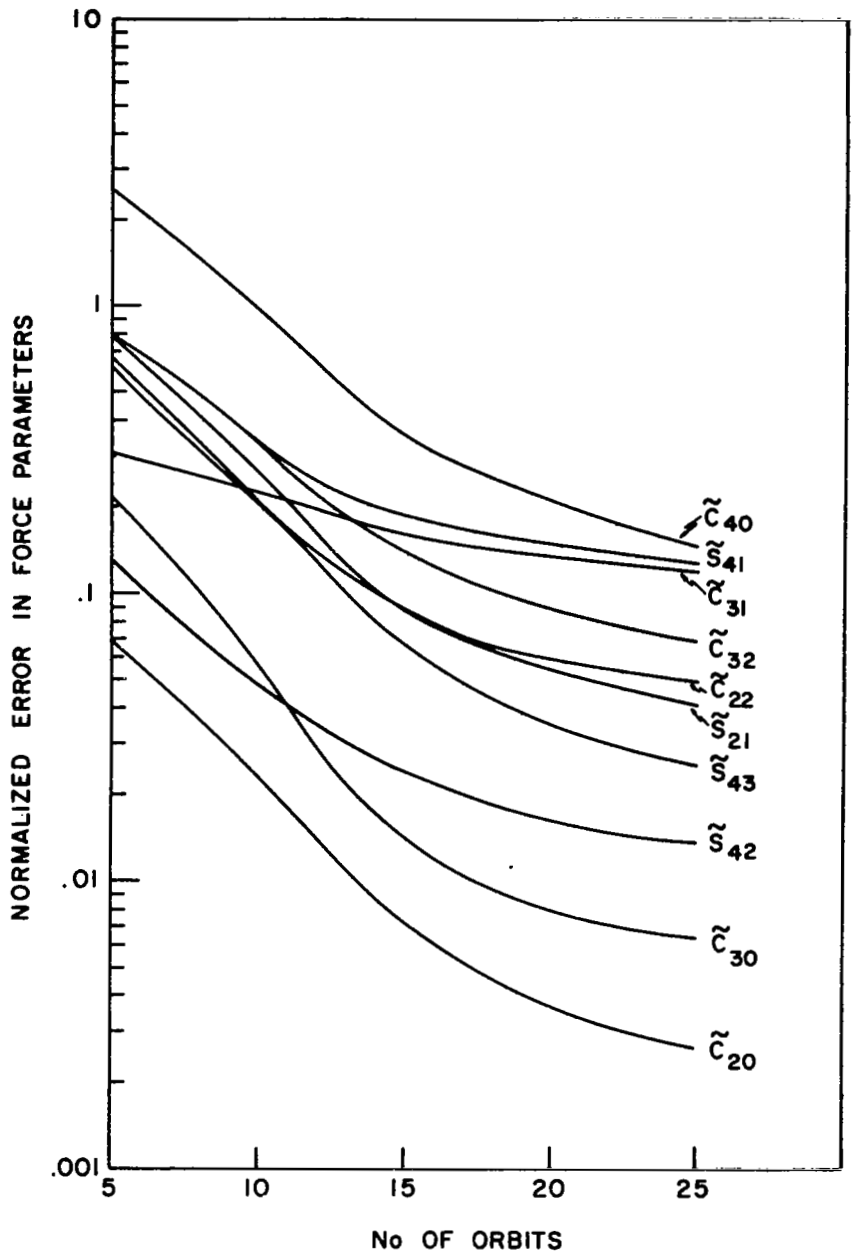

Figure 21: Normalized Error in Parameters as a Function of Data Interval. Case 2

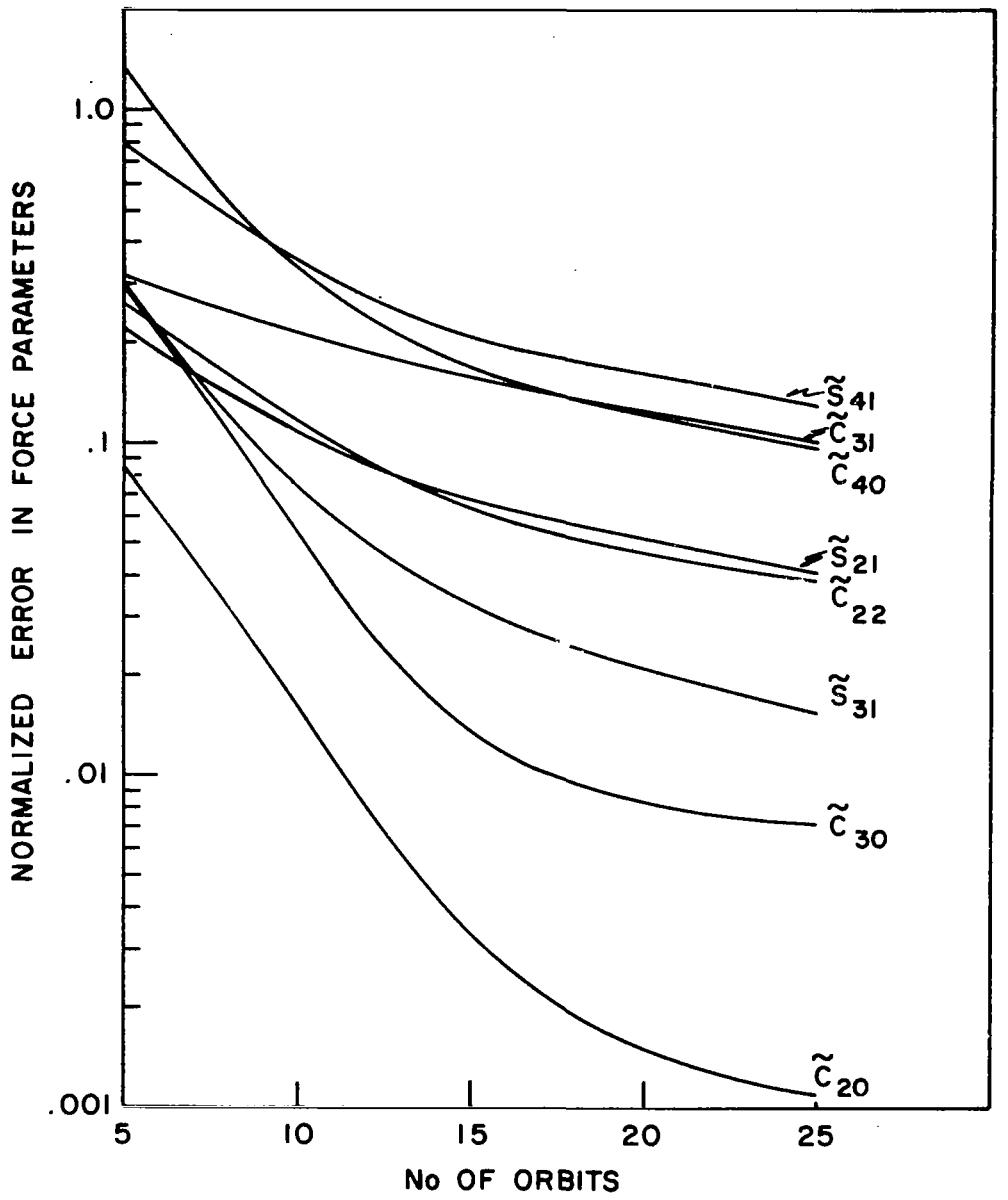

Figure 22: Normalized Error in Parameters as a Function of Data Interval. Case 3

TABLE XVI: Comparison of Results of Cases 2, 3, and 4. Data gathered over 25 Orbital Periods.

Parameter	Case 2	Case 3	Case 4
Σ (km)	.142	.131	.124
$\dot{\Sigma}$ (km/hr)	.121	.131	.137
$\tilde{C}_{20}$	.00270	.00253	.00250
$\tilde{C}_{30}$	.00633	.00640	.00630
$\tilde{C}_{40}$	.147	.0947	.0727
$\tilde{C}_{31}$	.117	.0788	.0567
$\tilde{C}_{22}$	.0491	.0357	.0299
$\tilde{S}_{21}$	.0423	.0285	.0226
$\tilde{C}_{32}$	.0664	.0515	.0435
$\tilde{S}_{41}$	.126	.0725	.0473
$\tilde{S}_{42}$	.0113	.00885	.00680
$\tilde{S}_{43}$	.0250	.0157	.0118

(2) As the orbital altitude is lowered (Case 2 to Case 3 to Case 4), the parameter errors decrease. A significant decrease is obtained in all parameters except C_{20} and C_{30} (see Table XVI).

(3) Again the improvement is gradual after 15 orbital periods.

(4) The improvement in accuracy of C_{31} is somewhat different from the other parameters in the interval from 5 to 15 orbital periods. Our conjecture for the cause of this more gradual improvement is the spacing of the sightings. Note that a factor of C_{31} in (20) is cos θ. Now, the ejection was placed at $\theta = 0$, and the probe nearly returns to the spacecraft for $\theta = 2\pi n$, $n = 1, 2, \ldots$. For this reason, no sightings were allowed within 36° of $\theta = 2\pi n$, which in turn generally implies a smaller coefficient of C_{31} than the other parameters at the time of probe sightings.

In Table XVII, we compare $\sigma(\delta C_{ji})$ and $\sigma(\delta S_{ji})$ as obtained by our analysis (Case 3, 25 orbits) with those values reported by Lorell and Sjogren in Reference [12]. The values of the standard deviations from Reference [12] were estimated from the residuals obtained from actual data furnished by Lunar Orbiters I-IV.

TABLE XVII: Comparison of Standard Deviations of Parameters Obtained by Probe Sighting and Lunar Orbiter Analysis

Standard Dev. x 10^6

Parameter	Probe Sighting	Lunar Orbiter	Probe/Orbiter
C_{20}	0.52	1.43	.36
C_{30}	0.29	2.62	.11
C_{40}	1.98	1.90	1.04
C_{31}	3.43	0.25	13.7
C_{22}	0.98	2.49	.40
C_{32}	.27	0.58	.46
S_{21}	1.17	1.39	.84
S_{41}	0.74	0.51	1.45
S_{42}	0.07	0.35	.20
S_{43}	0.04	0.15	.27

From Table XVII, we see that our method compares fairly well with radar measurements. However, our error in C_{31} is about 14 times larger. Moreover, we have not included the systematic errors which will arise in our method if an error in ejection speed is present. This point will now be considered.

Effect of Error in Ejection Speed

Thus far, we have assumed the ejection speed is given by $\Delta v = 4$ km/hr and was error-free. Let us now assume the ejection speed is in error so that $\delta\Delta v = .04$ km/hr. It seems reasonable that an ejection mechanism can be built so that $|\delta\Delta v| < .01\,\Delta v$.

In general, if an error in ejection speed exists, a systematic error in each output will result. In Figures 23, 24, and 25 we plot the systematic error in the outputs as a function of time. Also shown are the "one-sigma"

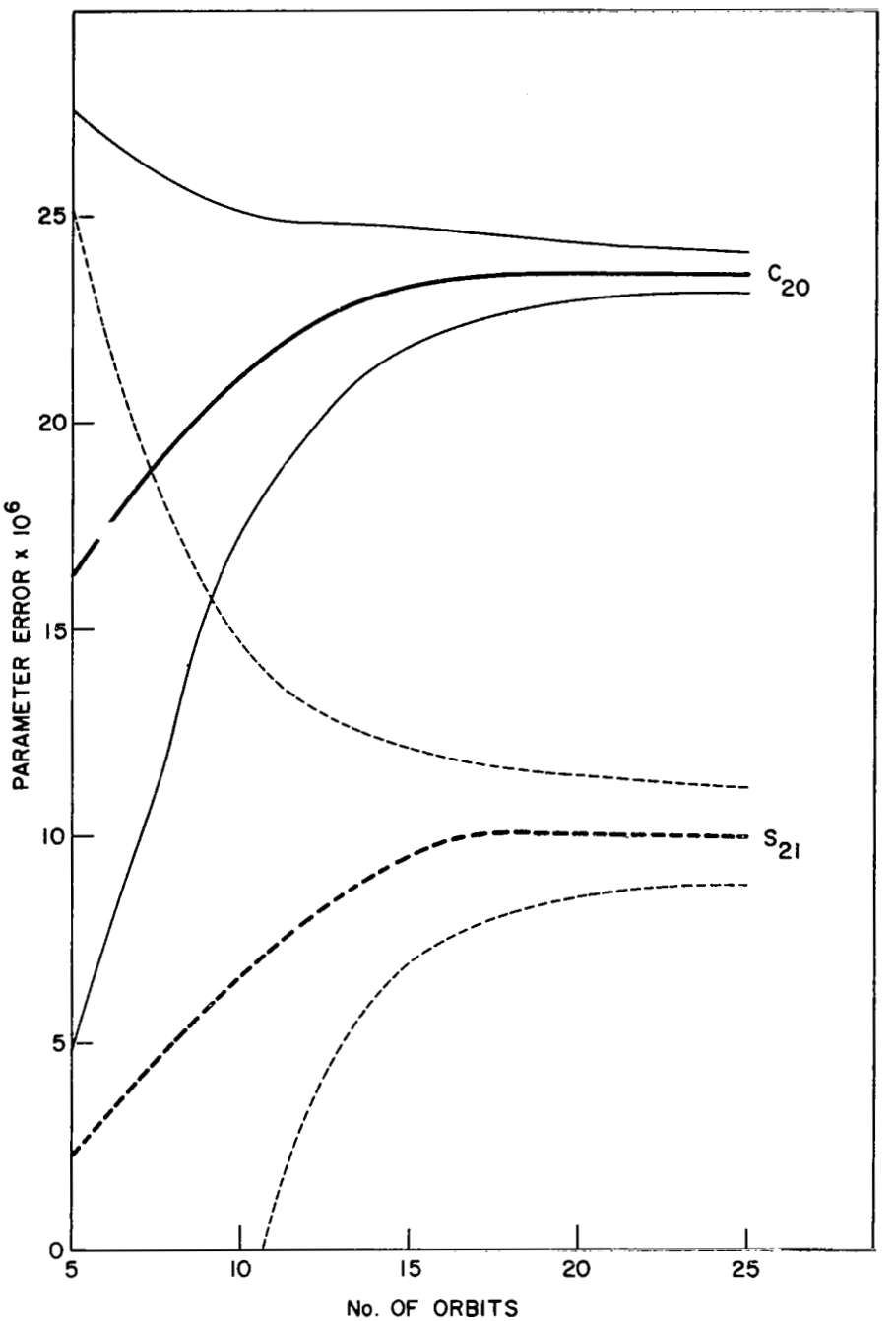

Figure 23: Mean Error and One Sigma Bounds for C_{20} and S_{21}. Case 3. $\delta\Delta v = .01\ \Delta v$

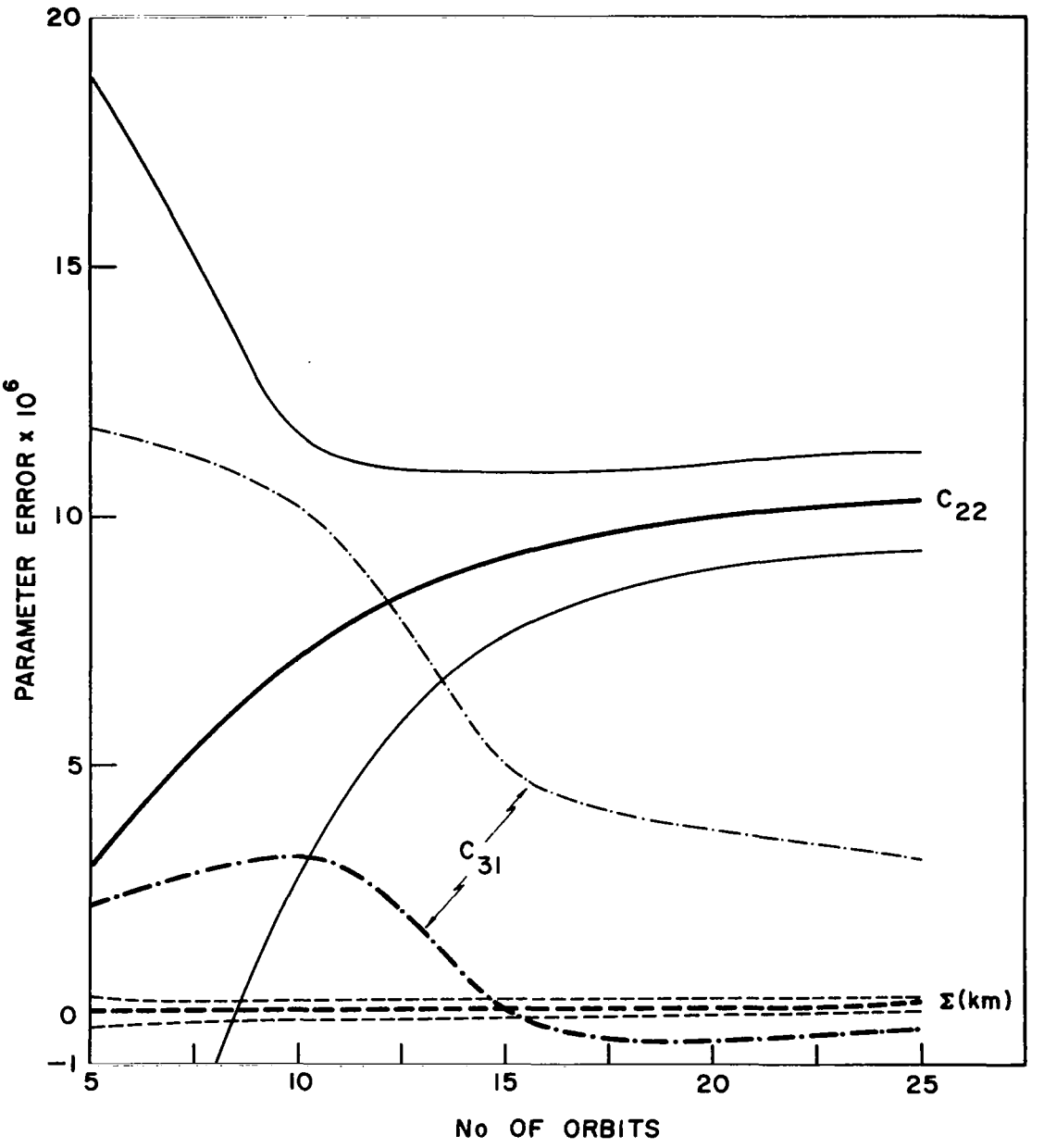

Figure 24: Mean Error and One Sigma Bounds for C_{22}, C_{31}, and Σ. Case 3. $\delta\Delta v = .01\ \Delta v$

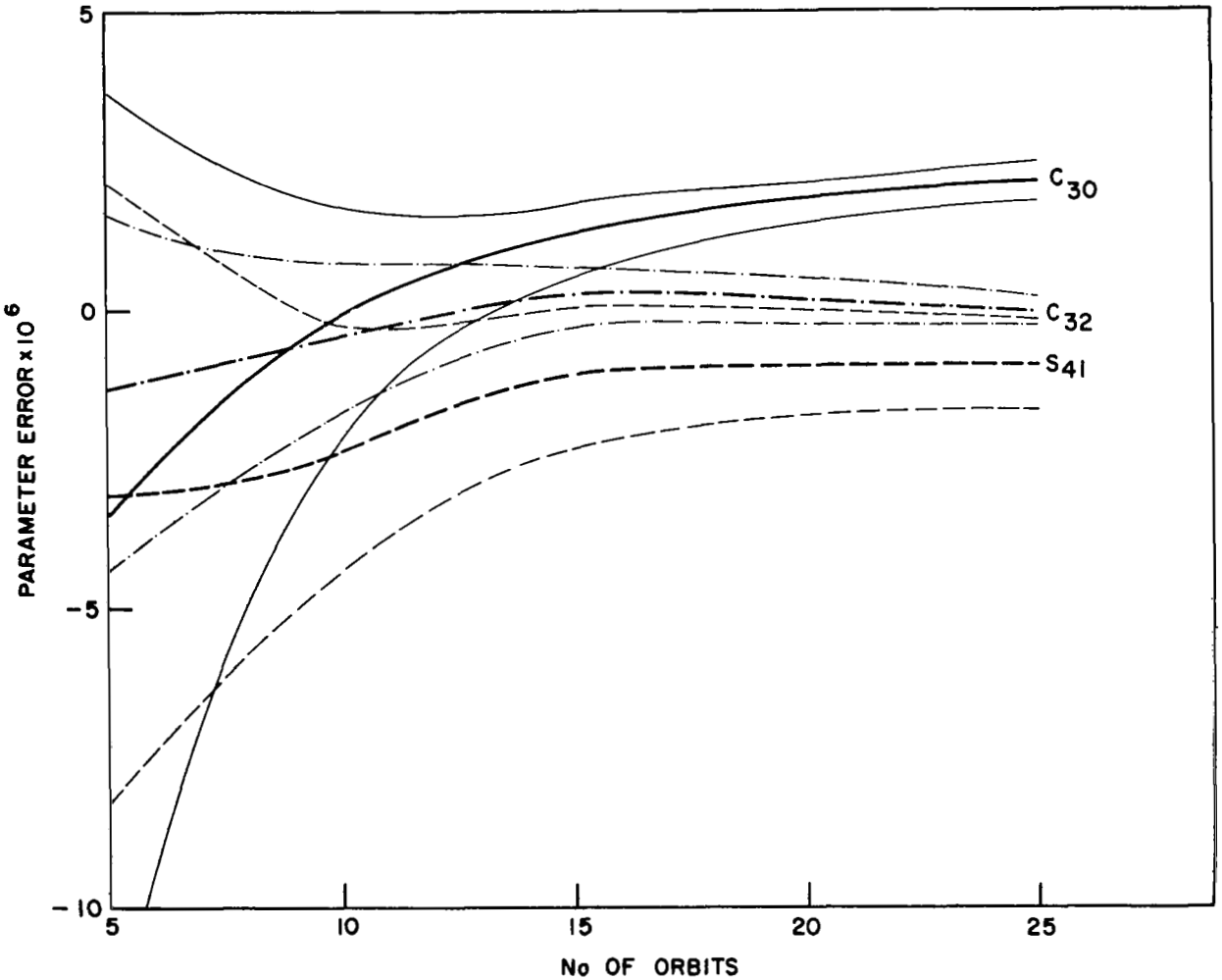

Figure 25: Mean Error and One Sigma Bounds for C_{30}, C_{32}, and S_{41}. Case 3. $\delta\Delta v = .01\,\Delta v$.

error bounds about the mean error. Case 3 is studied in these figures.

From Figure 23 we note that the mean error in C_{20} increases as more data is utilized, but the variance about the mean due to the random error decreases. Similar remarks are true for the other parameters. In these figures we omitted the parameters C_{40}, S_{21}, and S_{43}, but their behavior is quite similar to that exhibited in Figure 25.

EARTH ORBITS

Thus far, the only perturbing forces we have considered were those which arise from a potential. With each harmonic in the potential, there was an associated unknown.

In studying the application of our method for orbits about the earth, we will assume the potential is represented by three zonal harmonics such that the parameters J_2, J_3, and J_4 are known beforehand. Additional perturbing forces due to drag and radiation pressure will be allowed. These nonconservative forces will introduce two unknowns.

Two orbits will be used, a low altitude (632 kilometers) and a synchronous altitude orbit. The orbital parameters of the spacecraft are listed below. In all cases, five sightings per orbit will be utilized.

Orbit Elements	a	e	i	ω	Ω	t_p
Low Altitude	7,000 km	0	60^o	0^o	0^o	0
High Altitude	41,800 km	0	0^o	0^o	0^o	0

Let us now briefly discuss the forces produced by drag and radiation pressure.

Drag

The acceleration acting on a satellite caused by atmospheric drag may be approximated by

$$\bar{a}_d = - (1/2\ m)\ \rho\ v^2\ A_D C_D\ \hat{v}$$

where ρ = density of the atmosphere at the satellite,

A_D = cross-sectional area of satellite perpendicular to $\hat{v}$,

C_D = drag coefficient,

v = air speed,

$\hat{v}$ = unit vector in direction of satellite velocity with respect to atmosphere, and

m = mass of satellite.

If we assume the atmosphere rotates with the Earth as a rigid body, then

$$v\ \hat{v} = \dot{\bar{R}} - |\bar{R}|\ \Omega \cos \delta\ \hat{e},$$

where Ω = angular rotation rate of the Earth about its axis = $7.29215506 \times 10^{-5}$ rad/sec,

δ = declination of satellite,

$\hat{e}$ = unit vector in local East direction,

$\bar{R}$ = position vector of satellite.

The drag coefficient, C_D, is not constant, but is a function of angle of attack, temperature, and velocity. A brief, but enlightening, discussion of this parameter is given in Reference [13].

Here we will assume $c_d = \rho\ C_D$ is constant, but unknown. Hence,

$$\bar{a}_d = - (c_d\ A_D\ v^2/2\ m)\ \hat{v}.$$

Radiation Pressure

The acceleration of a satellite due to radiation pressure is given by

$$\bar{a}_p = - 1/m\ \gamma\ \nu\ P\ A_p\ \hat{s},$$

where γ = a factor which depends on the reflecting properties of the satellite,

= $1 + .5\lambda$, for a diffuse reflector,

= $2 - 2\lambda/3$, for a specular reflector; here

λ is the albedo of the satellite.

ν = 1, if satellite is sunlit,

= 0, if not sunlit,

P = solar radiation pressure in the vicinity of the Earth (approximately 4.5×10^{-5} dynes/cm^2),

A_p = cross-sectional area of satellite perpendicular to $\hat{s}$, and

$\hat{s}$ = unit vector in direction of sun.

Here we will assume P is constant, but unknown. Nominal parameters for drag and radiation pressure chosen here are listed in Table XVIII.

TABLE XVIII: Drag and Radiation Pressure Parameters

Parameter	Spacecraft	Probe
m	3000 kg	.3 kg
P	4.5×10^{-5} (dynes/cm^2)	4.5×10^{-5} (dynes/cm^2)
$A_D = A_p$	8×10^4 cm^2	40 cm^2
C_D	2.2	2.2
Reflector	specular	specular
λ (albedo)	0.5	0.9
$\gamma P A_p/m$	10^{-6} ν cm/sec^2	4.2×10^{-6} ν cm/sec^2
ρ (low alt.)	5.5×10^{-16} g/cm^3	5.5×10^{-16} g/cm^3
ρ (high alt.)	0	0
$\frac{\rho A_D C_D}{2m}$ (low)	1.613×10^{-17}/cm	1.473×10^{-16}/cm

The values of mass and area in Table XVIII imply that if the spacecraft and probe were spherical, then

spacecraft radius = 1.12 meters,

probe radius = 2.52 cm = 1 inch

mean spacecraft density = .498 g/cm^3, and

mean probe density = .141 g/cm^3.

Numerical Results for Earth Orbits

For our first case, let us consider the low altitude (a = 7000 kilometers) orbit. As with the case of the Moon, let the probe be ejected with no tangential component of velocity. Also, let Δv = 4 km/hr and $\delta \Delta v$ = .04 km/hr. This error in ejection speed will produce a systematic error in each output parameter. Moreover, a random error will also exist because of random errors in the measurement of the probe's direction. As before, these random errors in direction will be chosen with a standard deviation of 10 seconds of arc.

Our present problem has 10 unknowns: six define the initial position and velocity of the spacecraft, two define the radiation and drag parameters, and finally, two are parasitic and define the probe ejection direction.

Five sightings per orbital period of the spacecraft will be used. Each sighting will yield two equations.

Figure 26 is a plot of the mean error in initial position and the mean error in the initial velocity as a function of the number of orbits over which the measurements are taken. Also shown are the one sigma error bounds about the mean. These errors about the mean are produced by random input errors. Note that the random errors are almost insignificant compared to the systematic errors. Also, the systematic error in initial velocity increases quite rapidly as data over a longer interval is utilized.

In Figure 27 we plot the normalized systematic error in the radiation pressure and drag parameters. The random error in these parameters is about 10^{-2} times the systematic error and hence too small to be shown in this figure. Note the error in the radiation pressure parameter, δP, is almost as large as P. However, for the drag parameter $\delta c_d \doteq 10^{-3} c_d$ so the measurements will yield a good estimate of the product ρC_D. Note that only the product is calculable and not the individual factors.

It is not surprising that the $\delta P/P \gg \delta c_d/c_d$, for the acceleration due to drag is about 20 times greater than that due to radiation pressure. Moreover, no effect is produced by solar radiation over about 1/3 of each orbit.

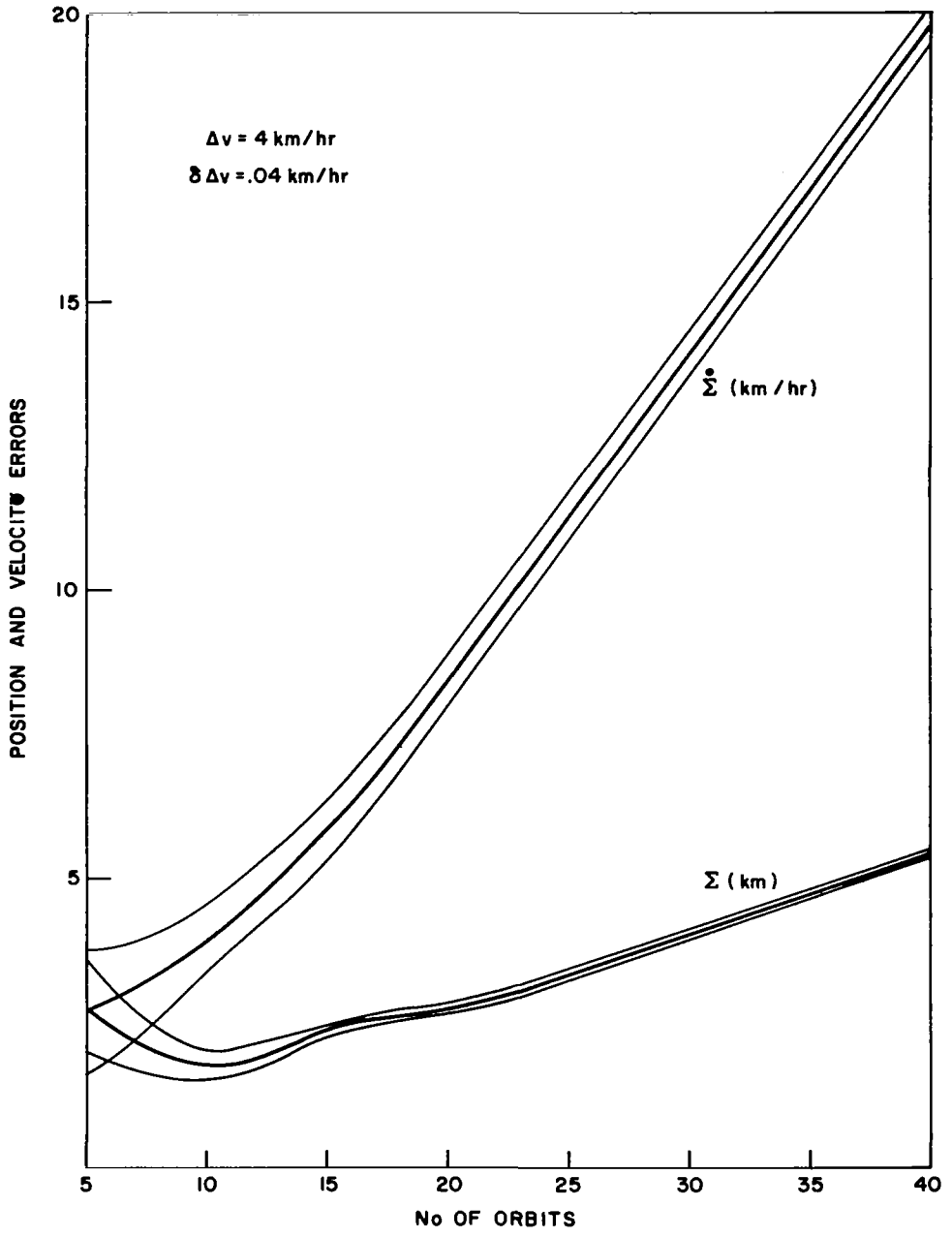

Figure 26: Mean Error and One Sigma Bounds for Initial Position and Velocity Errors. Low Altitude Earth Orbit

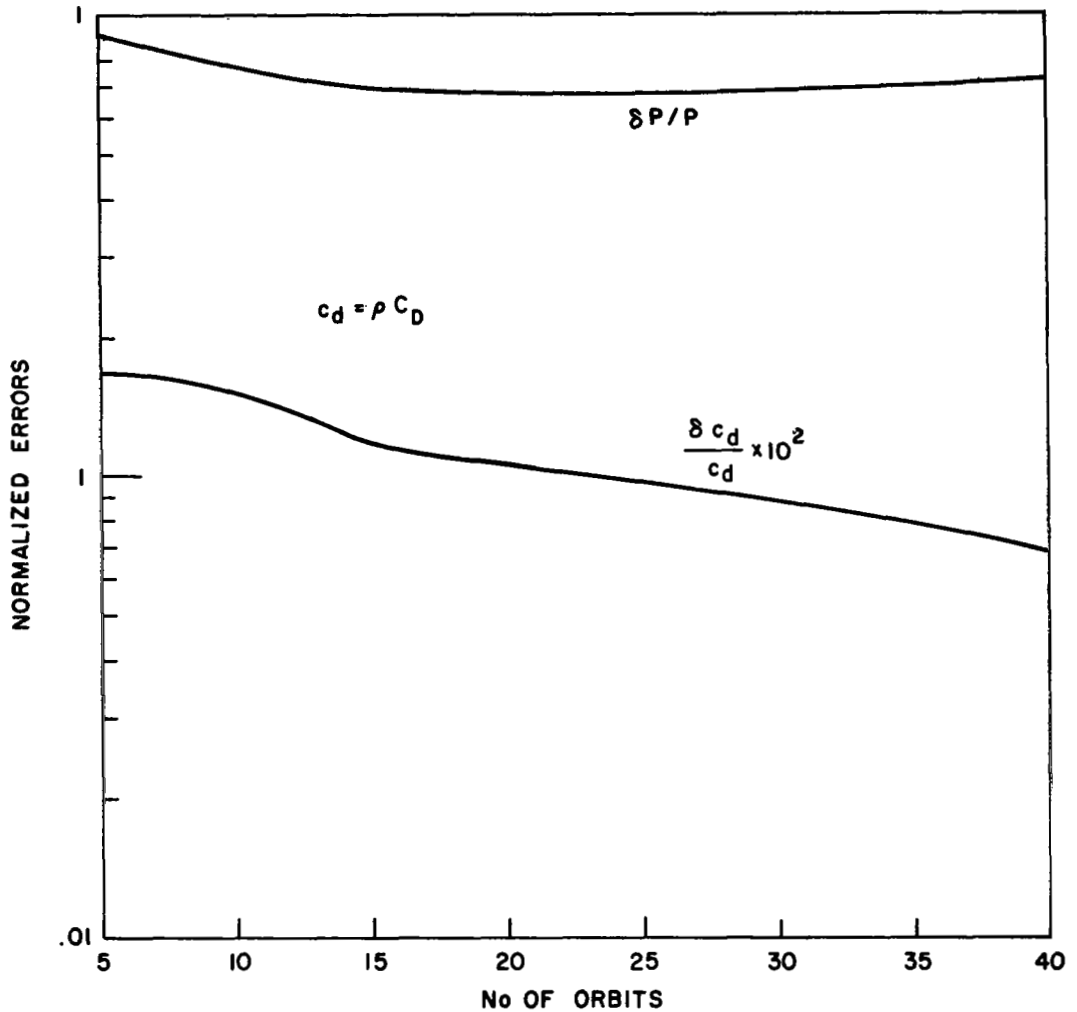

Figure 27: Normalized Errors in Drag and Radiation Parameters Caused by an Error in Ejection Speed. $\Delta\delta v$ = .04 km/hr Low Altitude Earth Orbit.

Since the effect of a systematic error in ejection speed outweighs the effect of random measurement errors in the previous case, it is highly desirable to reduce or eliminate the ejection speed error. We propose to accomplish this elimination by releasing the probe with zero differential speed, i.e., $\Delta v = \delta\Delta v = 0$. Drag and radiation pressure then is allowed to separate the spacecraft and probe. It is argumentative as to whether or not such a release is possible, but we will assume it is here.

The total problem has now only eight unknowns, for we lose the two unknowns associated with the ejection direction.

In Figure 28 we then plot the errors in initial position and velocity due to the random errors. Two orbital cases are shown: the low altitude case and the high altitude (synchronous). Note that the errors decrease with more measurements and are considerably less than those shown in Figure 26. Also note the plot begins at 10 orbits instead of five orbits. This is because no measurement was allowed if the distance between the probe and spacecraft was less than 100 meters. If this restriction were not imposed, parallax may produce an additional error. After five orbits, the distance between the probe and spacecraft for the low and high orbits is 420 and 910 meters, respectively. In Figure 29, we plot the normalized error in radiation and drag parameter for the low altitude orbit, and the noramlized error in the radiation parameter for the high altitude orbit. It was assumed $c_d = 0$ for the high altitude orbit.

Note that for the low altitude orbit the normalized drag error is about 10^{-2} times the normalized radiation pressure error. But, the normalized radiation pressure error for the high altitude orbit is smaller than either error in the low altitude case.

In conclusion, it appears that probe sightings are quite effective in calculating the parameters associated with drag and radiation pressure if systematic error in ejection speed can be avoided.

As a final note of interest, we plot the distance between the probe and spacecraft as a function of time for the three cases. We offer the following explanation for the somewhat strange behavior shown in Figure 30.

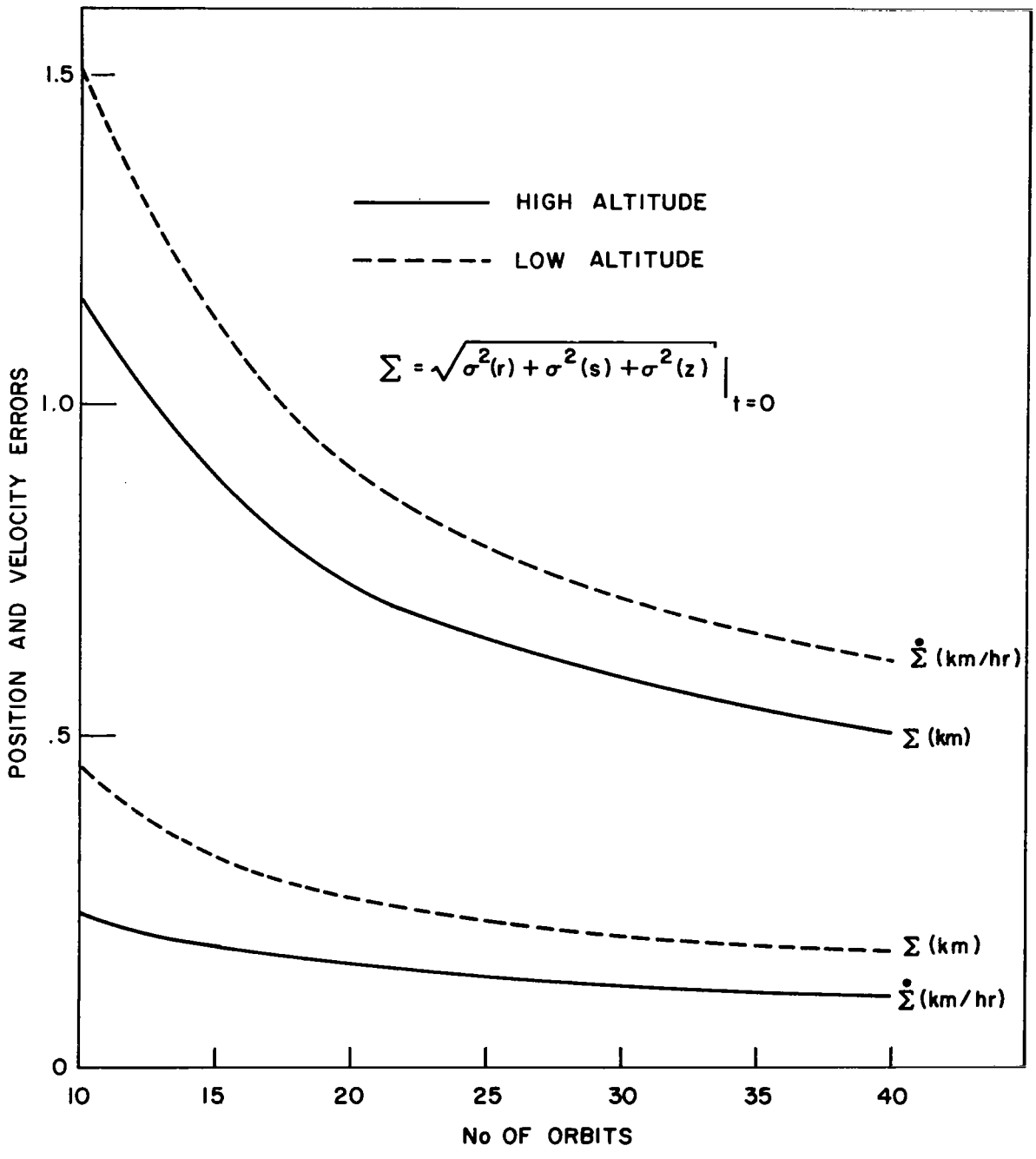

Figure 28: Initial Position and Velocity Errors for Low and High Altitude Earth Orbits. $\delta\Delta v = \Delta v = 0$

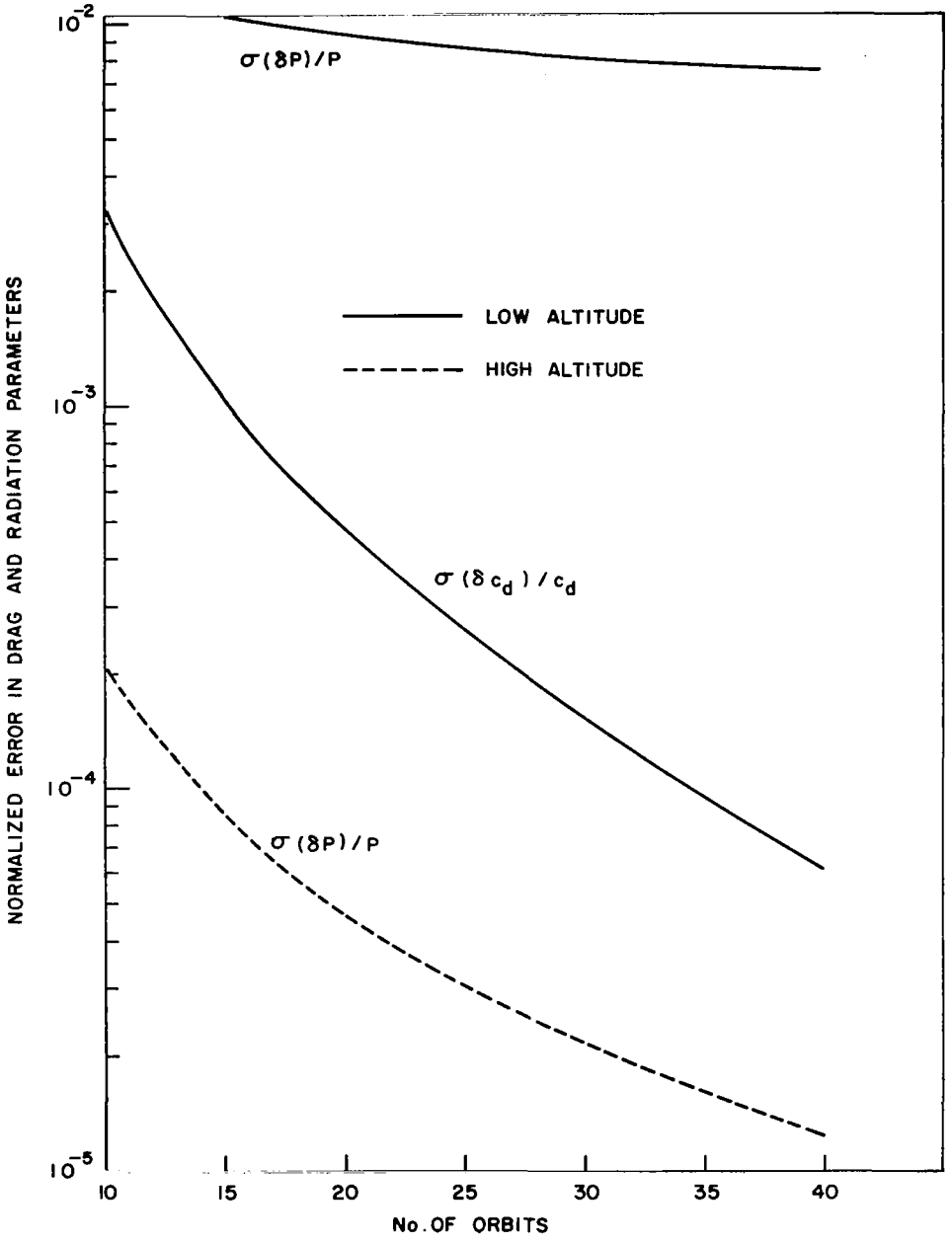

Figure 29: Normalized Error in Drag and Radiation Parameters Caused by Random Measurement Errors. $\delta\Delta v = \Delta v = 0$

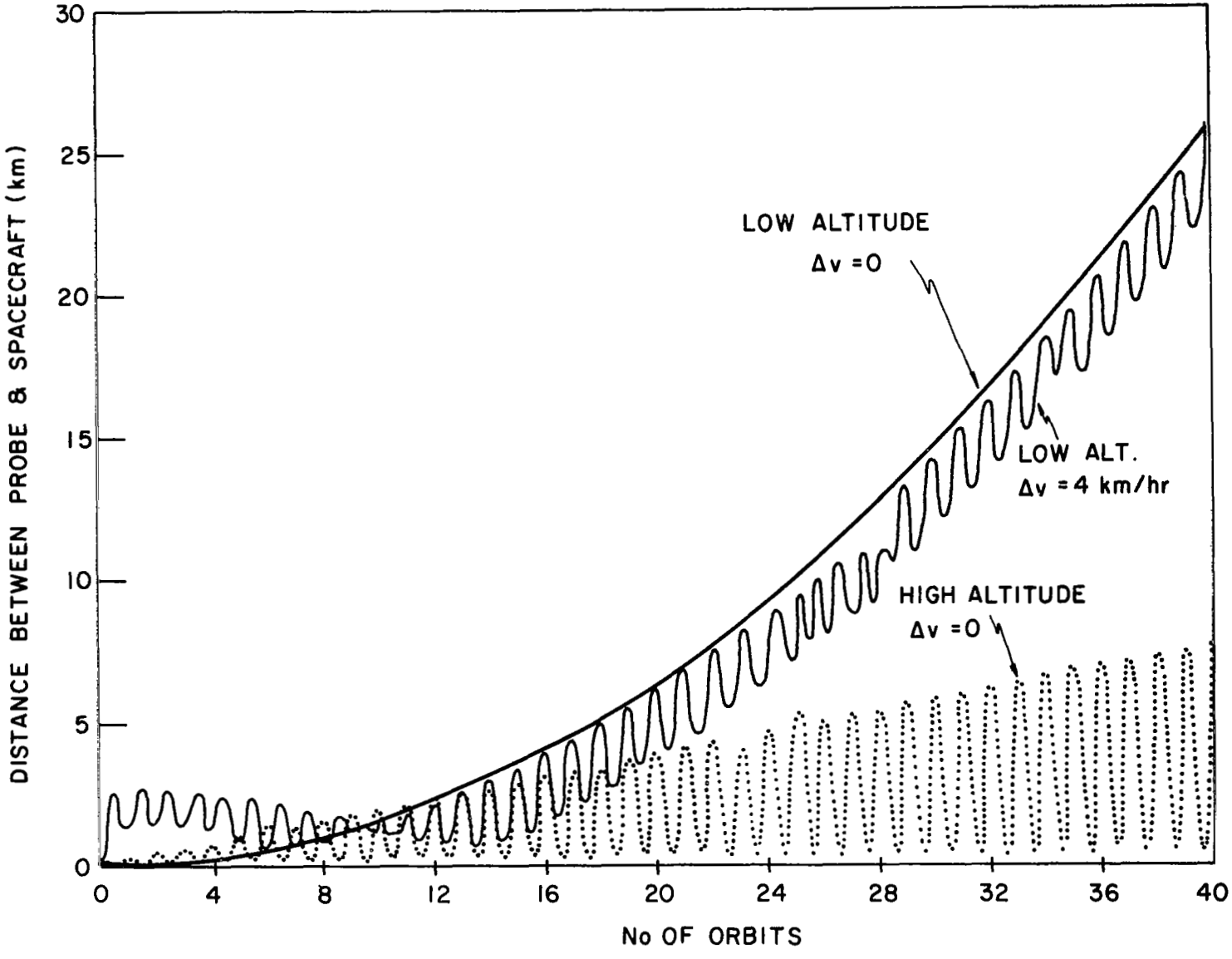

Figure 30: Distance Between Probe and Spacecraft as a Function of Time. Three Cases

(1) For the high altitude orbit in which the ejection speed is zero ($\Delta v = 0$), the only effect which separates the probe and spacecraft is the differential radiation pressure. But radiation pressure is approximately in the direction of motion over one-half the orbit and opposite the direct over the other one-half orbit. Hence, the distance may be expected to be oscillatory.

(2) For the low altitude orbit in which Δv, the main effect which causes separation is drag. Drag always acts to oppose the motion. Hence, the separation distance monotonically increases.

(3) If no drag or radiation forces exist, $\Delta v \neq 0$ but small, and ejection is such that no orbital tangential component of velocity is given to the particle, then the separation distance would be oscillatory. If drag and radiation are added, the effect shown in Figure 30 for $\Delta v = 4$ km/hr is reasonable.

CONCLUDING REMARKS

The major results of computer simulations indicating the manner in which instrument measurement errors propagate through the system into errors in the computed quantities is given below.

Mars Navigation Problem (Natural Satellites)

1. For the assumed conditions navigational accuracies ranging from 0.2 to 1.0 kilometer are obtained when viewing either Phobos or Deimos or both.

2. Introducing unknowns associated with the gravitational potential does not significantly degrade the accuracy of the spacecraft orbit determination; however, it does degrade the orbit determination of the artificial satellites (compared with the case in which the perturbing parameters are known).

3. Approximately two or three orbits of observations are needed to get the navigational error down to the region where the improvement is gradual and roughly proportional to the reciprocal of the square root of the number of observations. (Past studies have shown that one orbit is sufficient to arrive at this condition when using a test probe system. The fact that more orbits are taken here is a reflection of the fact that the orbital periods of the bodies being viewed are several times longer than that of the spacecraft orbital period.)

4. As a navigational system, the accuracy when viewing Deimos is poorer than when viewing Phobos. One of the reasons for this is that Deimos is simply further away and the angle errors propagate in proportion to the length of the sight line. Another reason is that Deimos' orbital period is longer and for a given observation time its motion around the central body is smaller.

Mars Perturbing Parameter Problem (Natural Satellites)

J_2, J_3, J_4*.-When the number of unknowns is expanded to include three terms in the gravitational potential (making a total of 15), a well conditioned problem exists: $10^{-7} < \sigma(\delta J_i) < 10^{-4}$, i = 2, 3, and 4.

* Only the unknown parameters are listed.

J_2, J_3, J_4, ξ_1, ξ_2.-Adding the unknown direction of the spin axis, ξ_1 and ξ_2, creates a problem in 17 unknowns. This problem is also well conditioned and the accuracy of the computed direction of the axis of dynamic symmetry varies from 1.0 to 10 minutes of arc. Some of the properties of this type of system are:

a. The terms in the gravitational potential only slowly improve in accuracy as the number of spacecraft orbits over which measurements are made is increased from 10 to 20;

b. The spin axis direction determination is improved by a factor of two to eight by extending the sampling period from 10 to 20 orbits;

c. An inclination of 60° generally produces a solution which is a factor of 10 more accurate than that produced by an inclination of 0; and

d. Changing the spacecraft altitude is not a dominant factor in changing the accuracy with which the unknowns can be computed.

J_2, J_3, J_4, ξ_1, ξ_2, m.-Adding the planetary mass as unknown expands the problem to a total of 18 unknowns. This produces a system which:

a. Errors in the computed spacecraft position become very large;

b. The error in the mass determination is also large;

c. Interestingly, there is no significant change in the accuracy with which the other parameters are computed (compared with the case in which mass was assumed to be known).

d. The addition of a linear measurement (such as would be supplied by radar) will rectify the above deficiency of systems in which mass is an unknown and permit an accurate computation of mass to be made.

Mars Ejected Probe (J_2, J_3, J_4, ξ_1, ξ_2, m)

Probe and Phobos.-Introducing an ejected probe expands the problem to a total of 20 unknowns in that two unknowns associated with the ejection direction must be added. The ejection speed cannot be used as an unknown without ill-conditioning the problem. It is assumed this speed is known exactly.

A significant improvement is obtained by use of the probe in all parameters. Moreover, the orbit of Phobos may be found more accurately by about a factor of four.

Probe Alone.-Deleting sightings of Phobos reduces the probelm to 14 unknowns. No great change in the accuracy of the parameters is obtained except that the error in m is about a factor of two larger.

Venus ($\delta\Delta V \equiv 0$)

J_2, ξ_1, ξ_2.-As J_2 becomes smaller, the errors become larger. The problem is ill-conditioned for $J_2 = 0$.

J_2, ξ_1, ξ_2, m.-Adding the mass of Venus as an unknown does not significantly degrade the determination of J_2, ξ_1, and ξ_2, but does degrade the initial position and velocity. The accuracy of the mass determination is poor and becomes poorer as J_2 becomes smaller. Mass should not be inserted into the problem as an unknown.

J_2, C_{21}, S_{21}.-In contrast to case 1 (J_2, ξ_1, ξ_2) in which ξ_1 and ξ_2 were unknown instead of C_{21} and S_{21}, the errors are almost independent of the magnitude of J_2, C_{21}, and S_{21}. The singularity is thus removed by this formulation.

Venus ($\delta\Delta v \neq 0$)

If an error exists in the ejection speed, a systematic error in each output will result. In general, as the perturbing forces become smaller, the systematic errors become smaller. However, as the time interval over which the measurements are taken is increased, the systematic errors are increased. But, in any event, an error in the ejection speed produced a very small error in the outputs.

J_2, ξ_1, ξ_2.-Consider the ratio of the systematic error in a quantity (produced by an error in ejection speed) to the random error in that quantity (produced by random errors in measuring the direction to the probe). This ratio is relatively large for the initial position and ξ_1 and small for other outputs.

If $|\delta\Delta v| \leq .01\ \Delta v$, then the systematic error in all outputs is relatively small if measurements are made over less than 12 orbits and $J_2 = 10^{-5}$. If $J_2 = 10^{-6}$, then they are relatively small for 32 orbits.

J_2, C_{21}, S_{21}.-For this set of unknowns, C_{21} has the largest relative error, but if $J_2 \leq 10^{-5}$ the systematic errors are relatively small.

Moon

1. The random errors in initial position and velocity are less than 0.2 kilometer and 0.2 km/hr, respectively, after 15 orbits of data collection
2. A higher altitude orbit yields larger errors in the harmonics, except for C_{20} and C_{30}.
3. The errors in the harmonics due to the random input errors have normalized values roughly between 0.1 and 1 after five orbits of data collection, and between 0.01 and 0.1 after 20 orbits.
4. If an error is present in the ejection speed, a systematic error in each harmonic will result whose properties are as follows:
   (a) As a longer data collection time interval is utilized, a larger systematic error generally occurs.
   (b) For some of the harmonics, the systematic error is about 10 to 20 times larger than the random error if $\delta\Delta v = .01\ \Delta v$.

Earth

1. Depending on the error in ejection speed, the product of atmospheric density (at the satellite) and the drag coefficient, ρC_D, can be determined to between one part in 1,000 and 10,000 by utilizing a low altitude orbit and a two inch diameter probe.
2. If there exists an error in ejection speed of $\delta\Delta v \approx .01\ \Delta v$, then the error in the radiation pressure, δP, is nearly as large as P.
3. If the probe is released so that $\delta\Delta v = \Delta v = 0$, then the following is true:
   (a) For a low altitude orbit, the drag forces are much greater than the solar radiation forces, and, hence, the normalized error in the radiation pressure is about 100 times greater than that of the drag parameter.
   (b) For a high altitude orbit, the drag forces are negligible. After 30 orbits of data, the normalized radiation pressure error, $\delta P/P$, is about 2×10^{-5}.

APPENDIX A

ACCURACY OF ORBIT DETERMINATION

We have proposed and utilized a method of orbit determination which relies on computing position and velocity by a linearization with respect to a reference trajectory. The reference trajectory is chosen to be a set of discontinuous Kepler arcs.

In order to test the accuracy of our method, the sponsor supplied a computer program called Lungfish. This program computes the position by a numerical method of solution to the differential equation. The three second order differential equations are used to obtain a 12th order Runge-Kutta type expansion for the solution.

In Figure 31, we plot the difference between the Lungfish solution and our solution as a function of time. The orbit in question is a low altitude orbit about Mars (Orbit No. 3, Table VI). Only two components are shown, but the third component is similar to those shown. We feel that curves shown can be interpreted as more simply the difference between the two solutions and is the error in our solution. We conclude this because the Lungfish solution implied a nearly constant kinetic energy and component of angular momentum which is parallel to the symmetric axis (within 10^{-7}).

Note the maximum error in our solution is 270 meters after 20 orbits. It is felt that this error has a negligible effect on the results of our error analysis. A test of the accuracy of our solution was also made using an orbit about Venus with $J_2 = 10^{-4}$. In this case, the maximum error was only five meters. It is not surprising that the error in our solution is considerably smaller for smaller perturbations; for our solution is exact for zero perturbations.

APPENDIX B

USE OF PROBE FOR AN ORBIT ABOUT SATURN

In our study of orbits about Venus, we found that the measurement of an

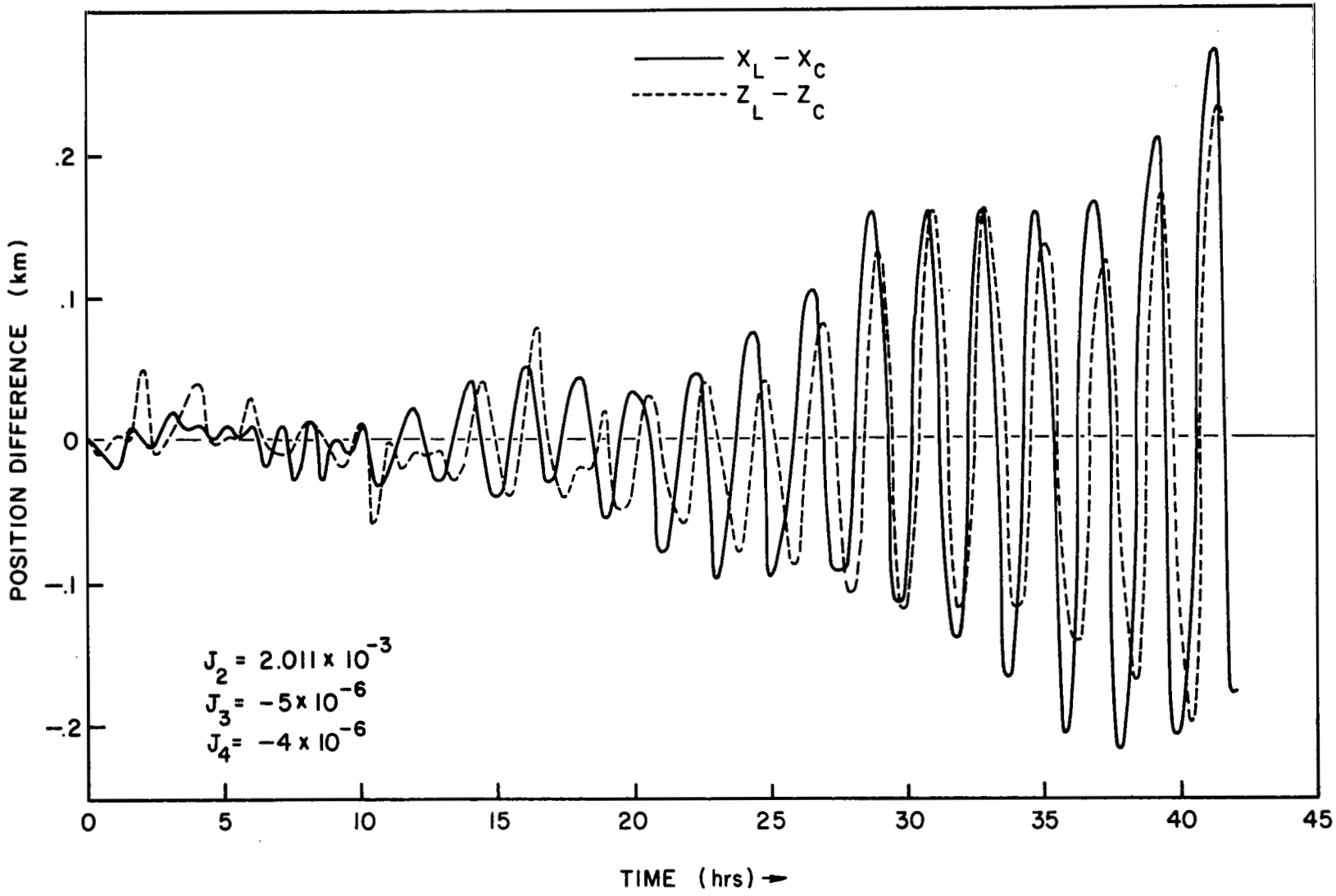

Figure 31: Error in X and Z - Components of Position Due to Method of Solution. Orbit about Mars.

ejected probe's direction as a function of time yielded a poor determination of mass and a relatively poor determination of the direction of the axis of symmetry. We reasoned that these facts were caused because of the almost spherical character of Venus. To test our reasoning, we now study an orbit about Saturn which is a highly oblate planet.

We now assume $J_2 = .0148$, $J_3 = 0$, and $J_4 = -3.5 \times 10^{-4}$, and an orbit whose semi-major axis has length 20% larger than the planet's equatorial radius, and eccentricity = .01. The following results are obtained for no error in ejection speed.

TABLE XIX: Standard Deviation of Parameters for an Orbit About Saturn. Mass Unknown

Parameter	No. of Orbits	
	10	20
$\sigma(\delta m)/m$	3.9×10^{-4}	1.9×10^{-4}
$\sigma(\delta\xi_1)$ (sec of arc)	43	17
$\sigma(\delta\xi_2)$ (sec of arc)	20	6
$\sigma(\delta J_2)$	2.4×10^{-6}	7.3×10^{-7}
$\sigma(\delta J_3)$	1.5×10^{-6}	8.0×10^{-7}
$\sigma(\delta J_4)$	1.0×10^{-6}	3.3×10^{-7}

Except for errors in J_2, the errors shown in Table XIX are somewhat less than those shown in Figure 12. However, the determination of the mass is still not impressive.

APPENDIX C

CHANGE IN DIRECTION PRODUCED BY HARMONICS IN MOON'S POTENTIAL

It is of interest to plot the change in direction of the probe produced by the small perturbing forces. We will do so now, utilizing a Moon orbit given by Orbit 1, Table XIV. To compute this change in direction, initial conditions and a Kepler field were first chosen. The right ascension of the probe was then computed as a function of time. The same initial conditions were rechosen but perturbing forces were added to the Kepler force. A new right ascension as a function of time was computed. The difference of these right

ascensions is shown in figure 32 (perturbed-unperturbed). Two cases are considered: one in which the oblateness term C_{20} produces the perturbing force, and a second in which this force is produced by the harmonics of Case 1, Table XV.

For the cases shown, the nominal orbital period is 2.93 hours. Also, the ejection direction was chosen so that the probe nearly returns after each orbital period. Because a small change in position produces a large direction change when the probe is near the spacecraft, large ($\approx \pm 4^{o}$) direction changes are apparent near multiples of the orbital period. Also, the deviation in azimuth as pictured in figure 32 is large enough so that our intuition is not strained by the fact that 10 arc second errors are small enough to yield results of useful accuracy.

The deviation in elevation is not shown, but this angle deviation is similar to that shown in the figure.

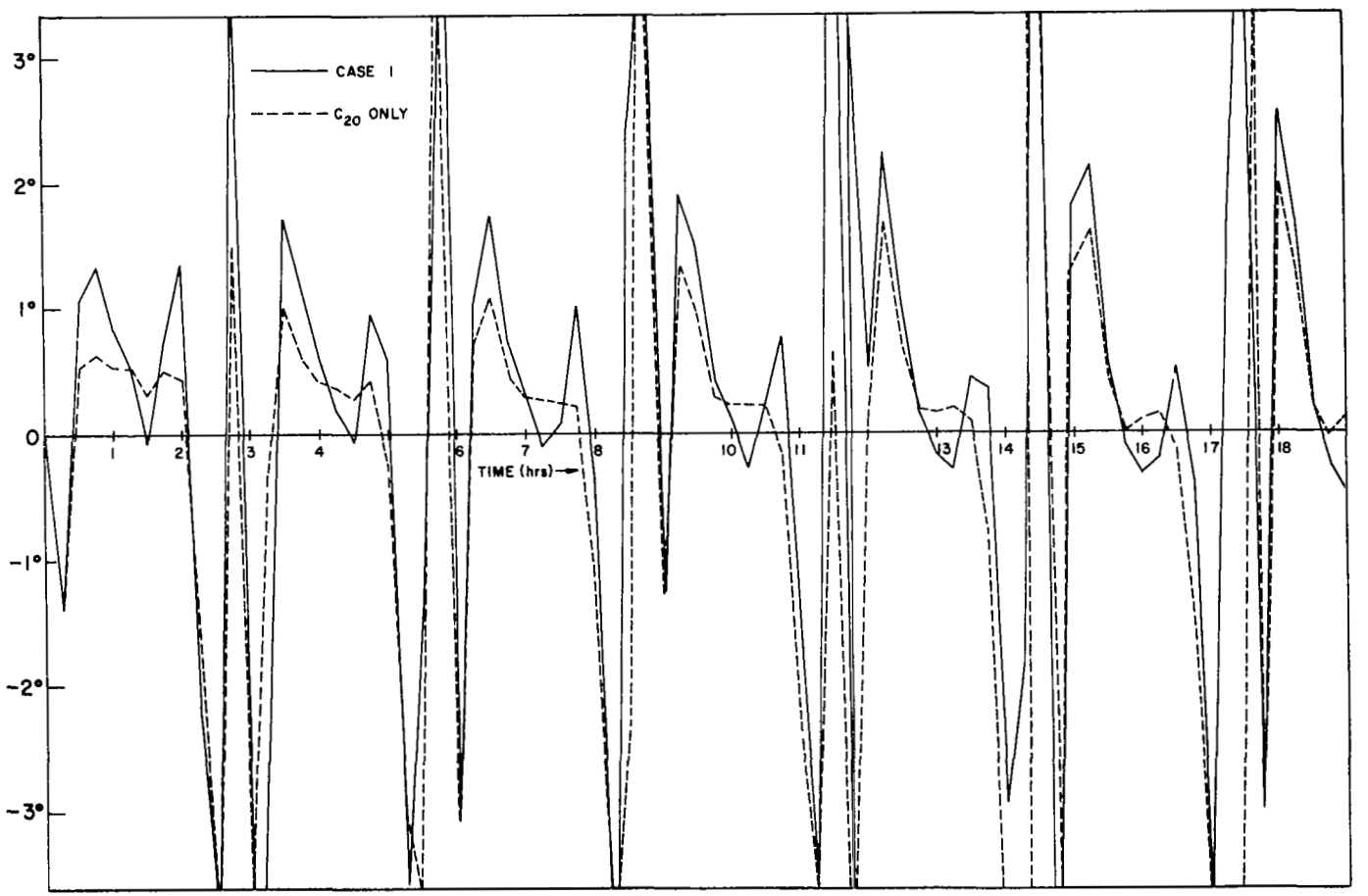

Figure 32: Effect of Harmonics on Direction of Probe

REFERENCES

1. Farrell, E. J. and R. L. Lillestrand, "Celestial Successor to Inertial Guidance," Electronics, March 21, 1955, pp. 94-105

2. Anderson, J. D., et al., "Mariner V Celestial Mechanics Experiment," Science, December 1967.

3. Makemson, M. W., et al., "Analysis and Standardization of Astrodynamic Constants," Journal of the Astronautical Sciences, Vol. VIII, No. 1 (Spring 1961), pp. 1-13.

4. Hamer, H. A. and K. G. Johnson, "Effect of Gravitational-Model Selection on Accuracy of Lunar Orbit Determination from Short Data Arcs," NASA TN D-5105, March 1969.

5. Allen, D. W., Astrophysical Quantities, University of London, Athlone Press, 1955.

6. Koenig, L. R., et al., Handbook of the Physical Properties of the Planet Venus, NASA SP-3029, Scientific and Technical Information Division, 1967.

7. Michaux, C. M., Handbook of the Physical Properties of the Planet Mars, NASA SP-3030, Scientific and Technical Information Division, 1967.

8. Coddington, E. and N. Levinson, Theory of Ordinary Differential Equations, McGraw-Hill, New York, 1955, pp. 67-75.

9. Battin, R. H., Astronautical Guidance, McGraw-Hill Book Company, New York, 1964, pp. 9-12.

10. Kochi, K. C., "Exact First-Order Navigation Guidance Mechanization and Error Propagation Equations for Two-Body Reference Orbits," AIAA Journal, Vol. 2, No. 2, February 1964, p. 365.

11. Brouwer, D. and G. M. Clemence, "Orbits and Masses of Planets and Satellites," in Planets and Satellites, Vol. III, ed. Kuiper and Middlehurst, University of Chicago Press, 1961.

12. Lorell, J. and W. L. Sjogren, "Lunar Gravity: Preliminary Estimates from Lunar Orbiter," Science, February 9, 1968.

13. King-Hele, D. G., Theory of Satellite Orbits in an Atmosphere, Butterworth Press, 1964.